# Optimal control of time-dependent targets

Diploma Thesis

Submitted to the Free University Berlin, Physics Department

Ioana Şerban

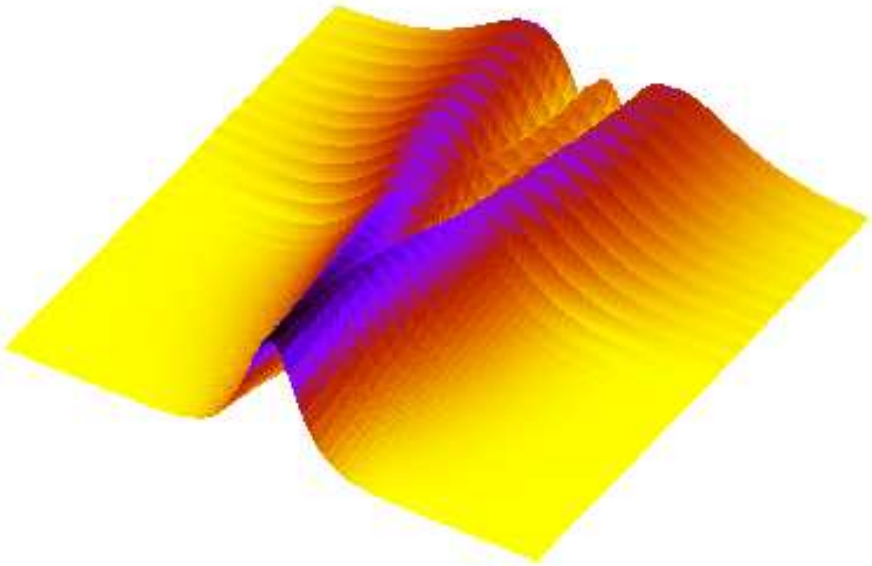

Advisor: Professor Dr. Eberhard Groß

Berlin, August 3, 2004

Title page: time-dependent electronic density; 1D hydrogen atom executes the transition from the ground-state to the $2nd$ excited state via $1st$ excited state.

# Contents

# Chapter 1

# Introduction

A common objective in many technical fields and economy is to find a control variable that commands a dynamic system to a desired output.

Optimal control theory describes strategies for maximizing a performance measure or minimizing a cost function as the state of a dynamic system evolves. The goal is to find a time-dependent control variable that drives the considered dynamical system from its initial to its final state and, at the same time, that optimizes the performance function. This requires choosing the optimum among a set of possible solutions. The resulting dynamics of the state of the system is an optimal trajectory. Examples include the trajectory of a climbing aircraft which requires a minimal quantity of fuel or an optimal financial investment strategy. Optimal control theory (OCT) as mathematical theory dates back to the late 1950s, starting with Pontryagin's maximum principle [1].

In physics and chemistry, due to techniques recently developed in the shaping of laser fields [2], the control of chemical reactions became possible. Typical problems include the search for the optimal laser pulse that selects one of several possible chemical reaction pathways e.g. selectively breaks a bond leaving the rest of the molecule intact. For example, starting with a molecule $ABC$ one can obtain two sets of reaction products $AB + C$ and $A + BC$, and the question therefore is how one can drive the system into only one of these two possible reaction channels. If one irradiates the molecule with a field which oscillates with the resonance frequency of the bond one wants to break, the energy of the field is rapidly redistributed to the rest of the molecule, so that selectivity is lost. Studies of the response of polyatomic molecules in response to laser fields have been given in [3, 4]. Another very general question is how one can excite a molecule or an atom into a desired state.

It is clear that the physical laws governing the processes described in the previous paragraph are the laws of quantum mechanics. Therefore, a formulation of OCT for quantum mechanics would allow to invert the formulation of such problems, i.e., one searches for the appropriate laser field that achieves a given objective. The theoretical formulation of OCT in quantum mechanics has started in the 1980s. The work of Huang, Tarn, Clark [5] considers a general formulation of the complete controllability[1] problem of quantum dynamics and gives sufficient conditions for complete control. Pierce et al. [6] have given an existence proof for the control variable in a system with localized states and a discrete spectrum. The proof has been generalized in [7] to systems with both continuous and discrete parts of the spectrum

[1] Complete controllability implies that the norm of the difference between the final state reached with the optimal control field and the target state can be made arbitrarily small, in the space of admissible fields

spectrum.

Tannor, Kosloff and Rice [8, 9] suggested a "pump-dump" technique to control the selectivity of chemical reactions. The first, "pump" pulse induces a vertical transition of the molecule into an excited Born-Oppenheimer-state surface, where the wave packet moves freely for a while. The second, "dump" pulse induces a vertical transition back to the ground state surface, according to the Franck-Condon principle. Depending on when and where on this surface the projection from the excited state ends, the molecule may go into one or the other reaction channel or remain intact. In ref. [10] the "pump-dump" technique is improved by optimizing the shapes of the "pump" and "dump" pulses.

Judson and Rabitz [11] suggested a closed loop algorithm to shape the optimal pulse that excites specific molecular states. Evolutionary algorithms are global optimization methods based on concepts from biological evolution. The properties of a laser pulse are coded in a "gene" which can be uniquely decoded to give the laser pulse. A performance function is defined to discriminate between individuals. From the initial population of pulses one chooses the individuals with best performance, mutates and combines their genes, obtains a new population and repeats the procedure. Evolutionary algorithms have been used in experiment to optimize population transfer from the ground to the first excited state [12], to control chemical reactions [13, 14] and selectively dissociate molecular bonds [15].

Tannor et al. [16] formulate the goal of optimization as a functional maximization and give an iterative method for solving the resulting variational equations, which guarantees the systematic increase of this functional. The solution of the optimal problem presented by Tannor et al. is based on the work of Krotov [17]. Similar algorithms are proposed by Rabitz et al. [18, 19]. A more general form of the iterative algorithm has been given by Maday and Turinici [20]. A non iterative method for the optimization of the same functional has been given in [21].

All the methods described so far have in common the goal to find the optimal laser field that optimizes the output of a quantum system at the end of the time interval. The path followed by the quantum mechanical system to reach the desired final state remains undetermined.

There is an application of OCT which attempts to control time averaged quantities, for example the time averaged population of a given state [22]. Nevertheless, the method is applicable only in a simple (two-level) system. There also exists a general formulation for OCT of time-dependent targets [23], but no method to solve the resulting equations has been given.

Apart from optimal control theory, there are also other methods to control the output of a quantum mechanical system. In the local control theory described in [24, 25, 26] one can determine a field which guarantees the monotonic increase of a "performance index". Nevertheless, there is no guarantee that one obtains an optimal field, i.e. that one reaches an maximum of the performance index with respect to the control field at the end of the time interval.

A very elegant method to control the trajectory of a system, namely tracking control, is proposed in ref. [27, 28, 29]. In this case, for an arbitrary time-dependent function $f(t)$ and a given operator $O$ one desires to find the external control field such that the solution of the Schrödinger equation $\Psi$ with this field satisfies $\langle\Psi|\hat{O}|\Psi\rangle = f(t)$. In this case the time dependence of the observable one desires to control is used to exactly invert the Schrödinger equation. The analytical solution gives the exact dependence between the field that solves the problem and the imposed function $f(t)$. It is a non-iterative method, therefore it is computationally inexpensive. The disadvantage of this method is that the exact field may experience

singularities, if the prescribed trajectory is not well posed, i.e. the prescribed trajectory cannot be reached in the space of admissible control fields. Furthermore, the derivation of this method strictly relies on the dipole approximation.

The goal of this diploma thesis is to find a general formulation of OCT that allows the control of the system not only at the final time, but also at each time within the control interval. If the path which the system takes to reach the final state, is undetermined, there will be many fields that are able to drive the system into this state. By imposing one trajectory for the whole time interval, the optimal control field has less degrees of freedom.

The starting point of this thesis will be the result of Zhu and Rabitz [19], where a method has been developed to determine the optimal field that maximizes the expectation of a positive definite operator at the end of the time interval. In chapter 2 we extend this formulation to the control of time averaged expectation value of a positive definite operator. The method is a general one and can be applied to systems more complex that the two level atom.

Following [19] we express the goal of optimization in the mathematical form of of functional maximization and derive optimal control equations. In chapter 4 we present an iterative method to solve these equations. For this method we prove the monotonic convergence of the cost functional. One of these control equations has the form of an inhomogeneous Schrödinger equation.

Our objective is to control the system at every time, and not only to use the time dependence of an observable in order to maximize its expectation value at the final state. We also do not desire only to maximize the time averaged expectation value of an operator, but also to control the trajectory followed by the system. We start, as in the tracking formulation, with an arbitrary function $f(t)$ and a given operator $\hat{O}$. First, we construct an "artificial" normalized time-dependent function $\varphi$ which satisfies $\langle\varphi|\hat{O}|\varphi\rangle = f(t)$. Note that for $\varphi$ we do not impose the constraint that it must satisfy the Schrödinger equation. Then we construct a projection operator on this function $\varphi(t)$. The maximization of the time averaged expectation value of this operator is then equivalent to finding that control field which maximizes at *all* times the overlap of the artificial function $\varphi$ with the solution $\Psi$ of the Schrödinger equation with the control field. We also search for the field that drives the time-dependent wave-function of the quantum mechanical system as closely as possible to the artificial function. Consequently, the expectation value of the given operator $\hat{O}$ follows the imposed function $f(t)$ as closely as possible.

A time-dependent wave-function contains all the information about the quantum system so that, by controlling it, we can control the time evolution of all observables. Nevertheless for finding the artificial function $\varphi$ physical intuition is needed. In chapter 5 we consider the control of the occupation number of a given state and the time-dependent dipole moment as examples. Using this approach, we are able not only to maximize the time averaged expectation value of an operator, but also to impose the time dependence of the observable.

Apart from this application, one can use the formalism we develop in chapters 2, 3 and 4 to control a time-dependent electronic density as one can see in section 6.2.2.

Atomic units are a convenient system of units used in atomic physics, in particular for describing the properties of electrons. Therefore, for the calculations used in this theses we will use atomic units exclusively, for which the conversion to SI is given in appendix A.

# Chapter 2

# Time dependent continuous control of a quantum mechanical system

In the past, optimal control theory has been used to find the optimal laser pulse that brings a quantum system from an initial state $A$ at $t = 0$ to a desired final state $B$ at $t = T$, but the path followed by the system between 0 and $T$ remained uncontrolled. We will refer to it as traditional optimal control. There are cases, e.g., the control of the time-dependent population in a specific state, where it is desirable to control this path. Another class of examples are problems one desires to bring a quantum system from a point $A$ in space to point $B$ under the restriction that one avoids a certain area in real space e.g. conical intersections.

The process of high harmonic generation[1] is also a process where the intensities of the harmonics depend not only on the initial and final state of the system but also on the state of the system at each time $t \in [0, T]$.

In this chapter we extend the optimal control theory to control a quantum system not only at the final time $T$ but also at every intermediate time $t \in [0, T]$. We formulate the optimization goal in the form of a functional which has to be maximized, and then derive the necessary condition for a maximum of this functional.

## 2.1 Formulation of the control problem

In this section we will formulate the problem of continuous time-dependent control of a single quantum-mechanical particle whose evolution is governed by the non-relativistic Schrödinger equation

$$i\frac{\partial}{\partial t}\Psi(x,t) = \widehat{H}\Psi(x,t), \tag{2.1}$$

$$\widehat{H} = \widehat{H}_0 - \hat{\mu}E(t), \tag{2.2}$$

$$\widehat{H}_0 = \widehat{T} + \widehat{V}, \tag{2.3}$$

In this thesis we will study systems like the two-level atom and the 1D hydrogen atom. $\widehat{T} = -\frac{\nabla^2}{2}$ is the kinetic energy operator, $\widehat{V}$ the potential of the nucleus (for the hydrogen atom see section 6.1.3), and $\hat{\mu} = qx$ the dipole moment operator. $q$ is the charge of the

[1] When an atom is exposed to an intense laser field, it responds in a nonlinear way and radiates the harmonics of the incident laser frequency.

particle and $E$ is the external electric field which, for example, can be realized with a laser beam.

For $\widehat{H}$ we use the dipole approximation of the Hamilton operator in an electromagnetic field (see Appendix B). In the dipole approximation we consider that the radiation field is uniform in the space occupied by the atom. This approximation is valid for radiation with wave lengths much larger than the dimension of the atom, which we will assume in the examples used in this thesis.

So far, studies of quantum control problems in the literature (for example [19]) have mostly focused on finding the optimal time-dependent field which brings the system from initial state $A$ to a state $B$ at final time $T$ irrespective of the path taken during the evolution. Mathematically this can be expressed as a maximization problem of the functional

$$J_1[\Psi(T)] = \langle\Psi(T)|\widehat{O}|\Psi(T)\rangle, \tag{2.4}$$

$$\langle\Psi(T)|\widehat{O}|\Psi(T)\rangle \geq 0 \quad \forall\Psi, \tag{2.5}$$

where for the positive definite operator $\widehat{O}$ has been chosen to be a projection operator on the desired final state or a local operator like $\delta(x - r(t))$.

The maximization of the functional (2.4) has been successfully used to drive the quantum system into the desired final state at the end of the time interval $T$. If we want to control the system not only at $T$ but also at intermediate points in time $\tau_1 < \tau_2 < \ldots T$ we define a new functional, namely $J_1[\Psi(t)] = J_1[\Psi(\tau_1)] + J_1[\Psi(\tau_2)] + \cdots + J_1[\Psi(T)]$ that has to be maximized. Since $t$ is a continuous variable, we can replace the sum with an integral

$$J_1[\Psi(t)] = \frac{1}{T}\int_0^T dt\, \langle\Psi(t)|\widehat{O}_t|\Psi(t)\rangle. \tag{2.6}$$

The normalization factor $1/T$ makes the maximal value of the functional independent on the length of the time interval $T$ and gives to $J_1$ the interpretation of time averaged expectation value.

Following [19] we choose the time-dependent operator to be hermitian $\widehat{O}_t = \widehat{O}_t^+$ and positive semi-definite, i.e.,

$$\langle\Psi(t)|\widehat{O}_t|\Psi(t)\rangle \geq 0, \quad \forall\ \Psi. \tag{2.7}$$

At this point we rewrite this operator to include traditional optimal control in our formulation

$$\widehat{O}_t = \widehat{O}_t^{(1)} + 2T\delta(t-T)\widehat{O}_t^{(2)}. \tag{2.8}$$

Both operators $\widehat{O}_t^{(1)}$ and $\widehat{O}_t^{(2)}$ are hermitian. For $\widehat{O}_t^{(1)} = 0$ and $\widehat{O}_t^{(2)} = \widehat{O}$ the functional of equation (2.6) reduces to equation (2.4). The restriction to the optimization of positive definite operators will be crucial for the proof of convergence of the algorithm for finding the optimal field.

Optimizing $J_1$ may possibly lead to fields with very high, or even infinite total intensity. In order to avoid these strong fields, we include an additional term in the functional which penalizes the total energy of the field

$$J_2[E,\alpha] = -\alpha\int_0^T dt\, E^2(t). \tag{2.9}$$

Here $\alpha$ is a positive parameter that weights this part of the functional against $J_1$. To keep $J_2$ dimensionless $\alpha$ must have the dimension of $\epsilon_0 c/\hbar$.

With the above formulation the problem reads as following: find the laser pulse that maximizes the difference between the time averaged overlap (2.6) and total intensity of the field. This goal sounds a little ambiguous, since $J_1$ separately is in fact what we want to maximize, but we will see later in this chapter that $J_2$ has a fundamental importance for the optimal control equations we will derive.

The wave function and the control field are connected through the time-dependent Schrödinger equation (2.1). We multiply this equation with a time- and space-dependent complex function $\chi(x,t)$, integrate over space and time and obtain like in [18] a third functional

$$\begin{aligned} J_3[E(t),\Psi(x,t),\chi(x,t)] &= 2\Im\int_0^T dt\int_{-\infty}^{\infty} dx\,\chi^*(x,t)\left(i\partial_t-\widehat{H}\right)\Psi(x,t) = \\ &= 2\Im\int_0^T dt\,\left\langle\chi(t)\left|\left(i\partial_t-\widehat{H}\right)\right|\Psi(t)\right\rangle = \\ &= 2\Re\int_0^T dt\,\left\langle\chi(t)\left|\left(\partial_t+i\widehat{H}\right)\right|\Psi(t)\right\rangle . \end{aligned} \tag{2.10}$$

By adding $J_3$ to the functional, we include the constraint that $\Psi$ satisfies the Schrödinger equation explicitly. Therefore we can treat $\Psi$ and $E$ as independent variables. The constraint is included as twice the imaginary part in order to make the functional symmetric in $\Psi$ and $\Psi^*$. The function $\chi$ plays the role of a Lagrange multiplier.

The Lagrange functional has the form

$$\begin{aligned} \mathcal{L}[\Psi,E,\chi,\alpha] &= J_1+J_2-J_3 = \\ &= \frac{1}{T}\int_0^T dt\,\langle\Psi(t)|\widehat{O}_t|\Psi(t)\rangle-\alpha\int_0^T dt\,E^2(t)- \\ &- 2\Im\int_0^T dt\,\left\langle\chi(t)\left|\left(i\partial_t-\widehat{H}\right)\right|\Psi(x)\right\rangle . \end{aligned} \tag{2.11}$$

The search for the maximum of $J_1+J_2$ under the constraint that $\Psi$ fulfills the Schrödinger equation becomes an unrestricted search for the maximum of $\mathcal{L}$.

## 2.2 Derivation of the control equations

By setting the variation of the Lagrange functional with respect to $\chi$, $E$ and $\Psi$ to 0 gives the *necessary* conditions for an local extremum of $\mathcal{L}$. Note that these equations are consistent not only with the global maximum but also with any local extremum (maximum, minimum or even saddle point). In chapter 4 we will give a method to solve these equations which guarantees that the solution is consistent with a (local) maximum. We follow in the derivation of the control equations [30] and generalize it for the functional $\mathcal{L}$.

### 2.2.1 Variation with respect to the wave function

The variation of $\Psi$ is independent from the variation of $\Psi^*$[2], and we should take the variation of the Lagrange functional with respect to both of them. Due to the symmetry of the Lagrange

[2] $\Psi$ is a complex function, it has two independent components $\Re\Psi$ and $\Im\Psi$ and one should vary $\mathcal{L}$ with respect to both of them. This is equivalent with varying $\mathcal{L}$ with respect to $\Psi$ and $\Psi^*$.

functional with respect to $\Psi$ and $\Psi^*$ this leads to the same equations for $\Psi^*$ and $\Psi$.

We consider the system at $t=0$ to be fixed in the initial state $\Psi(x,0)=\phi(x)$. It follows that the variation $\frac{\delta\Psi(0)}{\delta\Psi(\tau)}$ must vanish. The variation of $J_1$ gives

$$\begin{aligned}\frac{\delta J_1}{\delta\Psi(y,\tau)} &= \frac{1}{T}\int_0^T dt\int_{-\infty}^{\infty}dx\,\left(\widehat{O}_t^{(1)}\Psi(x,t)\right)^*\frac{\delta\Psi(x,t)}{\delta\Psi(y,\tau)}+\int_{-\infty}^{\infty}dx\,\left(\widehat{O}_T^{(2)}\Psi(x,T)\right)^*\frac{\delta\Psi(x,T)}{\delta\Psi(y,\tau)}= \\ &= \left(\frac{1}{T}\widehat{O}_\tau^{(1)}\Psi(y,\tau)\right)^*+\left(\hat{O}_T^{(2)}\Psi(y,T)\right)^*\delta(\tau-T). \qquad (2.12)\end{aligned}$$

We transform $J_3$ with the help of a partial integration, and using the fact that $\widehat{H}$ is hermitian

$$\begin{aligned}\int_0^T dt\,\left\langle\chi(t)\left|\left(i\partial_t-\widehat{H}\right)\right|\Psi(t)\right\rangle &= \int_0^T dt\,\left(\langle\chi(t)\,|i\partial_t|\,\Psi(t)\rangle+\left\langle\chi(t)\left|-\widehat{H}\right|\Psi(t)\right\rangle\right)= \\ &= \int_{-\infty}^{\infty}dx\int_0^T dt\,\chi^*(t)i\partial_t\Psi(t)+\int_0^T dt\left\langle-\widehat{H}\chi(t)\middle|\Psi(t)\right\rangle= \\ &= i\langle\chi(t)|\Psi(t)\rangle|_0^T+\int_0^T dt\left\langle\left(i\partial_t-\widehat{H}\right)\chi(t)\middle|\Psi(t)\right\rangle, \qquad (2.13)\end{aligned}$$

and then do a variation of $J_3$ with respect to $\Psi$

$$\begin{aligned}\frac{\delta J_3}{\delta\Psi(y,\tau)} &= -i\frac{\delta}{\delta\Psi(y,\tau)}\int_0^T dt\,\left(\left\langle\chi(t)\middle|\left(i\partial_t-\widehat{H}\right)\middle|\Psi(t)\right\rangle-\left\langle\left(i\partial_t-\widehat{H}\right)\Psi(t)\middle|\chi(t)\right\rangle\right)= \\ &= -i\frac{\delta}{\delta\Psi(y,\tau)}\left(\int_0^T dt\left\langle\left(i\partial_t-\widehat{H}\right)\chi(t)\middle|\Psi(t)\right\rangle+i\langle\chi(t)|\Psi(t)\rangle|_0^T\right)= \\ &= -i\left(\left(i\partial_\tau-\widehat{H}\right)\chi(y,\tau)\right)^*+\chi^*(y,T)\delta(T-\tau). \qquad (2.14)\end{aligned}$$

$\frac{\delta\Psi(x,0)}{\delta\Psi(y,\tau)}=0$, thus only the boundary term at T remains. Since $\Psi$ and $\Psi^*$ are independent variables, the variation of $\left\langle\left(i\partial_t-\widehat{H}\right)\Psi(t)\middle|\chi(t)\right\rangle$ with respect to $\Psi$ is zero.

$J_2$ does not depend on $\Psi$. Setting the variation of $\mathcal{L}$ with respect to $\Psi$ to zero gives

$$\begin{aligned}&-i\left(\left(i\partial_\tau-\widehat{H}\right)\chi(y,\tau)\right)^*+(\chi^*(y,T)\delta(T-\tau))= \\ &\frac{1}{T}\left(\widehat{O}_\tau^{(1)}\Psi(y,\tau)\right)^*+\left(\widehat{O}_T^{(2)}\Psi(y,T)\right)^*\delta(\tau-T). \qquad (2.15)\end{aligned}$$

Due to the symmetry of the Lagrange functional we obtain the complex conjugate of equation (2.15) after varying $\mathcal{L}$ with respect to $\Psi^*$

$$i\left(i\partial_t-\widehat{H}\right)\chi(x,t)+\chi(x,T)\delta(T-t) = \frac{1}{T}\widehat{O}_t^{(1)}\Psi(x,t)+\hat{O}_T^{(2)}\Psi(x,T)\delta(t-T). \qquad (2.16)$$

In the following we show how one can transform (2.16) to a differential equation with boundary condition. We state: if one requires the Lagrange multiplier $\chi(x,t)$ to be a continuous function at every time $t$ (including $t=T$), the solution $\chi(x,t)$ of equation (2.16) is unique. Equation (2.16) becomes equivalent to two other equations, which can be obtained by setting the terms which contain $\delta(T-\tau)$ and those which do not to zero separately. This yields

$$\left(i\partial_\tau-\widehat{H}\right)\chi(y,\tau) = -\frac{i}{T}\widehat{O}_t^{(1)}\Psi(y,\tau) \qquad (2.17)$$

$$\chi(y,T) = \widehat{O}_T^{(2)}\Psi(y,T). \qquad (2.18)$$

To show how equation (2.16) can be transformed to equations (2.17) and (2.18) we integrate (2.16)

$$\lim_{\kappa\to 0}\int_{T-\kappa}^{T+\kappa} dt\left(i\partial_t-\widehat{H}\right)\chi(x,t)+\frac{i}{T}\widehat{O}_t^{(1)}\Psi(x,t)=$$
$$\lim_{\kappa\to 0}\int_{T-\kappa}^{T+\kappa} dt\; i\left(\chi(x,t)-\widehat{O}_t^{(2)}\Psi(x,t)\right)\delta(t-T). \tag{2.19}$$

The left-hand side of (2.19) is zero because $\chi$ is a continuous function so that the integrand is also a continuous function and the length of the integration interval goes to zero. Performing the integration then yields equation (2.18). (2.17) is satisfied for every $t\neq T$ because the $\delta$ terms vanish. From (2.18) and (2.16) follows that (2.17) must be satisfied for every $t$.

The Lagrange multiplier $\chi$ satisfies an inhomogeneous Schrödinger equation (2.17) with initial condition (2.18), therefore it is uniquely determined.

### 2.2.2 Variation with respect to the field

The variation of $J_2$ with respect to $E$ gives

$$\frac{\delta J_2}{\delta E(\tau)} = -\frac{\delta}{\delta E(\tau)}\alpha\int_0^T dt\, E^2(t)=-2\alpha E(\tau). \tag{2.20}$$

Due to the dipole approximation we can explicitly write the dependence on $E(t)$ in the Hamilton operator, i.e. in $J_3$

$$\begin{aligned}\frac{\delta J_3}{\delta E(\tau)} &= \frac{\delta}{\delta E(\tau)}2\Im\int_0^T dt\,\left\langle\chi(t)\left|\left(i\partial_t-\widehat{H}\right)\right|\Psi(t)\right\rangle=\\ &= \frac{\delta}{\delta E(\tau)}2\Im\int_0^T dt\,\left\langle\chi(t)\left|\hat{\mu}E(t)\right|\Psi(t)\right\rangle=\\ &= 2\Im\left\langle\chi(\tau)\left|\hat{\mu}\right|\Psi(\tau)\right\rangle.\end{aligned} \tag{2.21}$$

Setting the variation of $\mathcal{L}$ with respect to $E$ to zero gives the field equation

$$\alpha E(\tau) = -\Im\langle\chi(\tau)|\hat{\mu}|\Psi(\tau)\rangle \tag{2.22}$$

The left-hand side results from the functional $J_2$. Without $J_2$ we would obtain

$$\Im\langle\chi(\tau)|\hat{\mu}|\Psi(\tau)\rangle=0 \tag{2.23}$$

so that no field can be determined.

### 2.2.3 Variation with respect to Lagrange multiplier

Similar to the variation with respect to $\Psi$ we do not have to take the variation of the Lagrange functional with respect to $\chi^*$ because $\mathcal{L}$ is symmetric in $\chi$ and $\chi^*$ and we would obtain the same equation.

$$\begin{aligned}\frac{\delta J_3}{\delta\chi(y,\tau)} &= -i\frac{\delta}{\delta\chi(y,\tau)}\int_0^T dt\,\left[\left\langle\chi(t)\right|\left(i\partial_t-\widehat{H}\right)\left|\Psi(t)\right\rangle-\left\langle\left(i\partial_t-\widehat{H}\right)\Psi(t)\middle|\chi(t)\right\rangle\right]=\\ &= i\frac{\delta}{\delta\chi(y,\tau)}\int_0^T dt\left\langle\left(i\partial_t-\widehat{H}\right)\Psi(t)\middle|\chi(t)\right\rangle=\\ &= i\left(\left(i\partial_t-\widehat{H}\right)\Psi(y,\tau)\right)^*=0\end{aligned} \tag{2.24}$$

By construction the variation with respect to the Lagrange multiplier gives the Schrödinger equation for $\Psi$, the constraint on $\Psi$ we wanted to enforce

The variation of $\mathcal{L}$ with respect to $\chi^*$ gives

$$-i\left(\left(i\partial_t - \widehat{H}\right)\Psi(y,\tau)\right) = 0. \tag{2.25}$$

### 2.2.4 Final set of optimal control equations equations

To summarize, the necessary conditions for a local extremum of the functional $\mathcal{L}$ is given by the following system of coupled integro-differential equations

$$\left(i\partial_t - \widehat{H}\right)\chi(x,t) = -\frac{i}{T}\widehat{O}_t^{(1)}\Psi(x,t), \tag{2.26}$$

$$\chi(x,T) = \widehat{O}_T^{(2)}\Psi(x,T), \tag{2.27}$$

$$\left(i\partial_t - \widehat{H}\right)\Psi(x,t) = 0, \tag{2.28}$$

$$\Psi(x,0) = \phi(x), \tag{2.29}$$

$$E(t) = -\frac{1}{\alpha}\Im\langle\chi(t)|\hat{\mu}|\Psi(t)\rangle, \tag{2.30}$$

were $\phi(x)$ is the initial state of the system.

The inhomogeneous Schrödinger equation for the Lagrange multiplier is a direct consequence of the target functional $J_1$, which depends on the trajectory followed by the system (i.e. $\Psi(x,t)$) and not only on the final state.

The field equation (2.30) has a very simple form due to the dipole approximation. Without the dipole approximation one obtains a second order differential equation for the vector potential (see Appendix C).

The coupled set of equations (2.26), (2.28) and (2.30) must be solved iteratively. This is mainly due to the fact that we have to deal with a two point boundary value problem. The wave function has an initial condition, while the Lagrange multiplier has a final condition. A possible method to solve these equations is: solve (2.28) using a known field $E(t)$, solve (2.26) using $E(t)$ and the solution of (2.28), and in the end calculate a new field using (2.30). In practice, we will use a more complicated iterative scheme (see chapter 4), which also guarantees the convergence to a local maximum. If we had equation (2.23) instead of equation (2.30), such an iterative scheme would not be applicable.

### 2.2.5 $\alpha$: Lagrange multiplier or penalty factor?

There is another way to formulate the problem such that the goal of the optimization becomes clearer. If we do not require to minimize the total intensity of the laser field, but want to find the laser pulse that has a predetermined intensity and maximizes $J_1$, we can rewrite $J_2$ in form of a constraint. We search for the optimal pulse in the subspace of pulses with a fixed energy $I_0$. The constraint is then expressed as

$$\widetilde{J}_2 = -\alpha\left(\int_0^T dt\; E^2(t) - I_0\right). \tag{2.31}$$

The Lagrange functional is

$$\widetilde{\mathcal{L}}[\alpha, E, \Psi, \chi] = J_1 + \widetilde{J}_2 - J_3, \tag{2.32}$$

where $\alpha$ is now a Lagrange multiplier. We express the necessary conditions for an extremum of $\widetilde{\mathcal{L}}$ in the form of a system of equations

$$\left(i\partial_t - \widehat{H}\right)\chi(x,t) = -\frac{i}{T}\widehat{O}_t^{(1)}\Psi(x,t)\,, \quad \chi(x,T) = \widehat{O}_T^{(2)}\Psi(x,T), \tag{2.33}$$

$$\left(i\partial_t - \widehat{H}\right)\Psi(x,t) = 0\,, \quad \Psi(x,0) = \phi(x), \tag{2.34}$$

$$\alpha E(\tau) = -\Im\langle\chi(\tau)|\hat{\mu}|\Psi(\tau)\rangle \tag{2.35}$$

$$\int_0^T dt\; E^2(t) = I_0 \tag{2.36}$$

This is a system of four coupled differential and integral equations with unknown $\alpha$, $E(t)$, $\Psi(x,t)$ and $\chi(x,t)$. For a given $\alpha$ the first three equations of this system restate the necessary conditions for an extremum of the functional $\mathcal{L}[E,\Psi,\chi]$ of functional (2.11) which we derived in section 2.2.4.

To solve the system of equations (2.33)-(2.36) we start by solving equations (2.33), (2.34) and (2.35) for a fixed value of $\alpha$. Suppose we have found a method to solve this three and also that the solution ($E$, $\Psi$, $\chi$) is compatible with a *maximum* of the Lagrange functional $\mathcal{L}[E,\Psi,\chi] = J_1 + J_2 - J_3$ (one possible algorithm that serves this purpose will be presented in chapter 4). In this case, we can determine the optimal field $E$ and its total intensity $I$, which is a function of $\alpha$: $I(\alpha)$. The iterative method presented in chapter 4 only finds a local maximum of $\mathcal{L}$, which also depends on the initial guess for the field, therefore $I = I(\alpha, E_{guess})$. But for the discussion here, we consider $E_{guess}$ fixed, and consider only the dependence of $I$ on $\alpha$.

Furthermore, we find the root of the function $f(\alpha) = I(\alpha) - I_0$ using the following scheme

$$\begin{array}{ccccc} \alpha_{init.\ guess} \longrightarrow \alpha & \longrightarrow & \boxed{\text{solve (2.33), (2.34),(2.35)}} \\ \uparrow & & \downarrow \\ \boxed{I(\alpha) = \int_0^T E^2(t)dt} & \longleftarrow & (E,\Psi,\chi)_\alpha \end{array} \tag{2.37}$$

We start with an initial guess for the Lagrange multiplier $\alpha$ and solve equations (2.33), (2.34) and (2.35) to obtain $E$, $\Psi$ and $\chi$. We then calculate the total intensity of the laser field and compare it with the target value $I_0$. Depending on $I(\alpha)$ we determine a new $\alpha$ (see section 5.3.3). The whole process is iterated until we find $\alpha_0$ such that $I(\alpha_0) = I_0$ and thus equation (2.36) is also satisfied. With the iteration (2.37) we can solve the system (2.33) - (2.36). The solution ($\alpha$, $E$, $\Psi$, $\chi$) is consistent with an extremum (maximum, minimum or saddle point) of the functional $\widetilde{\mathcal{L}} = J_1 + \widetilde{J}_2 - J_3$.

In every step of the iteration (2.37) the solution ($E$, $\Psi$, $\chi$) corresponds to a maximum of the functional $\mathcal{L}[E,\Psi,\chi] = \widetilde{\mathcal{L}}[\alpha,E,\Psi,\chi] - \alpha I_0$ for a given $\alpha$, i.e. we maximize $\widetilde{\mathcal{L}}$ with respect to $E$, $\Psi$, $\chi$. The outer loop finds the extremum of $\widetilde{\mathcal{L}}[\alpha,E,\Psi,\chi]$ with respect to $\alpha$, which can be either a minimum or a maximum. In section 5.3.3 we show a simple implementation of the iterative scheme (2.37).

For $\alpha = 0$, $J_1 + J_2 - J_3$ reduces to $J_1 - J_3$, so that the field for which $J_1 + J_2 - J_3$ reaches its absolute maximum is the same as the field which absolute maximizes $J_1 - J_3$. In other words

$$\lim_{\alpha\to 0} I(\alpha) = I_1, \tag{2.38}$$

where $I_1$ is the intensity of the field which maximizes $J_1 - J_3$ separately. In practice we cannot use $\alpha = 0$ due to equation 2.23. In the case $\alpha \to \infty$, for every field $E(t) \neq 0$ the functional $(J_1 + J_2 - J_3)[E]$ has the value $-\infty$. Only for $E(t) = 0$ the functional $(J_1 + J_2 - J_3)[E]$ has a positive value, so that the absolute maximum of $(J_1 + J_2 - J_3)[E]$ is reached for $E(t) = 0$. Therefore

$$\lim_{\alpha \to \infty} I(\alpha) = 0. \tag{2.39}$$

# Chapter 3

# Inhomogeneous Schrödinger equation

## 3.1 Formal solution

In order to find the optimal field which maximizes the target functional $J_1 + J_2$ under the constraint that the wave function satisfies the Schrödinger equation, we have to solve the system of coupled differential equations (2.26), (2.28) and (2.30). The solution of (2.30) can be achieved by integration once we know $\chi$ and $\Psi$. In this chapter we present the solution of the equations (2.26) and (2.28). We briefly restate the solution of the homogeneous Schrödinger equation (2.28). We rewrite the wave function

$$\Psi(x,t) = \widehat{U}_{t_0}^{t}\Psi(x,t_0), \tag{3.1}$$

where $\Psi(x,t_0)$ is the initial state at time $t_0$ and $\widehat{U}_{t_0}^{t}$ is the time evolution operator. Using this ansatz for $\Psi(x,t)$ in the Schrödinger equation (2.28) we obtain

$$\left(\frac{d}{dt}\widehat{U}_{t_0}^{t} + i\widehat{H}_t\widehat{U}_{t_0}^{t}\right)\Psi(x,t_0) = 0. \tag{3.2}$$

Since this equation must be satisfied for every $\Psi(x,t_0)$, we conclude that the evolution operator must satisfy the equation

$$\frac{d}{dt}\widehat{U}_{t_0}^{t} = -i\widehat{H}_t\widehat{U}_{t_0}^{t}, \tag{3.3}$$

with initial condition

$$\widehat{U}_{t_0}^{t_0} = \widehat{I}, \tag{3.4}$$

where $\widehat{I}$ is the identity operator. The solution of (3.3) can formally be written as [31]

$$\begin{aligned}\widehat{U}_{t_0}^{t} &= \widehat{I} + \int_{t_0}^{t} d\tau(-i\widehat{H}_\tau) + \int_{t_0}^{t} d\tau \int_{t_0}^{\tau} d\tau'(-i\widehat{H}_\tau)(-i\widehat{H}_{\tau'}) \\ &+ \int_{t_0}^{t} d\tau \int_{t_0}^{\tau} d\tau' \int_{t_0}^{\tau'} d\tau''(-i\widehat{H}_\tau)(-i\widehat{H}_{\tau'})(-i\widehat{H}_{\tau''}) + \ldots \\ &= \mathcal{T}\exp\left[\int_{t_0}^{t} d\tau(-i\widehat{H}_\tau)\right]\end{aligned} \tag{3.5}$$

where $\mathcal{T}$ is the time ordering operator. Therefore the solution of the Schrödinger equation is

$$\Psi(x,t) = \mathcal{T}\exp\left[\int_{t_0}^{t} d\tau(-i\widehat{H}_\tau)\right]\Psi(x,t_0). \tag{3.6}$$

The evolution operator $\widehat{U}_{t_0}^{t}$ has the following properties

$$\widehat{U}_{t_0}^{t} = \left(\widehat{U}_{t}^{t_0}\right)^{-1} \quad \text{(unitary)} \tag{3.7}$$

$$\widehat{U}_{t_0}^{t} = \widehat{U}_{t_1}^{t}\widehat{U}_{t_0}^{t_1} \quad \text{(group property)}. \tag{3.8}$$

Using the group property of the time evolution operator we can write

$$\Psi(t+\Delta t) = U_{t}^{t+\Delta t}\Psi(t) \tag{3.9}$$

$$\begin{aligned}\Psi(t+2\Delta t) &= U_{t}^{t+2\Delta t}\Psi(t) = U_{t+\Delta t}^{t+2\Delta t}U_{t}^{t+\Delta t}\Psi(t)\\ &= U_{t+\Delta t}^{t+2\Delta t}\Psi(t+\Delta t).\end{aligned} \tag{3.10}$$

From equations (3.9) and (3.10) we can see that we can propagate the solution of the Schrödinger equation, using the infinitesimal time evolution operator.

The solution of (2.26) contains an additional complication since the differential equation is inhomogeneous. Using the solution of the homogeneous Schrödinger equation that we just derived we try to find the formal solution of the inhomogeneous equation:

$$\frac{d}{dt}\chi(x,t) = -i\widehat{H}\chi(x,t) + f(x,t). \tag{3.11}$$

In analogy to (3.1) we suppose there is an "evolution" operator for $\chi$ as well, so that we can write:

$$\chi(x,t) = \widehat{W}_{t_0}^{t}\chi(x,t_0). \tag{3.12}$$

As in the case of the homogeneous equation we use this ansatz in (3.11) and obtain for the operator $\widehat{W}_{t_0}^{t}$ the equation:

$$\frac{d}{dt}\widehat{W}_{t_0}^{t} = -i\widehat{H}_t\widehat{W}_{t_0}^{t} + \widehat{A}_t, \tag{3.13}$$

with the initial condition:

$$\widehat{W}_{t_0}^{t_0} = \widehat{I}, \tag{3.14}$$

and $\widehat{A}_t = \widehat{I}\frac{f(x,t)}{\chi(x,t_0)}$, for $\chi(x,t_0) \neq 0$. The solution of equation (3.13), (see [32, 33]) is

$$\widehat{W}_{t_0}^{t} = \widehat{U}_{t_0}^{t} + \int_{t_0}^{t} d\tau\, \widehat{U}_{\tau}^{t}\widehat{A}_\tau. \tag{3.15}$$

To show this we make the ansatz

$$\widehat{W}_{t_0}^{t} = \widehat{U}_{t_0}^{t}\widehat{Z}_t. \tag{3.16}$$

The time derivative of $\widehat{W}^t_{t_0}$ then becomes

$$\frac{d}{dt}\widehat{W}^t_{t_0} = -i\widehat{H}_t\widehat{W}^t_{t_0} + \widehat{U}^t_{t_0}\frac{d}{dt}\widehat{Z}_t, \tag{3.17}$$

where we used (3.3) for the derivative of $\widehat{U}^t_{t_0}$. A comparison with equation (3.13) yields

$$\frac{d}{dt}\widehat{Z}_t = \left[\widehat{U}^t_{t_0}\right]^{-1}\widehat{A}_t. \tag{3.18}$$

Integration from $t_0$ to $t$ of the previous equation gives

$$\widehat{Z}_t - \widehat{Z}_{t_0} = \int_{t_0}^t d\tau \left[\widehat{U}^\tau_{t_0}\right]^{-1}\widehat{A}_\tau = \int_{t_0}^t d\tau \widehat{U}^{t_0}_\tau \widehat{A}_\tau, \tag{3.19}$$

where we used (3.7). From the initial conditions for $\widehat{U}^{t_0}_\tau$ and $\widehat{W}^t_{t_0}$ we can conclude that $\widehat{Z}_{t_0} = \widehat{I}$. Therefore we get

$$\widehat{Z}_t = \widehat{I} + \int_{t_0}^t d\tau \widehat{U}^{t_0}_\tau \widehat{A}_\tau. \tag{3.20}$$

We insert this expression in (3.16) and obtain

$$\widehat{W}^t_{t_0} = \widehat{U}^t_{t_0} + \int_{t_0}^t d\tau \underbrace{\widehat{U}^t_{t_0}\widehat{U}^{t_0}_\tau}_{\widehat{U}^t_\tau}\widehat{A}_\tau. \tag{3.21}$$

If we study the properties of this operator we see that it does not have the group property

$$\begin{aligned}
\widehat{W}^t_{t_1}\widehat{W}^{t_1}_{t_0} &= \left(\widehat{U}^t_{t_1} + \int_{t_1}^t d\tau\, \widehat{U}^t_\tau\widehat{A}_\tau\right)\left(\widehat{U}^{t_1}_{t_0} + \int_{t_0}^{t_1} d\tau\, \widehat{U}^{t_1}_\tau\widehat{A}_\tau\right) \\
&= \underbrace{\widehat{U}^t_{t_1}\widehat{U}^{t_1}_{t_0}}_{\widehat{U}^t_{t_0}} + \widehat{U}^t_{t_1}\int_{t_0}^{t_1} d\tau\, \widehat{U}^{t_1}_\tau\widehat{A}_\tau + \int_{t_1}^t d\tau\, \widehat{U}^t_\tau\widehat{A}_\tau\widehat{U}^{t_1}_{t_0} + \int_{t_1}^t d\tau\, \widehat{U}^t_\tau\widehat{A}_\tau\int_{t_0}^{t_1} d\tau'\, \widehat{U}^{t_1}_{\tau'}\widehat{A}_{\tau'} \\
&= \widehat{U}^t_{t_0} + \int_{t_0}^{t_1} d\tau\, \underbrace{\widehat{U}^t_{t_1}\widehat{U}^{t_1}_\tau}_{\widehat{U}^t_\tau}\widehat{A}_\tau + \int_{t_1}^t d\tau\, \widehat{U}^t_\tau\widehat{A}_\tau + \int_{t_1}^t d\tau\, \widehat{U}^t_\tau\widehat{A}_\tau\left(\widehat{U}^{t_1}_{t_0} - \widehat{I} + \int_{t_0}^{t_1} d\tau'\, \widehat{U}^{t_1}_{\tau'}\widehat{A}_{\tau'}\right) \\
&= \widehat{W}^t_{t_0} + \int_{t_1}^t d\tau\, \widehat{U}^t_\tau\widehat{A}_\tau\left(\widehat{W}^{t_1}_{t_0} - \widehat{I}\right) \\
&\neq \widehat{W}^t_{t_0}
\end{aligned} \tag{3.22}$$

therefore it cannot be used as the infinitesimal evolution operator of the inhomogeneous equation to propagate $\chi$. But using equations (3.12) and (3.15) we can write the formal solution of the inhomogeneous equation

$$\begin{aligned}
\chi(x,t) &= \widehat{W}^t_{t_0}\chi(x,t_0) = \left(\widehat{U}^t_{t_0} + \int_{t_0}^t d\tau\, \widehat{U}^t_\tau\widehat{A}_\tau\right)\chi(x,t_0) \\
&= \widehat{U}^t_{t_0}\chi(x,t_0) + \int_{t_0}^t d\tau\, \widehat{U}^t_\tau\widehat{I}\frac{f(x,\tau)}{\chi(x,t_0)}\chi(x,t_0) \\
&= \underbrace{\widehat{U}^t_{t_0}\chi(x,t_0)}_{\chi_{hom}} + \underbrace{\int_{t_0}^t d\tau\, \widehat{U}^t_\tau f(x,\tau)}_{\chi_{inh}}.
\end{aligned} \tag{3.23}$$

We observe, by simply inserting this solution in the inhomogeneous Schrödinger equation and using equation (3.3), that it satisfies equation (3.11) also for the case $\chi(x,t_0)=0$. As expected, the solution is the sum of the general solution of the homogeneous equation $\chi_{hom}$ and a particular solution of the inhomogeneous one $\chi_{inh}$. The inhomogeneous solution has the initial condition $\chi_{inh}(x,t_0)=0$ and is independent of the initial state.

Now we show that it is possible to calculate $\chi(x,t+\Delta t)$ using $\chi(x,t)$, even if the operator $\widehat{W}_{t_0}^{t}$ does not have the group property. We use the solution (3.23)

$$\begin{aligned}
\chi_{inh}(x,t+\Delta t) &= \int_{t_0}^{t+\Delta t} d\tau\, \widehat{U}_{\tau}^{t+\Delta t} f(x,\tau) = \int_{t_0}^{t} d\tau\, \widehat{U}_{\tau}^{t+\Delta t} f(x,\tau) + \int_{t}^{t+\Delta t} d\tau\, \widehat{U}_{\tau}^{t+\Delta t} f(x,\tau) \\
&= \widehat{U}_{t}^{t+\Delta t}\left(\int_{t_0}^{t} d\tau\, \widehat{U}_{\tau}^{t} f(x,\tau) + \int_{t}^{t+\Delta t} d\tau\, \widehat{U}_{\tau}^{t} f(x,\tau)\right) \\
&= \widehat{U}_{t}^{t+\Delta t}\left(\chi_{inh}(x,t) + \int_{t}^{t+\Delta t} d\tau\, \widehat{U}_{\tau}^{t} f(x,\tau)\right). \qquad (3.24)
\end{aligned}$$

For the homogeneous part of the solution we have:

$$\chi_{hom}(x,t+\Delta t) = \widehat{U}_{t}^{t+\Delta t}\chi_{hom}(x,t). \qquad (3.25)$$

Adding the two components we obtain for $\chi$:

$$\chi(x,t+\Delta t) = \widehat{U}_{t}^{t+\Delta t}\left(\chi(x,t) + \int_{t}^{t+\Delta t} d\tau\, \widehat{U}_{\tau}^{t} f(x,\tau)\right). \qquad (3.26)$$

As we see, even if the operator $\widehat{W}_{t_0}^{t}$ does not have the group property, we can propagate the Lagrange multiplier in a manner similar to the propagation of the wave function.

In practice, to propagate the solution of the Schrödinger equation, we need an approximation for the infinitesimal time evolution operator $\widehat{U}_{t}^{t+\Delta t}$. This will be discussed in chapters 5 and 6. It is crucial that for the approximation of $\widehat{U}_{t}^{t+\Delta t}$ we only need to know the time-dependent field $\epsilon$ at time $t$.

## 3.2 Analytical solution for a simple inhomogeneity

One method to test equation (3.23) is to compare the numerical and the analytical solution of (3.11). For a particular type of inhomogeneity, $f(x,t)=\widetilde{f}(t)\Psi(x,t)$, if one knows the solution of the homogeneous equation

$$\frac{\partial}{\partial t}\Psi(x,t) = -i\widehat{H}\Psi(x,t), \qquad (3.27)$$

one can find the analytical solution of the inhomogeneous equation

$$\frac{\partial}{\partial t}\chi(x,t) = -i\widehat{H}\chi(x,t) + \widetilde{f}(t)\Psi(x,t). \qquad (3.28)$$

We make the ansatz $\chi(x,t)=\Psi(x,t)c(t)$ for $\chi(x,t)$ in equation (3.28). This leads to the following equation for $c(t)$:

$$c(t)\frac{\partial}{\partial t}\Psi(x,t) + \Psi(x,t)\frac{\partial}{\partial t}c(t) = c(t)\left(-i\widehat{H}\right)\Psi(x,t) + \widetilde{f}(t)\Psi(x,t). \qquad (3.29)$$

Using equation (3.27) for $\Psi(x,t)$ this reduces to

$$\Psi(x,t)\frac{\partial}{\partial t}c(t) = \widetilde{f}(t)\Psi(x,t), \tag{3.30}$$

from which we can conclude that

$$\frac{\partial}{\partial t}c(t) = \widetilde{f}(t). \tag{3.31}$$

Integration of equation (3.31) finally results in

$$c(t) = \int_{t_0}^{t} d\tau\, \widetilde{f}(\tau) + c_{t_0}. \tag{3.32}$$

If one knows the homogeneous solution $\Psi$, then the solution for $\chi$ is

$$\chi(x,t) = \Psi(x,t)\left(\int_{t_0}^{t} d\tau\, \widetilde{f}(\tau) + c_{t_0}\right). \tag{3.33}$$

The constant $c_{t_0}$ is determined from the initial condition for $\chi(x,t)$

$$\chi(x,t_0) = \Psi(x,t_0)c_{t_0}. \tag{3.34}$$

Therefore, we know the solution of the inhomogeneous equation (3.28) once we have solved the homogeneous Schrödinger equation (3.27). Two examples of systems where one can solve the homogeneous Schrödinger equation exactly are given in Appendix D.

# Chapter 4

# Iterative algorithm for the solution of the optimal control equations

We have to solve the system of coupled differential equations

$$\left(i\partial_t - \widehat{H}\right)\chi(x,t) = -\frac{i}{T}\widehat{O}_t^{(1)}\Psi(x,t), \tag{4.1}$$

$$\chi(x,T) = \widehat{O}_T^{(2)}\Psi(x,T), \tag{4.2}$$

$$\left(i\partial_t - \widehat{H}\right)\Psi(x,t) = 0, \tag{4.3}$$

$$\Psi(x,0) = \phi(x), \tag{4.4}$$

$$E(t) = -\frac{1}{\alpha}\Im\langle\chi(t)|\hat{\mu}|\Psi(t)\rangle, \tag{4.5}$$

In the previous chapter we have shown that one can construct the solution of (4.1) and (4.3) step by step, but for this one needs a starting point. We can propagate (4.3) forward, taking as starting point $\Psi(x,0)$, where the wave function is analytically known (see (4.4)), and (4.1) backward, taking as starting point $\chi(x,T)$ according to equation (4.2). To solve the equation for the Lagrange multiplier $\chi$ we need the field $E(t)$ and also the wave function $\Psi(x,t), \forall t \in [0,T]$, due to the inhomogeneity. Furthermore, the field $E(t)$ , which we need for the propagation of $\Psi$ and $\chi$, itself depends on $\Psi$ and $\chi$ via equation (4.5). In conclusion, we cannot solve these three equations with only one propagation, so that we need an iterative scheme.

The purpose of this chapter is to show how one can deal with the coupling of the equations. We assume that we can determine the exact solution of the Schrödinger equation (homogeneous and inhomogeneous) for every time, once $E(t)$ is given for *all* times and the boundary conditions $\Psi(x,0)$ and $\chi(x,T)$ are known. Methods to approximate the infinitesimal time evolution operator will be discussed separately for the two systems studied in this thesis (two level atom and 1D hydrogen). For now, we suppose we can solve equations (4.1) and (4.3) exactly.

In the first section we present an iteration algorithm similar to the one used in [19] and [20]. Then we show that this iteration must converge to a local maximum of the functional $\mathcal{L}$ (2.11). In the last part of this chapter we discuss a more general form of $\mathcal{L}$ and the convergence of the algorithm for this generalized functional.

## 4.1 Iterative scheme

Schematically, we can represent the iteration as follows

$$\text{Step} \quad 0. \quad \boldsymbol{\Psi_1(0)} \xrightarrow{E_1} \Psi_1(T) \tag{4.6}$$

$$\text{Step} \quad k. \quad \boldsymbol{\chi_k(T)} \xrightarrow{\widetilde{E}_k,\, \Psi_k} \chi_k(0) \tag{4.7}$$

$$\boldsymbol{\Psi_{k+1}(0)} \xrightarrow{E_{k+1}} \Psi_{k+1}(T) \tag{4.8}$$

We start with an initial guess field $E_1(t)$ and propagate the solution of (4.3) starting with the initial condition (4.4). $\chi$ is known at $T$, therefore we start to propagate the solution of (4.1) backwards using the initial condition (4.2), $\Psi(x,t)$ calculated in the previous step and the new field $\widetilde{E}_k(t)$. (4.7) is equivalent to solving

$$\left(i\partial_t - \widetilde{H}_k\right)\chi_k(x,t) = -\frac{i}{T}\widehat{O}_t^{(1)}\Psi_k(x,t), \tag{4.9}$$

$$\chi_k(x,T) = \widehat{O}_T^{(2)}\Psi_k(x,T). \tag{4.10}$$

where

$$\widetilde{H}_k = \widehat{H}_0 - \hat{\mu}\widetilde{E}_k(t), \tag{4.11}$$

$$\widetilde{E}_k(t) = (1-\eta)E_k(t) - \frac{\eta}{\alpha}\Im\langle\chi_k(t)|\hat{\mu}|\Psi_k(t)\rangle \tag{4.12}$$

and $\widehat{H}_0$ is the field-free Hamiltonian. Here we have again a self-consistency problem in the sense that $\chi_k$ depends on $\widetilde{E}_k$ and the field $\widetilde{E}_k$ depends on the Lagrange multiplier $\chi_k$.

In the chapters 5 and 6 we give a method to approximate the infinitesimal time evolution operator needed in equation (3.26). In this approximation to calculate $\widehat{U}_t^{t-\Delta t}$ we need to know the field $\widetilde{E}_k$ only at time $t$. Therefore we can propagate $\chi_k$ and at the same time calculate the field needed for the propagation.

$$\begin{array}{ccc} \chi_k(x,t) & \xrightarrow{(b)} & \chi_k(x,t-\Delta t) \\ (a)\searrow & & \nearrow(b') \\ & \widetilde{E}_k(t) & \end{array} \tag{4.13}$$

For $(a)$ we use equation (4.12) and for $(b)$ and $(b')$ we use (3.26). The method is called immediate feedback [16]. Nevertheless, for the rest of the proof we assume that we can solve the Schrödiger equation (4.9) with the field given in (4.12) exactly.

We propagate $\Psi_{k+1}$ forward and at the same time calculate the field needed for propagation. (4.8) is equivalent to solving

$$\left(i\partial_t - \widehat{H}_{k+1}\right)\Psi_{k+1}(x,t) = 0, \tag{4.14}$$

$$\Psi_{k+1}(x,0) = \phi(x). \tag{4.15}$$

where $phi(x)$ is the initial state wave-function of the quantum mechanical system and

$$\widehat{H}_{k+1} = \widehat{H}_0 - \hat{\mu}E_{k+1}(t), \tag{4.16}$$

$$E_{k+1}(t) = (1-\gamma)\widetilde{E}_k(t) - \frac{\gamma}{\alpha}\Im\langle\chi_k(t)|\hat{\mu}|\Psi_{k+1}(t)\rangle \tag{4.17}$$

In writing the equations for the field (4.12) and (4.17) we follow [20]. Similar to [20] we will see in the next section that for our proof of convergence it is necessary that both parameters $\gamma$ and $\eta$ have values in interval $[0, 2]$.

For the proof of convergence we assume that we can solve equations (4.14) and (4.17) exactly, in one propagation. In practice we use immediate feedback.

## 4.2 Proof of convergence for the iterative scheme

For the iteration described in the previous section we will now demonstrate that in every iteration step the functional must increase its value. This is an important feature because the control equations are compatible not only with a maximum but also with a minimum of the functional. Since the Lagrange functional has an upper bound, namely the value 1 for the case that $\widehat{O}^{(1)}$ is a projection operator on a time dependent wave-function or $\delta(x - r(t))$, this implies that the algorithm converges to a solution of the system of coupled differential equations. The solution corresponds thus to a local maximum. Depending on the initial guess for the field, the iteration can end in different local maxima.

In each iteration step we solve (2.26) and (2.28) therefore, the value of the functional $J_3$ is zero. The difference in $\mathcal{L}$ between iteration step $k + 1$ and $k$ is thus

$$\delta\mathcal{L}_{k+1,k} = J_1[\Psi_{k+1}] + J_2[\Psi_{k+1}] - J_1[\Psi_k] - J_2[\Psi_k]. \tag{4.18}$$

Using for $J_1$ and $J_2$ the expressions (2.6) and (2.9) we obtain

$$\begin{aligned}\delta\mathcal{L}_{k+1,k} &= \int_0^T dt\Big(\frac{1}{T}\langle\Psi_{k+1}(t)|\widehat{O}_t|\Psi_{k+1}(t)\rangle - \frac{1}{T}\langle\Psi_k(t)|\widehat{O}_t|\Psi_k(t)\rangle \\ &- \alpha\left(E_{k+1}^2(t) - E_k^2(t)\right)\Big).\end{aligned} \tag{4.19}$$

With the short-hand notation $\delta\Psi_{k+1,k}(x,t) = \Psi_{k+1}(x,t) - \Psi_k(x,t)$ we can rewrite equation (4.19) as

$$\begin{aligned}\delta\mathcal{L}_{k+1,k} &= \int_0^T dt\Big(\frac{1}{T}\langle\Psi_k(t)|\widehat{O}_t|\delta\Psi_{k+1,k}(t)\rangle + \frac{1}{T}\langle\delta\Psi_{k+1,k}(t)|\widehat{O}_t|\Psi_k(t)\rangle \\ &+ \frac{1}{T}\langle\delta\Psi_{k+1,k}(t)|\widehat{O}_t|\delta\Psi_{k+1,k}(t)\rangle - \alpha\left(E_{k+1}^2(t) - E_k^2(t)\right)\Big) \\ &= \int_0^T dt\Big(\frac{1}{T}2\Re\langle\Psi_k(t)|\widehat{O}_t|\delta\Psi_{k+1,k}(t)\rangle \\ &+ \frac{1}{T}\langle\delta\Psi_{k+1,k}(t)|\widehat{O}_t|\delta\Psi_{k+1,k}(t)\rangle - \alpha\left(E_{k+1}^2(t) - E_k^2(t)\right)\Big).\end{aligned} \tag{4.20}$$

We define

$$A_{k+1,k} := \int_0^T dt\ \frac{1}{T}\langle\delta\Psi_{k+1,k}(t)|\widehat{O}_t|\delta\Psi_{k+1,k}(t)\rangle \geq 0, \tag{4.21}$$

which follows from the fact that $\widehat{O}_t$ is positive semi-definite. $A_{k+1,k}$ is the first contribution to $\delta\mathcal{L}_{k+1,k}$ that can only be positive or zero. We write the difference in $\mathcal{L}$ as

$$\begin{aligned}\delta\mathcal{L}_{k+1,k} &= A_{k+1,k} + \int_0^T dt\Big(\frac{1}{T}2\Re\langle\Psi_k(t)|\widehat{O}_t|\delta\Psi_{k+1,k}(t)\rangle \\ &- \alpha\left(E_{k+1}^2(t) - E_k^2(t)\right)\Big).\end{aligned} \tag{4.22}$$

Now we want to transform the first term of the integrand. First we use the hermiticity of $\widehat{O}$ and bring the operator to the other side. After that we use equations (4.9) and (4.10) to obtain

$$\begin{aligned}\int_0^T dt\frac{1}{T}\langle\Psi_k(t)|\widehat{O}_t|\delta\Psi_{k+1,k}(t)\rangle &= \int_0^T dt\frac{1}{T}\langle\widehat{O}_t\Psi_k(t)|\delta\Psi_{k+1,k}(t)\rangle \\ &= \int_0^T dt\frac{1}{T}\langle\widehat{O}_t^{(1)}\Psi_k(t)|\delta\Psi_{k+1,k}(t)\rangle + \langle\widehat{O}_T^{(2)}\Psi_k(T)|\delta\Psi_{k+1,k}(T)\rangle \\ &= \int_0^T dt\langle i\left(i\partial_t - \widetilde{H}_k\right)\chi_k(t)|\delta\Psi_{k+1,k}(t)\rangle \\ &+ \langle\chi(T)|\delta\Psi_{k+1,k}(T)\rangle. \end{aligned} \tag{4.23}$$

Making a partial integration and using the hermiticity of $\widetilde{H}_k$ we can transform the first term on the right-hand side into

$$\begin{aligned}-i\int_0^T dt\langle\left(i\partial_t - \widetilde{H}_k\right)\chi_k(t)|\delta\Psi_{k+1,k}(t)\rangle &= -i\int_0^T dt\langle\chi_k(t)|\left(i\partial_t - \widetilde{H}_k\right)\delta\Psi_{k+1,k}(t)\rangle - \\ &- \underbrace{\langle\chi_k(t)|\delta\Psi_{k+1,k}(t)\rangle|_0^T}_{\langle\chi_k(T)|\delta\Psi_{k+1,k}(T)\rangle}. \end{aligned} \tag{4.24}$$

Here we used the fact that, due the initial condition $\Psi_k(x,0) = \Psi_{k+1}(x,0) = \phi(x)$, only the boundary term at $T$ contributes. In equation (4.23) we only have the real part of equation (4.24). Using $\Re(-i(a+ib)) = b = \Im(a+ib)$ we can rewrite the first part of the integrand in (4.23) as

$$\begin{aligned}\int_0^T dt2\Re\langle\Psi_k(t)|\widehat{O}_t|\delta\Psi_{k+1,k}(t)\rangle &= \int_0^T dt2\Re\left(-i\langle\chi_k(t)|\left(i\partial_t - \widetilde{H}_k\right)\delta\Psi_{k+1,k}(t)\rangle\right) \\ &\quad \underbrace{-2\Re\langle\chi_k(T)|\delta\Psi_{k+1,k}(T)\rangle + 2\Re\langle\chi_k(T)|\delta\Psi_{k+1,k}(T)\rangle}_{0} \\ &= \int_0^T dt2\Im\left(\langle\chi_k(t)|\left(i\partial_t - \widetilde{H}_k\right)\delta\Psi_{k+1,k}(t)\rangle\right). \end{aligned} \tag{4.25}$$

The remaining boundary term and a similar one coming from $\widehat{O}_2$ cancel each other. Plugging the results above into $\delta\mathcal{L}_{k+1,k}$ yields

$$\begin{aligned}\delta\mathcal{L}_{k+1,k} &= A_{k,k+1} + \int_0^T dt\Big(-\alpha\left(E_{k+1}^2(t) - E_k^2(t)\right) \\ &+ 2\Im\langle\chi_k(t)|\left(i\partial_t - \widetilde{H}_k\right)\delta\Psi_{k+1,k}(t)\rangle\Big). \end{aligned} \tag{4.26}$$

In the next step we use the Schrödinger equation (4.14) for $k$ and $k+1$ and we replace the terms $i\partial_t\Psi_j(x,t)$ by $\widehat{H}_j\Psi_j(x,t)$, $j = k, k+1$

$$\left(i\partial_t - \widetilde{H}_k\right)\delta\Psi_{k+1,k}(x,t) = \left(i\partial_t - \widetilde{H}_k\right)(\Psi_{k+1}(x,t) - \Psi_k(x,t)) = \tag{4.27}$$

$$\begin{aligned} &= \left(\widehat{H}_{k+1} - \widetilde{H}_k\right)\Psi_{k+1}(x,t) - \left(\widehat{H}_k - \widetilde{H}_k\right)\Psi_k(x,t) = \\ &= -\left(E_{k+1}(t) - \widetilde{E}_k(t)\right)\hat{\mu}(x)\Psi_{k+1}(x,t) \\ &+ \left(E_k(t) - \widetilde{E}_k(t)\right)\hat{\mu}(x)\Psi_k(x,t). \end{aligned} \tag{4.28}$$

As we can see from equations (4.11) and (4.16) the Hamilton operators above differ only in the term $\hat{\mu}E(t)$, so that the difference reduces to a difference of the electric fields. Consequently, the change in the Lagrange functional becomes

$$\begin{aligned}\delta\mathcal{L}_{k+1,k} &= A_{k,k+1} + \int_0^T dt\Big( - \alpha\left(E_{k+1}^2(t) - E_k^2(t)\right) \\ &- 2\Im\langle\chi_k(t)|\hat{\mu}|\Psi_{k+1}(t)\rangle(E_{k+1}(t) - \widetilde{E}_k(t)) \\ &+ 2\Im\langle\chi_k(t)|\hat{\mu}|\Psi_k(t)\rangle(E_k(t) - \widetilde{E}_k(t))\Big). \end{aligned} \tag{4.29}$$

In order to replace the imaginary parts in equation (4.29) we transform equations (4.12) and (4.17) into

$$\Im\langle\chi_k|\hat{\mu}|\Psi_{k+1}\rangle = -\left(E_{k+1} - (1-\gamma)\widetilde{E}_k\right)\frac{\alpha}{\gamma}, \tag{4.30}$$

$$\Im\langle\chi_k|\hat{\mu}|\Psi_k\rangle = -\left(\widetilde{E}_k - (1-\eta)E_k\right)\frac{\alpha}{\eta}, \tag{4.31}$$

and, after regrouping the terms we obtain the final expression for the difference between the Lagrange functional in two consecutive iteration steps

$$\begin{aligned}\delta\mathcal{L}_{k+1,k} &= A_{k,k+1} + \int_0^T dt\,\alpha\Big[(E_k(t) - \widetilde{E}_k(t))^2\left(\frac{2}{\eta} - 1\right) \\ &+ (E_{k+1}(t) - \widetilde{E}_k(t))^2\left(\frac{2}{\gamma} - 1\right)\Big]. \end{aligned} \tag{4.32}$$

As we can see all terms in equation(4.32) are either zero or positive under the conditions that $0 \leq \gamma \leq 2$, $0 \leq \eta \leq 2$ and $\alpha \geq 0$. As in ref. [19] this iteration converges monotonically and quadratically in terms of the field deviations between two iterations. In this case we made a couple of assumptions.

1. The proof holds true only if both the homogeneous and the inhomogeneous Schrödinger equations (2.28) and (2.26) are solved exactly in each time step. Therefore one expects the method to be sensitive to numerical errors. For the effect of numerical errors see Appendix F.

2. $\alpha$ is hold constant during the iteration. If one tries to change its value between two iterations, it is not possible to construct the squared deviations of the field and the proof given here breaks down. $\alpha$ can also be a time dependent positive function (see ref. [34])

3. Since the method is not a global one, the convergence is guaranteed only to a local maximum. Therefore the calculations should be repeated with different initial guesses for the field. Since we know the upper bound of the functional for some operators, the quality of the maximum can be judged directly.

## 4.3 Proof of convergence for a more general functional

In this section we generalize the proof of convergence given in section (4.2) to functionals of the form

$$J_1 = \frac{1}{T}\int_0^T dt\,\langle\Psi(t)|\widehat{O}_t^{(1)}|\Psi(t)\rangle^n + \langle\Psi(T)|\widehat{O}^{(2)}|\Psi(T)\rangle$$

where $n > 1$, $n \in \mathbb{N}$. The operator is still positive definite. Note that the term depending only on $\Psi(T)$ remains unchanged. Again, the operators $\widehat{O}_t^{(1)}$ and $\widehat{O}^{(2)}$ are assumed to be hermitian and positive semidefinite. The equation for the Lagrange multiplier then has the form

$$(i\partial_t - H)\chi(x,t) = -\frac{1}{T} n i \langle \Psi(t)|\widehat{O}_t^{(1)}|\Psi(t)\rangle^{n-1} \widehat{O}_t^{(1)} \Psi(x,t) \tag{4.33}$$

$$\chi(x,T) = \widehat{O}^{(2)} \Psi(x,T) \tag{4.34}$$

We start by calculating the difference $\delta\mathcal{L}_{k+1,k}$

$$\begin{aligned} \delta\mathcal{L}_{k+1,k} &= \int_0^T dt \left( \frac{1}{T} \underbrace{\langle \Psi_{k+1}(t)|\widehat{O}_t^{(1)}|\Psi_{k+1}(t)\rangle^n}_{a^n} - \frac{1}{T} \underbrace{\langle \Psi_k(t)|\widehat{O}_t^{(1)}|\Psi_k(t)\rangle^n}_{b^n} \right. \\ &+ \left. \alpha \left[E_k(t)\right]^2 - \alpha \left[E_{k+1}(t)\right]^2 \right) \\ &+ \langle \Psi_{k+1}(T)|\widehat{O}^{(2)}|\Psi_{k+1}(T)\rangle - \langle \Psi_k(T)|\widehat{O}^{(2)}|\Psi_k(T)\rangle. \end{aligned} \tag{4.35}$$

Since the operator $\widehat{O}^{(1)}$ is positive semi-definite and hermitian the expectation values $\langle \Psi_{k+1}(t)|\widehat{O}_t^{(1)}|\Psi_{k+1}(t)\rangle$ and $\langle \Psi_k(t)|\widehat{O}_t^{(1)}|\Psi_k(t)\rangle$ are two real positive numbers. We rename $a(t) = \langle \Psi_{k+1}(t)|\widehat{O}_t^{(1)}|\Psi_{k+1}(t)\rangle$ and $b(t) = \langle \Psi_k(t)|\widehat{O}_t^{(1)}|\Psi_k(t)\rangle$ and, using

$$a^n - b^n = n b^{n-1}(a-b) + a^n + (n-1)b^n - n b^{n-1} a, \tag{4.36}$$

we obtain

$$\begin{aligned} \delta\mathcal{L}_{k+1,k} &= \int_0^T dt \left( A(t) + \alpha \left[E_k(t)\right]^2 - \alpha \left[E_{k+1}(t)\right]^2 \right. \\ &+ n \frac{1}{T} \langle \Psi_k(t)|\widehat{O}_t^{(1)}|\Psi_k(t)\rangle^{n-1} \\ &\times \left. \left( \langle \Psi_{k+1}(t)|\widehat{O}_t^{(1)}|\Psi_{k+1}(t)\rangle - \langle \Psi_k(t)|\widehat{O}_t^{(1)}|\Psi_k(t)\rangle \right) \right) \\ &+ \langle \Psi_{k+1}(T)|\widehat{O}^{(2)}|\Psi_{k+1}(T)\rangle - \langle \Psi_k(T)|\widehat{O}^{(2)}|\Psi_k(T)\rangle \end{aligned} \tag{4.37}$$

with

$$A(t) = a^n(t) + (n-1)b^n(t) - n b^{n-1}(t) a(t). \tag{4.38}$$

One can show (see Appendix G) that $A(t)$ is positive or zero. Therefore, we have separated the first positive contribution in $\delta\mathcal{L}_{k+1,k}$ and can now transform the difference $\langle \Psi_{k+1}(t)|\widehat{O}^{(j)}|\Psi_{k+1}(t)\rangle -$

$\langle\Psi_k(t)|\widehat{O}^{(j)}|\Psi_k(t)\rangle$, $j=1,2$ as in the last section. We can rewrite equation (4.37) as

$$\begin{aligned}
\delta\mathcal{L}_{k+1,k} &= \int_0^T dt\,\Big(A(t)+\alpha\,[E_k(t)]^2-\alpha\,[E_{k+1}(t)]^2 \\
&+ n\langle\Psi_k(t)|\widehat{O}_t^{(1)}|\Psi_k(t)\rangle^{n-1}\Big(\langle\delta\Psi_{k+1,k}(t)|\widehat{O}_t^{(1)}|\delta\Psi_{k+1,k}(t)\rangle \\
&+ 2\Re\langle\Psi_k(t)|\widehat{O}_t^{(1)}|\delta\Psi_{k+1,k}(t)\rangle\Big) \\
&+ \langle\delta\Psi_{k+1,k}(T)|\widehat{O}^{(2)}|\delta\Psi_{k+1,k}(T)\rangle+2\Re\langle\Psi_k(T)|\widehat{O}^{(2)}|\delta\Psi_{k+1,k}(T)\rangle \qquad (4.39)\\
\delta\mathcal{L}_{k+1,k} &= C+\int_0^T dt\,\Big(A(t)+B(t)+\alpha\,[E_k(t)]^2-\alpha\,[E_{k+1}(t)]^2 \\
&+ n\langle\Psi_k(t)|\widehat{O}_t^{(1)}|\Psi_k(t)\rangle^{n-1}2\Re\langle\Psi_k(t)|\widehat{O}_t^{(1)}|\delta\Psi_{k+1,k}(t)\rangle\Big) \\
&+ 2\Re\langle\Psi_k(T)|\widehat{O}^{(2)}|\delta\Psi_{k+1,k}(T)\rangle \qquad (4.40)
\end{aligned}$$

where

$$\begin{aligned}
B(t) &= n\langle\Psi_k(t)|\widehat{O}_t^{(1)}|\Psi_k(t)\rangle^{n-1}\langle\delta\Psi_{k+1,k}(t)|\widehat{O}_t^{(1)}|\delta\Psi_{k+1,k}(t)\rangle\geq 0 \qquad (4.41)\\
C &= \langle\delta\Psi_{k+1,k}(T)|\widehat{O}^{(2)}|\delta\Psi_{k+1,k}(T)\rangle\geq 0 \qquad (4.42)
\end{aligned}$$

The remaining terms $n\langle\Psi_k(t)|\widehat{O}_t^{(1)}|\Psi_k(t)\rangle^{n-1}2\Re\langle\Psi_k(t)|\widehat{O}_t^{(1)}|\delta\Psi_{k+1,k}(t)\rangle$ and $2\Re\langle\Psi_k(T)|\widehat{O}^{(2)}|\delta\Psi_{k+1,k}(T)\rangle$ can be transformed using the inhomogeneous Schrödinger equation (4.33) with initial condition (4.34) for $\chi$ which yields

$$\begin{aligned}
\delta\mathcal{L}_{k+1,k} &= C+\int_0^T dt\,\Big(A(t)+B(t)+\alpha\,[E_k(t)]^2-\alpha\,[E_{k+1}(t)]^2 \\
&+ 2\Re\langle-\left(\partial_t+i\widetilde{H}_k\right)\chi(t)|\delta\Psi_{k+1,k}(t)\rangle\Big)+2\Re\langle\chi_k(T)|\delta\Psi_{k+1,k}(T)\rangle. \qquad (4.43)
\end{aligned}$$

Partial integration results in

$$\begin{aligned}
\delta\mathcal{L}_{k+1,k} &= C+\int_0^T dt\,\Big(A(t)+B(t)+\alpha\,[E_k(t)]^2-\alpha\,[E_{k+1}(t)]^2 \\
&+ 2\Re\langle\chi(t)|\left(\partial_t+i\widetilde{H}_k\right)|\delta\Psi_{k+1,k}(t)\rangle\Big) \\
&- 2\Re\langle\chi(t)|\delta\Psi_{k+1,k}(t)\rangle|_0^T+2\Re\langle\chi(T)|\delta\Psi_{k+1,k}(T)\rangle \qquad (4.44)
\end{aligned}$$

$\delta\Psi_{k+1,k}(x,0)=0$ since the initial state for the wave function is fixed, so that only the boundary term at T contributes. Therefore the last two terms cancel each other and we have

$$\begin{aligned}
\delta\mathcal{L}_{k+1,k} &= C+\int_0^T dt\,\Big(A(t)+B(t)+\alpha\,[E_k(t)]^2-\alpha\,[E_{k+1}(t)]^2 \\
&+ 2\Re\langle\chi(t)|\left(\partial_t+i\widetilde{H}_k\right)|\delta\Psi_{k+1,k}(t)\rangle\Big) \qquad (4.45)
\end{aligned}$$

(4.45) is similar to (4.26) and the proof of convergence from this point on is identical to the proof in the previous section. In the end one obtains expression (4.32) where $A_{k+1,k}$ is replaced by $C+\int_0^t dt(A(t)+B(t))$.

# Chapter 5

# Time dependent optimal control of a two-level system

As a first application of the optimization algorithm presented in the previous chapters we consider a two-level atom. Although no such atom exists, many interactions with electromagnetic fields involve only two of the levels of an atom. The two-level system has many applications in physics from spin models, to the micro-maser [35] and quantum computers [36]. In the so-called rotating wave approximation (RWA) see ref. [37, 38] and appendix E the Schrödinger equation may be solved exactly.

In this chapter we use the two level system to test the algorithm presented in chapter 4. We discuss the role of the penalty factor $\alpha$ and also give an practical implementation of the scheme suggested in section 2.2.5. As the positive semi-definite operator of chapter 2 we here choose a projection operator onto the two eigenstates, which may be used to define time-dependent occupation numbers. We then give the time evolution of these occupation numbers and let the algorithm find the optimal pulse which drives the system along this trajectory.

Using RWA we can calculate the time dependence of the occupation numbers of the two levels for a given laser field. In this chapter we address the inverse question of what shape does the external field have, in order to obtain a certain time evolution of the population of the two levels. As a last example we suggest a method to control the time dependent dipole moment.

## 5.1 Control equations for the two-level system

The field-free Hamilton operator of a two level system has only two eigenstates: $|0\rangle$ and $|1\rangle$. The corresponding energies are $\omega_0$ and $\omega_1$. Therefore, one can express every wave function as $\Psi(t) = \Psi_0(t)|0\rangle + \Psi_1(t)|1\rangle$. Thus also the function

$$\partial_t \Psi(t) + i\widehat{H}\Psi(t) \tag{5.1}$$

consists only in a linear combination of the eigenstates of the field-free Hamiltonian. Since in the functional $J_3$ we have the scalar product of the Lagrange multiplier $\chi$ with a function from the vector space of the two states $|0\rangle$ and $|1\rangle$, it follows that only the projection of $\chi$ onto this space is relevant. Therefore we can define $\chi$ also as a linear combination of the states $|0\rangle$ and $|1\rangle$: $\chi(t) = \chi_0(t)|0\rangle + \chi_1(t)|1\rangle$. The Hamiltonian with laser field can be represented as a

2×2 matrix [37]

$$\widehat{H} = \widehat{H}_0 - \hat{\mu}E(t) = \begin{pmatrix} \omega_0 - E(t)\mu_{00} & -E(t)\mu_{01} \\ -E(t)\mu_{10} & \omega_1 - E(t)\mu_{11} \end{pmatrix}, \tag{5.2}$$

where $\mu_{ij} = \langle i|\hat{\mu}|j\rangle$ is the dipole matrix element. The optimal control equations (2.26)-(2.30) are

$$\frac{d}{dt}\begin{pmatrix} \chi_0(t) \\ \chi_1(t) \end{pmatrix} = -i\begin{pmatrix} \omega_0 - E(t)\mu_{00} & -E(t)\mu_{01} \\ -E(t)\mu_{10} & \omega_1 - E(t)\mu_{11} \end{pmatrix}\begin{pmatrix} \chi_0(t) \\ \chi_1(t) \end{pmatrix} - \frac{1}{T}\widehat{O}_t^{(1)}\begin{pmatrix} \Psi_0(t) \\ \Psi_1(t) \end{pmatrix}, \tag{5.3}$$

$$\begin{pmatrix} \chi_0(T) \\ \chi_1(T) \end{pmatrix} = \widehat{O}_T^{(2)}\begin{pmatrix} \Psi_0(T) \\ \Psi_1(T) \end{pmatrix}, \tag{5.4}$$

$$\frac{d}{dt}\begin{pmatrix} \Psi_0(t) \\ \Psi_1(t) \end{pmatrix} = -i\begin{pmatrix} \omega_0 - E(t)\mu_{00} & -E(t)\mu_{01} \\ -E(t)\mu_{10} & \omega_1 - E(t)\mu_{11} \end{pmatrix}\begin{pmatrix} \Psi_0(t) \\ \Psi_1(t) \end{pmatrix}, \tag{5.5}$$

$$\begin{pmatrix} \Psi_0(0) \\ \Psi_1(0) \end{pmatrix} = \begin{pmatrix} \phi_0 \\ \phi_1 \end{pmatrix}, \tag{5.6}$$

$$E(t) = -\frac{1}{\alpha}\Im(\Psi_0\chi_0^*\mu_{00} + \Psi_1\chi_0^*\mu_{01} + \Psi_0\chi_1^*\mu_{10} + \Psi_1\chi_1^*\mu_{11}). \tag{5.7}$$

## 5.2 Numerical setup

To solve the control equations we first perform a transformation of variable. We introduce new variables $\widetilde{\Psi}_i(t) = \Psi_i(t)e^{i\omega_i t}$ and $\widetilde{\chi}_i(t) = \chi_i(t)e^{i\omega_i t}$, $i = 1, 2$ and obtain from equations (5.5) and (5.6)

$$\frac{d}{dt}\begin{pmatrix} \widetilde{\Psi}_0(t) \\ \widetilde{\Psi}_1(t) \end{pmatrix} = -i\underbrace{\begin{pmatrix} -E(t)\mu_{00} & -E(t)\mu_{01}e^{i\omega_{01}t} \\ -E(t)\mu_{10}e^{-i\omega_{01}t} & -E(t)\mu_{11} \end{pmatrix}}_{\widetilde{H}}\begin{pmatrix} \widetilde{\Psi}_0(t) \\ \widetilde{\Psi}_1(t) \end{pmatrix}, \tag{5.8}$$

$$\begin{pmatrix} \widetilde{\Psi}_0(0) \\ \widetilde{\Psi}_1(0) \end{pmatrix} = \begin{pmatrix} \phi_0 \\ \phi_1 \end{pmatrix}, \tag{5.9}$$

with $\omega_{01} = \omega_0 - \omega_1$. We write the operators $\widehat{O}^{(i)}$, $i = 1, 2$ as $2 \times 2$ matrices

$$\widehat{O}^{(i)} = \begin{pmatrix} O_{00}^{(i)} & O_{01}^{(i)} \\ O_{10}^{(i)} & O_{11}^{(i)} \end{pmatrix}. \tag{5.10}$$

The inhomogeneous Schrödinger equation (5.3) becomes

$$\begin{aligned} \frac{d}{dt}\begin{pmatrix} \widetilde{\chi}_0(t) \\ \widetilde{\chi}_1(t) \end{pmatrix} &= \frac{-i}{\hbar}\begin{pmatrix} -E(t)\mu_{00} & -E(t)\mu_{01}e^{i\omega_{01}t} \\ -E(t)\mu_{10}e^{-i\omega_{01}t} & -E(t)\mu_{11} \end{pmatrix}\begin{pmatrix} \widetilde{\chi}_0(t) \\ \widetilde{\chi}_1(t) \end{pmatrix} \\ &- \frac{1}{T}\begin{pmatrix} O_{00}^{(1)} & O_{01}^{(1)}e^{i\omega_{01}t} \\ O_{10}^{(1)}e^{-i\omega_{01}t} & O_{11}^{(1)} \end{pmatrix}\begin{pmatrix} \widetilde{\Psi}_0(t) \\ \widetilde{\Psi}_1(t) \end{pmatrix}, \end{aligned} \tag{5.11}$$

with the initial condition

$$\begin{pmatrix} \widetilde{\chi}_0(T) \\ \widetilde{\chi}_1(T) \end{pmatrix} = \begin{pmatrix} O_{00}^{(2)} & O_{01}^{(2)}e^{i\omega_{01}t} \\ O_{10}^{(2)}e^{-i\omega_{01}t} & O_{11}^{(2)} \end{pmatrix}\begin{pmatrix} \widetilde{\Psi}_0(T) \\ \widetilde{\Psi}_1(T) \end{pmatrix}. \tag{5.12}$$

Furthermore, the field equation (5.7) transforms to

$$E(t) = -\frac{1}{\alpha}\Im(\widetilde{\Psi}_0\widetilde{\chi}_0^*\mu_{00} + \widetilde{\Psi}_1\widetilde{\chi}_0^*\mu_{01}e^{i\omega_{01}t} + \widetilde{\Psi}_0\widetilde{\chi}_1^*\mu_{10}e^{-i\omega_{01}t} + \widetilde{\Psi}_1\widetilde{\chi}_1^*\mu_{11}). \tag{5.13}$$

For the dipole operator $\hat{\mu}$ we chose $\mu_{00} = \mu_{11} = 0$ so that the transformed Hamilton matrix is given by

$$\widetilde{H} = \begin{pmatrix} 0 & -E(t)\mu_{01}e^{i\omega_{01}t} \\ -E(t)\mu_{10}e^{-i\omega_{01}t} & 0 \end{pmatrix}. \tag{5.14}$$

It has the following eigenvalues

$$\lambda_1 = -|E(t)\mu_{01}| = -\lambda, \tag{5.15}$$
$$\lambda_2 = |E(t)\mu_{01}| = \lambda, \tag{5.16}$$

due to the hermiticiy of $\hat{\mu}$ i.e. $\mu_{01} = \mu_{10}^*$. The corresponding eigenvectors are

$$\vec{u}_1 = \frac{1}{\sqrt{2}}\begin{pmatrix} \frac{E(t)\mu_{01}e^{i\omega_{01}t}}{|E(t)\mu_{01}|} \\ 1 \end{pmatrix} = \frac{1}{\sqrt{2}}\begin{pmatrix} \frac{\sigma(E(t))\mu_{01}e^{i\omega_{01}t}}{|\mu_{01}|} \\ 1 \end{pmatrix}, \tag{5.17}$$

$$\vec{u}_2 = \frac{1}{\sqrt{2}}\begin{pmatrix} \frac{-E(t)\mu_{01}e^{i\omega_{01}t}}{|E(t)\mu_{01}|} \\ 1 \end{pmatrix} = \frac{1}{\sqrt{2}}\begin{pmatrix} \frac{-\sigma(E(t))\mu_{01}e^{i\omega_{01}t}}{|\mu_{01}|} \\ 1 \end{pmatrix}, \tag{5.18}$$

where $\sigma$ is the sign function

$$\sigma(x) = \begin{cases} 1 & x \geq 0 \\ -1 & x < 0 \end{cases}. \tag{5.19}$$

To solve the Schrödinger equations[1] (homogeneous and inhomogeneous) we use (3.6) and (3.23). For the propagation of the Schrödinger equation we need an approximation for the time evolution operator. If we neglect the time ordering operator and use the simplest approximation for the time integral we have

$$\widetilde{U}_t^{t+\Delta t} = \mathcal{T}\exp\left[\int_t^{t+\Delta t} d\tau(-i\widetilde{H}_\tau)\right] \approx \exp\left[-i\Delta t\widetilde{H}_t\right]. \tag{5.20}$$

We see that for the approximation of $\widetilde{U}_t^{t+\Delta t}$ we need to know the field $E$ only at time $t$. Therefore, we can use the immediate feedback mentioned in section 4.1. The infinitesimal evolution operator is

$$\begin{aligned} \widetilde{U}_t^{t+\Delta t} &\approx \exp\left[-i\Delta t\widetilde{H}_t\right] = \begin{pmatrix} u_{11} & u_{21} \\ u_{12} & u_{22} \end{pmatrix}\begin{pmatrix} e^{-i\Delta t\lambda_1} & 0 \\ 0 & e^{-i\Delta t\lambda_2} \end{pmatrix}\begin{pmatrix} u_{11}^* & u_{12}^* \\ u_{21}^* & u_{22}^* \end{pmatrix} \\ &= \begin{pmatrix} u_{11} & u_{21} \\ u_{12} & u_{22} \end{pmatrix}\begin{pmatrix} e^{-i\Delta t\lambda_1}u_{11}^* & e^{-i\Delta t\lambda_1}u_{12}^* \\ e^{-i\Delta t\lambda_2}u_{21}^* & e^{-i\Delta t\lambda_2}u_{22}^* \end{pmatrix} \\ &= \begin{pmatrix} e^{-i\Delta t\lambda_1}|u_{11}|^2 + e^{-i\Delta t\lambda_2}|u_{21}|^2 & e^{-i\Delta t\lambda_1}u_{11}u_{12}^* + e^{-i\Delta t\lambda_2}u_{21}u_{22}^* \\ e^{-i\Delta t\lambda_1}u_{12}u_{11}^* + e^{-i\Delta t\lambda_2}u_{22}u_{21}^* & e^{-i\Delta t\lambda_1}|u_{12}|^2 + e^{-i\Delta t\lambda_2}|u_{22}|^2 \end{pmatrix}, \end{aligned} \tag{5.21}$$

[1]For the transformed equations there is also a time evolution operator with the same properties (group property etc.) as the one for the initial equations.

where $u_{j1}$ and $u_{j2}$ are the elements of the eigenvector $\vec{u}_j$, $j = 1, 2$. We observe that the eigenvectors of the Hamiltonian satisfy the relations

$$u_{11} = -u_{21}, \tag{5.22}$$
$$u_{12} = u_{22}, \tag{5.23}$$

as well as

$$|u_{11}|^2 = |u_{21}|^2 = |u_{12}|^2 = |u_{22}|^2 = 1/2. \tag{5.24}$$

Using equation (5.22)-(5.24) the exponentials appearing in the matrix elements of $\widetilde{U}_t^{t+\Delta t}$ can be rewritten as

$$e^{-i\Delta t\lambda_1} + e^{-i\Delta t\lambda_2} = e^{i\Delta t\lambda} + e^{i\Delta t\lambda} = 2\cos(\Delta t\lambda), \tag{5.25}$$
$$e^{-i\Delta t\lambda_1} - e^{-i\Delta t\lambda_2} = e^{i\Delta t\lambda} - e^{-i\Delta t\lambda} = 2i\sin(\Delta t\lambda). \tag{5.26}$$

The time evolution operator $\widetilde{U}_t^{t+\Delta t}$ therefore reduces to

$$\widetilde{U}_t^{t+\Delta t} = \begin{pmatrix} \cos(\Delta t\lambda) & u_{11}u_{12}^* 2i\sin(\Delta t\lambda) \\ u_{12}u_{11}^* 2i\sin(\Delta t\lambda) & \cos(\Delta t\lambda) \end{pmatrix} =$$
$$= \begin{pmatrix} \cos(\Delta t|E(t)\mu_{01}|) & \frac{i\hat{\mu}_{01}e^{i\omega_{01}t}}{|\hat{\mu}_{01}|}\sigma(E(t))\sin(\Delta t|E(t)\mu_{01}|) \\ \frac{i\hat{\mu}_{01}^* e^{-i\omega_{01}t}}{|\hat{\mu}_{01}|}\sigma(E(t))\sin(\Delta t|E(t)\mu_{01}|) & \cos(\Delta t|E(t)\mu_{01}|) \end{pmatrix}. \tag{5.27}$$

**Time step and penalty factor**

In a large number of tests we found that 0.01 a.u. is an acceptable value for the time step $\Delta t$, as long as the amplitude of the field remains below the value of 0.05 a.u.. For stronger fields one should use smaller time steps in order to get reasonable results for the field. Since a smaller penalty factor leads to stronger fields, one also has to adjust the time steps to the value of $\alpha$.

## 5.3 Results

We have introduced the operator $\widehat{O}^{(2)}$ to establish the link between optimal control of time-dependent targets and traditional optimal control. For the rest of this thesis we will set it to zero. This yields (see equation (2.27))

$$\chi(T) = 0. \tag{5.28}$$

$\chi$ is not normalized. If we consider equation (2.26) and also the results from section 3.2 we see that the norm of $\chi$ need not be constant. Thus $\chi$ need not remain zero for all times even if it satisfies equation (5.28). From equations (5.28) and (2.30) it follows that $E(T) = 0$. To compute the results in this section we use the iterative scheme presented in section 4.1 using

$$\eta = \gamma = 1. \tag{5.29}$$

For the initial state of the wave-function we choose

$$\Psi(0) = |0\rangle \tag{5.30}$$

As time-dependent operator $\widehat{O}_t^{(1)}$ we choose a projection operator on a time-dependent function $\Phi$

$$\widehat{O}_t^{(1)} = |\Phi(t)\rangle\langle\Phi(t)| = \begin{pmatrix} |\Phi_0(t)|^2 & \Phi_0(t)\Phi_1(t)^* \\ \Phi_1(t)\Phi_0(t)^* & |\Phi_1(t)|^2 \end{pmatrix}. \tag{5.31}$$

$\widehat{O}_t^{(1)}$ is therefore positive semi-definite and hermitian, so that we can use all previously derived formulas. Using this operator, the goal of optimization process is that the wave-function $\Psi$ becomes identical with the target $\Phi$. Thus, the maximal value of the Lagrange functional is unity. Thus the maximization of the time averaged expectation value of $\widehat{O}_t^{(1)}$ becomes equivalent to the inversion of the Schrödinger equation, i.e., for a given function $\Phi$ we find the field $E(t)$ so that

$$i\partial_t\Psi = (\widehat{H}_0 - e\hat{\mu}E)\Psi(t), \tag{5.32}$$

so that the calculated wave-function $\Psi$ comes as close as possible to the target $\Phi$ in the space of admissible fields

$$\Psi \approx \Phi. \tag{5.33}$$

A target wave-function is not a quantity one can measure in experiment. But it can be used to control the expectation value of operators that are not necessarily positive definite. Suppose one desires to find the optimal field $E$ so that the solution $\Psi$ of the Schrödinger equation with this field satisfies

$$\langle\Psi(t)|\hat{A}|\Psi(t)\rangle = S(t), \tag{5.34}$$

where $S(t)$ is a given time-dependent function and $\hat{A}$ is the operator of an observable. Starting with the function $S(t)$, we can construct an "artificial" wave-function $\Phi$ that is normalized and satisfies

$$\langle\Phi(t)|\hat{A}|\Phi(t)\rangle = S(t). \tag{5.35}$$

Then we invert the Schrödinger equation i.e. we find the field $E$ and the wave-function $\Psi$ for which equation (5.32) is satisfied, and the overlap integral $J_1$ is maximal. Consequently

$$\langle\Psi(t)|\hat{A}|\Psi(t)\rangle \approx S(t). \tag{5.36}$$

We can summarize this procedure as

$$S(t) \xrightarrow{(a)} \Phi(t) \xrightarrow{(b)} E(t), \Psi \approx \Phi, \tag{5.37}$$

where for step (b) we use the optimization of the expectation value of operator $\widehat{O}$ from equation (5.31). For step (a) one must use physical intuition.

The time-dependent target wave-function $\Phi$ can be described as a linear combination of the two eigenstates with time-dependent coefficients $\Phi(t) = \Phi_0(t)|0\rangle + \Phi_1(t)|1\rangle$. At the beginning of each section we will specify which functions we choose for $\Phi_0(t)$ and $\Phi_1(t)$. The inhomogeneous part of equation (5.11) becomes

$$-\frac{1}{T}\begin{pmatrix} |\Phi_0(t)|^2\widetilde{\Psi}_0 + \Phi_0(t)\Phi_1(t)^*\widetilde{\Psi}_1 e^{i\omega_{01}t} \\ \Phi_1(t)\Phi_0(t)^*\widetilde{\Psi}_0 e^{-i\omega_{01}t} + |\Phi_1(t)|^2\widetilde{\Psi}_1 \end{pmatrix}. \tag{5.38}$$

If we define $\widetilde{\Phi}_i(t) = \Phi_i(t)e^{i\omega_i t}$ we can rewrite this inhomogeneity

$$-\frac{1}{T}\begin{pmatrix}\widetilde{\Phi}_0\\ \widetilde{\Phi}_1\end{pmatrix}(\widetilde{\Psi}_0(t)\widetilde{\Phi}_0^*(t) + \widetilde{\Phi}_1(t)^*\widetilde{\Psi}_1(t)). \tag{5.39}$$

We observe that

$$\begin{aligned}\langle\Psi(t)|\Phi(t)\rangle &= \Psi_0(t)^*\Phi_0(t) + \Psi_1(t)^*\Phi_1(t)\\ &= \widetilde{\Psi}_0(t)^*\widetilde{\Phi}_0(t) + \widetilde{\Psi}_1(t)^*\widetilde{\Phi}_1(t)\\ &= \langle\widetilde{\Psi}(t)|\widetilde{\Phi}(t)\rangle.\end{aligned} \tag{5.40}$$

In the next sections we will use as target the transformed wave-function $\widetilde{\Phi}$. The energies $\omega_0$ and $\omega_1$ enter the formalism not directly but only through their difference $\omega_{01}$.

### 5.3.1 Test of optimization process

In this section we test step (b) of scheme (5.37). To see how close the inversion process comes to the true solution of the problem, we use a function $\Phi$ for which we know the field $E(t)$. We want to test the convergence of the algorithm (see chapter 4) and the focus here is the relevance of the penalty factor $\alpha$. As one can see, the functional which we want to maximize has two competing components $J_1$ and $J_2$.

$$\begin{aligned}\mathcal{L}[\Psi, E, \chi] &= J_1 + J_2 - J_3 =\\ &= \frac{1}{T}\int_0^T dt\,\langle\Psi(t)|\widehat{O}_t|\Psi(t)\rangle - \alpha\int_0^T dt\,E^2(t) -\\ &- 2\Im\int_0^T dt\,\left\langle\chi(t)\left|\left(i\partial_t - \widehat{H}\right)\right|\Psi(x)\right\rangle.\end{aligned} \tag{5.41}$$

On the one hand we want to maximize the overlap of the wave-function with a time-dependent target in $J_1$. To achieve this we need an external field $E(t)$. On the other hand, there is a part of the functional ($J_2$) that reaches its maximum in the absence of an external field. In this section we want to check how the competition between the two parts of the functional $\mathcal{L}$ influences the results. Since the penalty factor $\alpha$ weighs the second term with respect to the first one we examine the results for different values of $\alpha$.

As a target state $\Phi(t)$ we choose the solution of the Schrödinger equation with the field

$$E_{target}(t) = \frac{\pi}{|\mu_{01}|T}\sin(\omega_{01}\cdot(T-t)) \tag{5.42}$$

The field is chosen such that $E_{target}(T) = 0$. The amplitude $\frac{\pi}{|\mu_{01}|T}$, is chosen such that at least in the RWA[2](see also appendix E), the system will experience a complete transfer of population from $|0\rangle$ to $|1\rangle$. To start the iteration we choose the same field as initial guess $E_{guess}(t) = \frac{\pi}{|\mu_{01}|T}\sin(\omega_{01}\cdot(t-T))$, which means that we start at the absolute maximum of the functional $J_1$. We perform the same calculation with different penalty factors $\alpha = 0.01$, 0.1, 1, 10 and 100 and 20 iterations in each calculation. Table 5.1 gives the other parameters. The results of the calculations are shown in figure 5.1 and 5.2.

[2]In the RWA the population oscillates between the two levels like $\sin^2(\Omega_R t/2)$ with the Rabi frequency $\Omega_R = A|\mu_{01}|$. For the system to make the complete transition from $|0\rangle$ to $|1\rangle$ in the time interval $T$ , under the influence of a field with the resonance frequency the relation $\Omega_R T = \pi$ must be satisfied. This leads to $A = \frac{\pi}{|\mu_{01}|T}$.

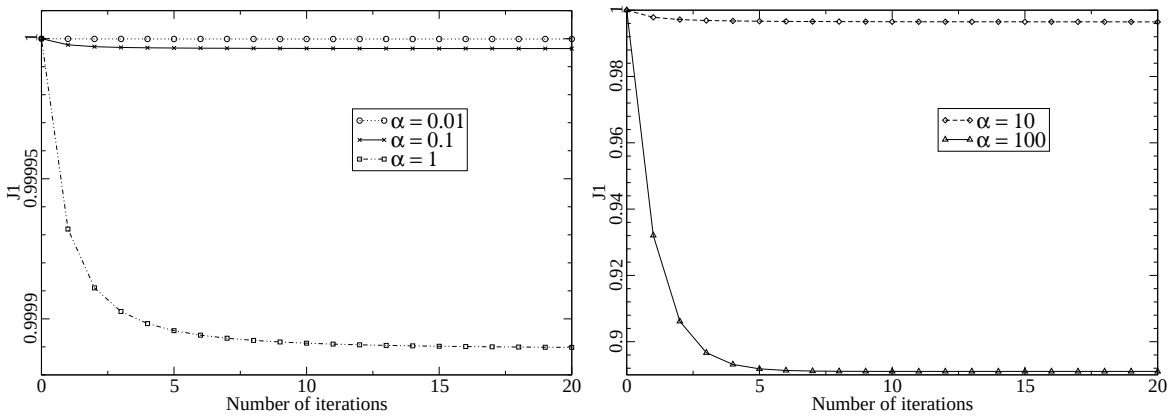


Figure 5.1: $J_1$ for different values of $\alpha$

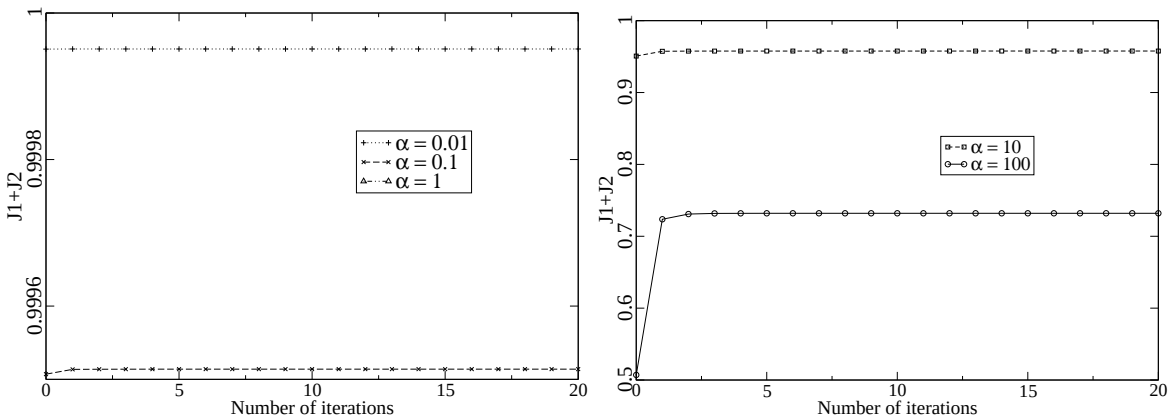


Figure 5.2: $J_1 + J_2$ for different values of $\alpha$'s

As expected, $J_1$ in loop 0 has its maximum value 1.0. It decreases in the next iteration steps, and this decrease is larger for larger values of the penalty factor $\alpha$. The value of the functional $J_1 + J_2$ grows, as expected from the convergence proof (see chapter 4). Therefore $J_2$ grows, and its increase over-compensates the decrease of $J_1$. The increase of $J_2$ means that the total intensity of the external field decreases.

For larger values of $\alpha$, the functional $J_2$ plays a more important role in $J_1 + J_2$, and the algorithm converges to fields with smaller energy. Consequently, the overlap with the target is smaller. For small $\alpha$ the functional $J_2$ is less important, and the maximum of $J_1 + J_2$ is closer to the one of $J_1$. For $\alpha \to 0$ we expect the optimal field to converge to the target generating field $E_{target}$, because in this case we have to maximize only $J_1$ (see equation (2.38)). In practice we cannot solve the problem with $\alpha = 0$ because we obtain a singular optimal control problem (see equation (2.23)), but we can use very small values of $\alpha$.

| $\mu_{01}$ | $\Delta t$ | $\omega_{01}$ | T |
|---|---|---|---|
| 1 | 0.001 | 0.4 | 1000 |

Table 5.1: Parameters for the test of optimization

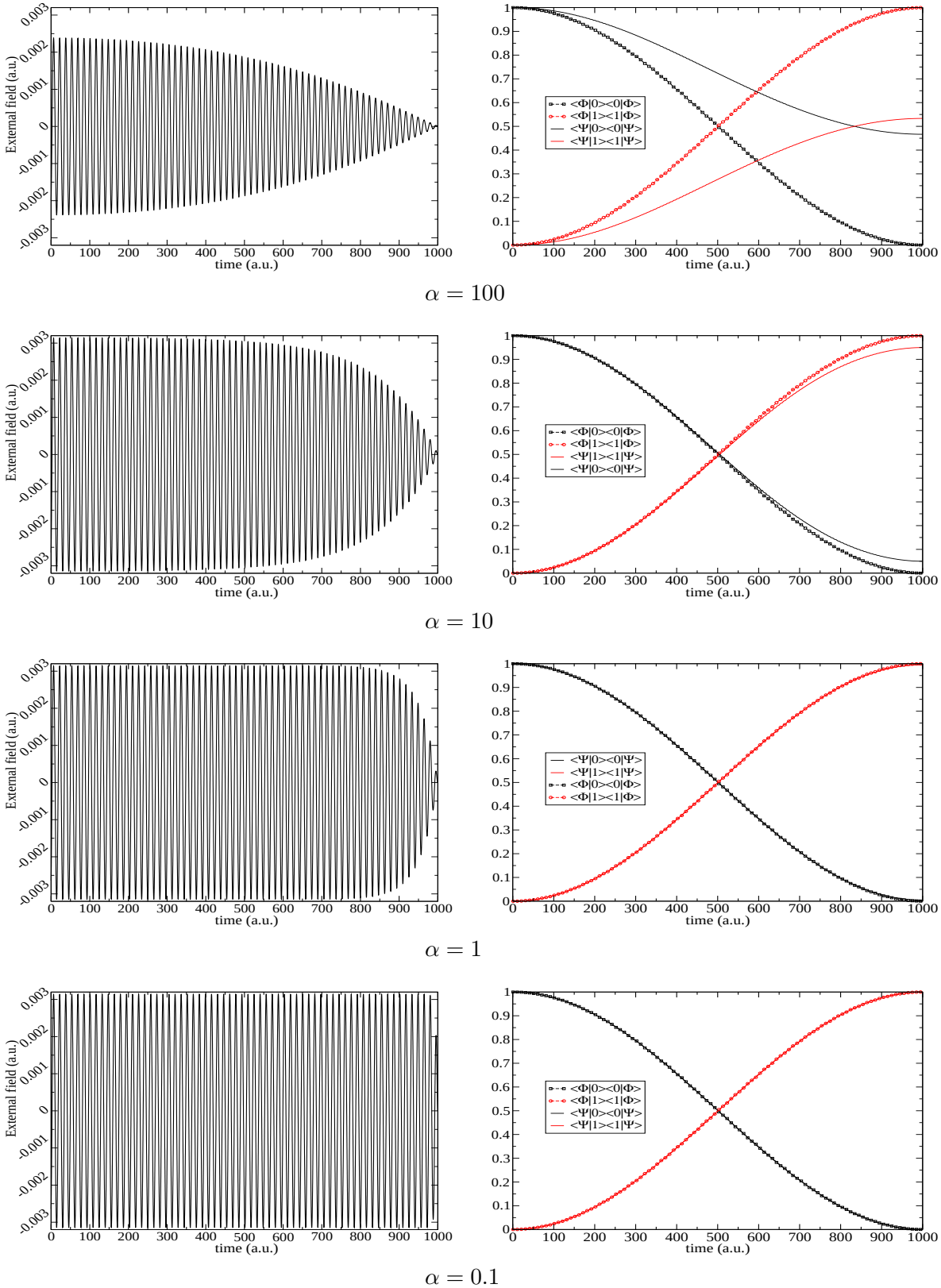


Figure 5.3: Optimal field and time dependence of population of the two levels after 230 iterations for $\alpha$=100, 10, 1, 0.1 from top to bottom.

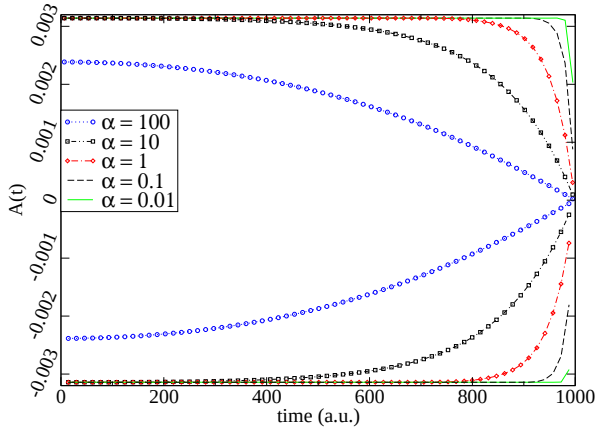


Figure 5.4: Envelope of the field for different $\alpha$'s. The plot summarizes figure 5.3

In figure 5.3 one can see that the optimal field satisfies $E(T) = 0$. Furthermore, the envelope of the field is also zero at $t = T$ and one can see that the intensity of the optimal field is being reduced at the end of the time interval. We found this behavior in all the calculations performed in the two-level system, so it seems to be independent of the type of the problem.

As expected, the deviation of the optimal field from the target generating field increases for increasing value of the penalty factors. We also see that $\alpha = 0.1$ is small enough for the time averaged overlap of the calculated wave-function with the target (functional $J_1$) to be larger than 99.9% (see Fig. 5.1). For $\alpha$ small enough we can come arbitrarily close to the absolute maximum of $J_1$, which is 1.0. For larger values of $\alpha$ the optimal field does not have the energy that is necessary for the wave-function to follow the target.

In figure 5.3 one can see that the optimal field has the structure

$$E(t) \quad = \quad A(t)\sin(\omega_{01} \cdot t). \tag{5.43}$$

This describes a harmonic oscillation with the resonance frequency $\omega_{01}$ multiplied with a time-depending envelope. We extract the envelope function from the results for $E(t)$ at the end of the calculation. They are plotted in figure 5.4 for different values of $\alpha$. The envelope of the field obtained after the optimization can be fitted to a curve of the type

$$A(t) = \frac{\pi}{T}\left(1 - \exp(-(T-t)\cdot\beta)\right) \tag{5.44}$$

where $\beta$ is the parameter to be fitted and we can see that

$$\lim_{\beta\to\infty} \frac{\pi}{T}\left(1 - \exp(-(T-t)\cdot\beta)\right) \quad = \quad \frac{\pi}{T}. \tag{5.45}$$

For $\beta$ large enough we therefore retrieve the target generating field. The values of $\beta$ for different values of $\alpha$ are given in the table 5.2. We also see that the agreement of the fitted curve with the calculated envelope is better for small values of $\alpha$.

Now we parameterize the field with respect to $\beta$. The functional $J_1 + J_2$ depends on an infinite number of variables, i.e. $E(t)$ at each $t$. By parameterizing the field the functional $J_1 + J_2$ reduces to a function of $\beta$, which is simple to visualize. It can be written as

$$(J_1 + J_2)[\alpha, \beta] \quad = \quad \int_0^t dt \left(|\langle\Psi(t)|\Phi(t)\rangle|^2 - \alpha E_\beta^2(t)\right). \tag{5.46}$$

| $\alpha$ | $\beta$ | SSR [3] |
|---|---|---|
| 0.01 | 0.227993 | $7.70464 \cdot 10^{-12}$ |
| 0.1 | 0.0697594 | $1.19946 \cdot 10^{-9}$ |
| 1 | 0.0222404 | $9.47338 \cdot 10^{-10}$ |
| 10 | 0.00698218 | $1.03182 \cdot 10^{-9}$ |
| 100 | 0.00171991 | $2.55678 \cdot 10^{-7}$ |

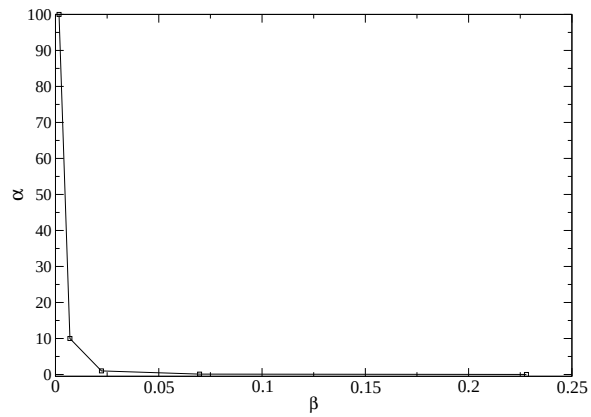


Table 5.2: The parameter $\beta$ for different penalty factors and the error SSR

where $\Psi(t)$ is the solution of the time-dependent Schrödinger equation with the external field $E_\beta(t) = \frac{\pi}{T}(1 - \exp(-(T-t)\cdot\beta))\sin(\omega_{01}t)$. The functional $J_1(\beta)$ reaches its maximum for $\beta \to \infty$. In figure 5.5 one can see the plot of the functional $(J_1 + J_2)(\alpha, \beta)$, where the dependence on the function $E$ has been reduced to the dependence on only one parameter $\beta$. Here, each value of $\beta$ complete determines a field $E_\beta(t)$. On this surface, the functional evaluated with the initial guess field used in the previous calculations is represented for each $\alpha$ as the point $\beta \to \infty$ as one can deduce from equation (5.45). We see that for growing values of $\alpha$ the distance between this point and the point where the functional reaches its maximum with respect to $\beta$ (given by the dotted blue line) grows.

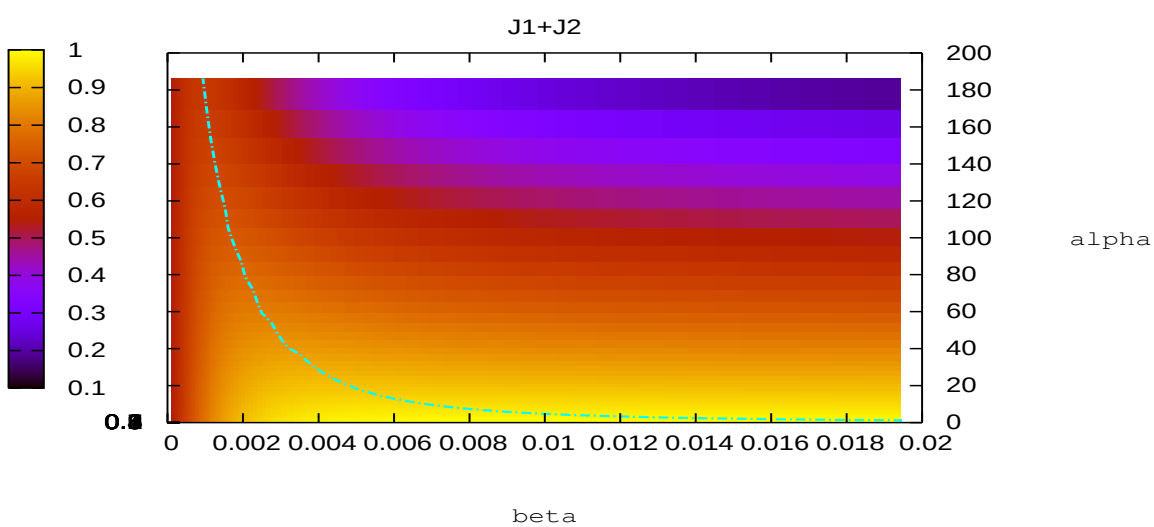


Figure 5.5: The functional $(J_1 + J_2)(\beta)$

[3]SSR = sum of the squared differences (residuals) between the input data points and the function values, evaluated at the same places.

### 5.3.2 Control of the time-dependent population

In the previous section we used as target a wave-function about which we already knew that it is the solution of the time-dependent Schrödinger equation. In this section we define as target an "artificial" wave-function and study the optimal field. In this case we cannot be certain that there is an optimal field so that the overlap functional $J_1$ is 1, i.e. if the guessed wave-function is actually a physical wave-function which can be obtained as solution of some time-dependent Schrödinger equation. We study the dependence of the maximum of $J_1$ and $J_1 + J_2$ on $\alpha$. We also investigate the influence of $\alpha$ on the number of iterations needed to achieve convergence.

For the components of the target wave-function we choose two time-dependent wave-functions

$$\widetilde{\Phi}_1(t) = \sqrt{\exp\left(-\frac{\left(t-\frac{T}{4}\right)^2}{2\left(\frac{T}{20}\right)^2}\right) + \exp\left(-\frac{\left(t-\frac{2T}{3}\right)^2}{2\left(\frac{T}{10}\right)^2}\right)} \tag{5.47}$$

$$\widetilde{\Phi}_0(t) = \sqrt{1-\widetilde{\Phi}_1^2(t)} \tag{5.48}$$

The target wave-function is normalized and at times $t = 0$ and $t = T$ in the state $|1\rangle$. The observable we want to control is the occupation number of one of state $|0\rangle$. Using this specific target we wan to demonstrate that we can precisely control the trajectory followed by the population, also if the system executes many transitions between the two states. With our approach we can not only maximize the population of level $|1\rangle$, but also determine on which path the system executes the transition from $|0\rangle$ to $|1\rangle$, and if necessary, invert the process, or repeat it in a different time interval. To demonstrate this we have chosen four consequent transitions between the two levels, which must be executed in different times. The parameters used are given in table 5.3.2. We start with the initial guess

| $\mu_{01}$ | $\Delta t$ | $\omega_{01}$ | T |
|---|---|---|---|
| 1 | 0.01 | 0.4 | 2000 |

Table 5.3: Parameters for the control of population

$$E_{guess}(t) = -10^{-4} \tag{5.49}$$

and let the algorithm iterate until $\delta\mathcal{L}_{k,k-1} \leq 10^{-8}$.

In figure 5.6 one can see the value of the functional $J_1$ versus the number iterations for different values of $\alpha$. For each value of $\alpha$ we extract the maximum value reached by $J_1$ and $J_1 + J_2$ and also the total number of iterations needed to achieve convergence. In figure 5.7 (a) we observe that for smaller $\alpha$ the functionals $J_1$ and $J_1 + J_2$ converge to larger values. As mentioned before, a small value of $\alpha$ allows a large total energy for the optimal field. A field with larger energy is then able to drive the system closer to the prescribed path and thus the value of the overlap functional $J_1$ becomes larger. At the same time, a small value of $\alpha$ makes the quantity we have to subtract from $J_1$, namely $J_2$ smaller, even if the intensity of the field is large. Therefore also $J_1 + J_2$ becomes larger for smaller values of the penalty factor.

In figure 5.7 (b) we see that the total number of iterations grows with decreasing $\alpha$, thus we obtain better results (larger value of the functional $J_1 + J_2$) at the cost of considerably

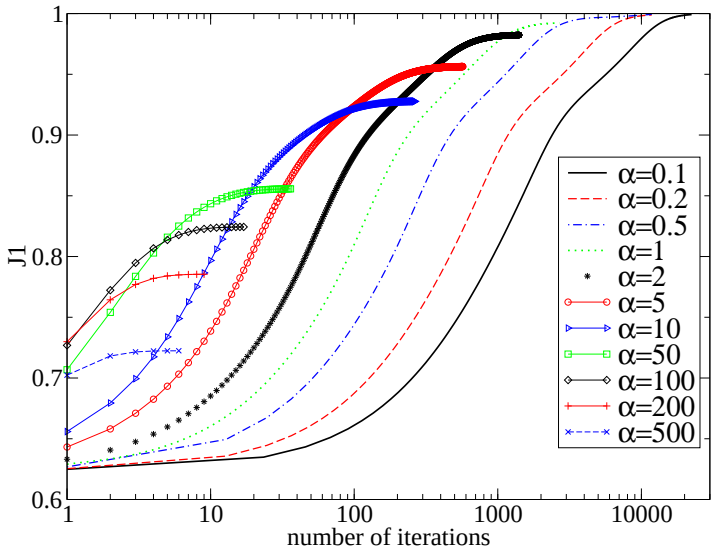


Figure 5.6: Evolution of $J_1$ during the iteration for different values of $\alpha$

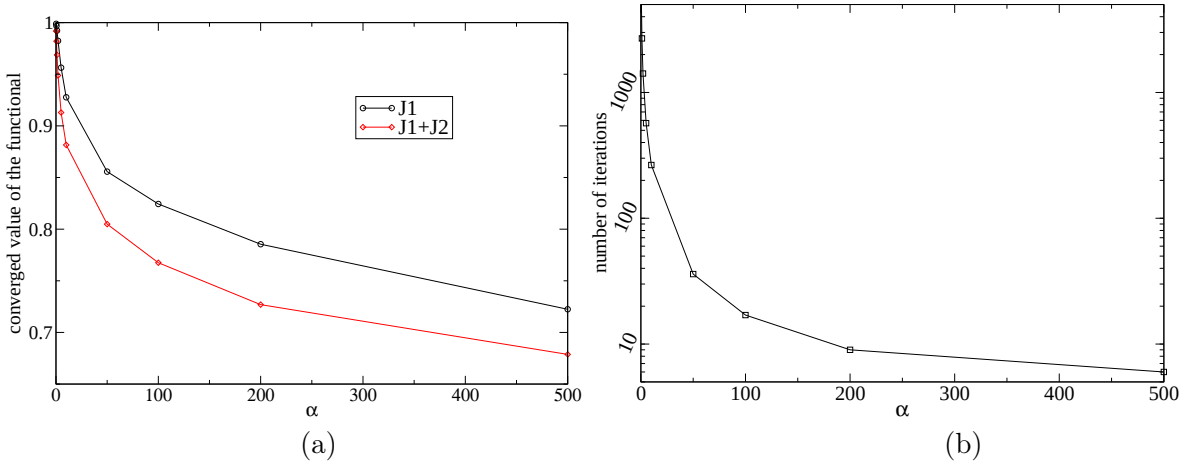


Figure 5.7: Maximal value of functionals $J_1$ and $J_1 + J_2$ (b) and final number of iterations as function of the penalty factor $\alpha$

larger number of iterations. We can understand this behavior if we look at the initial guess field, which is very small ($\approx 0$). The "distance" between this initial guess field and the optimal field is simply the total intensity of the optimal field. For a large value of $\alpha$, the optimal field has a small intensity. Thus, the initial guess is "closer" to the optimal field for large values of $\alpha$. For small values of the penalty factor, the optimal field is stronger i.e. it differs more from the initial guess and more iterations are needed to find it. Coming back to the figure 5.2 we can see the inverse behavior. In that case we have started with the target generating field as initial guess, so that for very small values of $\alpha$ the initial guess was very close to the optimal field, and the functional $J_1 + J_2$ converged very fast. For larger values of $\alpha$ the optimal field (see figure 5.3, uppermost row) differs considerably from the initial guess, and the convergence is slower. In conclusion, the total number of iterations gives a measure for the "distance" between the initial guess field $E_{guess}$ and the field for which the functional has

a local maximum.

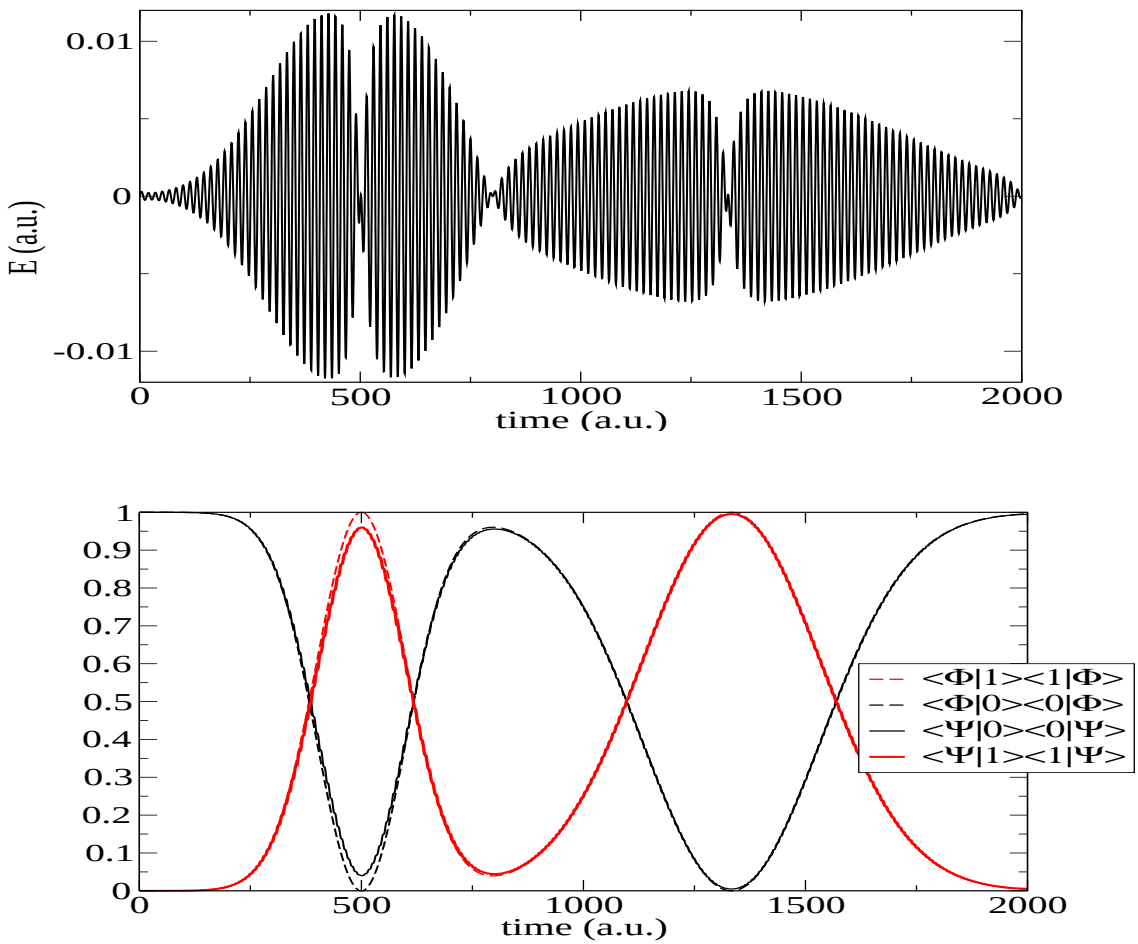


Figure 5.8: Optimal field $E(t)$ (top) and $|\Phi_0(t)|^2$, $|\Phi_1(t)|^2$, $|\Psi_0(t)|^2$ and $|\Psi_1(t)|^2$ (bottom) for $\alpha = 0.1$

A very important result of this section can be seen in figure 5.8. Comparing the squared absolute value of the two components of the target and the calculated wave-function, we can see that the prescribed path is followed very closely by the optimized wave-function. The overlap of the target and calculated wave-function, averaged over the whole time interval reaches a value larger than 99% (see figure 5.6, the curve for $\alpha = 0.1$). Thus, even if we constructed an "artificial" target, with no guarantee that it satisfies the Schrödinger equation, the algorithm finds a wave-function that is very close to the target.

Another point of interest is the shape of the external field. We can see in figure 5.8 that the prescribed wave-function experiences four transitions: from state $|0\rangle$ to state $|1\rangle$ in 500 a.u. and back in roughly the same time, and than again from $|0\rangle$ to $|1\rangle$ and back, but in a longer time interval. We observe that the maximal amplitude reached by the optimal field is larger in the first part and also its envelope is steeper than in the second part.

In our simulations, turning down the field leaves the population of each level unchanged

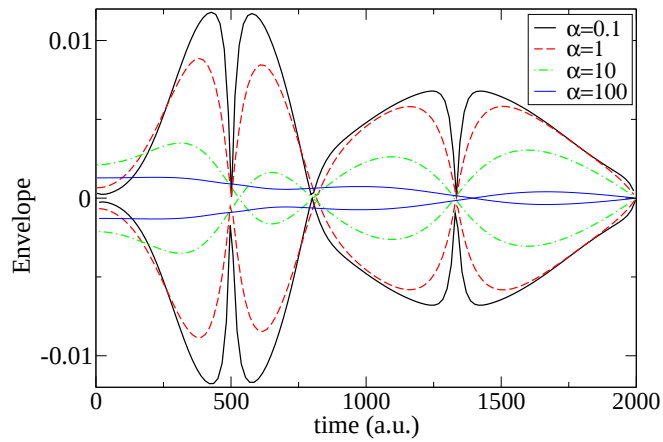


Figure 5.9: The envelope of the field for several penalty factors $\alpha$

for indefinite time. We can easily see this if we analyze the infinitesimal time evolution operator $\widetilde{U}_t^{t+\Delta t}$ in equation (5.27). For $E(t) = 0$ it becomes the identity matrix. This has the consequence that for vanishing external field every state will be conserved. In figure 5.8 we see that at the points where the time derivative of the prescribed population becomes zero, the envelope of the field goes through zero. This behavior is conserved for larger penalty factors as can be seen in figure 5.9.

### 5.3.3 Optimal field of a prescribed intensity

We have shown in section 2.2.5 how one can, at least in principle, search for the field that maximizes $J_1$ in the subspace of fields with a given intensity $I_0$. In chapter 4 we have given an iterative method to solve equations (2.33), (2.34) and (2.35) for a given positive parameter $\alpha$. In this section we give a practical implementation of the scheme (2.37).

We want to determine the Lagrange multiplier $\alpha$ so that equation (2.36) is satisfied. For this we need some knowledge about the function $I(\alpha)$. Keeping in mind the results from section 5.3.1 we make the assumption that $I(\alpha)$ is a monotonically decreasing function of $\alpha$. To make this plausible consider $\alpha_2 \geq \alpha_1$. The functional $J_2[\alpha_2]$, that penalizes the total intensity, weighs more than $J_2[\alpha_1]$, so that the field that maximizes $(J_1 + J_2)[\alpha_2]$ has a smaller total intensity than the one that optimizes $(J_1 + J_2)[\alpha_1]$.

We calculate a target wave-function $\Phi(t)$ as the solution of the Schrödinger equation with the external field

$$E_{target}(t) \quad = \quad A \sin(\omega_{01} \cdot t) = \frac{\pi}{T\mu_{01}} \sin(\omega_{01} \cdot t), \tag{5.50}$$

which is the same as the one used for the test in section 5.3.1. The parameters are now

| $\mu_{01}$ | $\Delta t$ | $\omega_{01}$ | T |
|---|---|---|---|
| 1 | 0.01 | 0.4 | 400 |

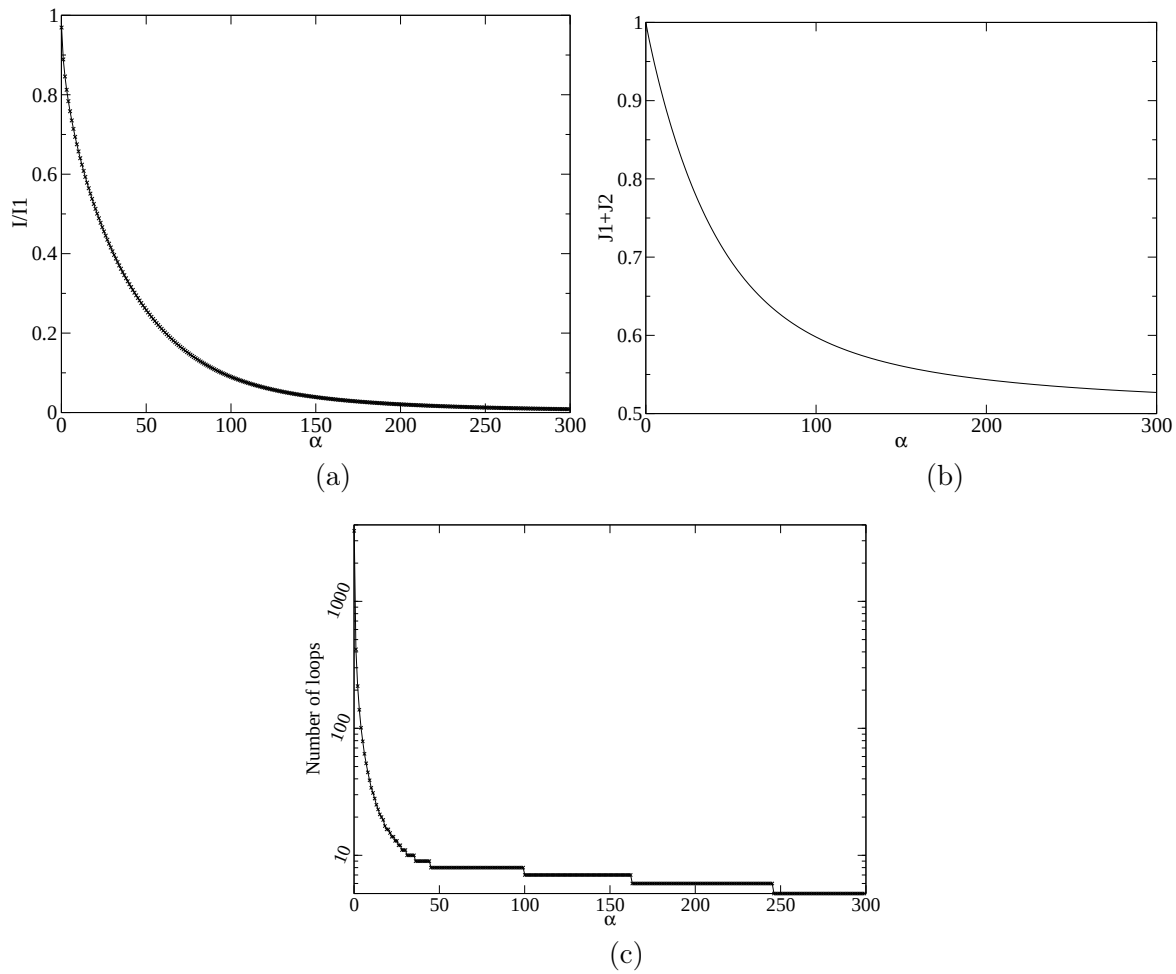


Figure 5.10: $I/I_1$ (a) $J_1 + J_2$ (b) and the final number of loops (c)

We scanned an interval $\alpha \in [0.1, 300]$ with steps of 1; for each value of $\alpha$ we started the iteration described in section 4, using $E_{guess}(t) = 10^{-6}$ as initial guess field. The algorithm was adjusted to iterate until the difference in $\mathcal{L}$ between two consecutive loops was smaller than $10^{-7}$.

Figure 5.10 (a) confirms equations (2.38) and (2.39) and also the assumption that $I(\alpha)$ is a monotonically decreasing function. $I_1$ is the intensity of the target generating field, i.e. the field that maximizes $J_1$ separately. From this considerations we conclude that it is not possible to find a field with total intensity that is larger than $I_1$.

For $J_1 + J_2$ (figure 5.10 (b)) and the total number of iterations (figure 5.10 (c)) we observe the same dependence on $\alpha$ as in section 5.3.2.

We use this information to find the root of the function

$$f(\alpha) \quad = \quad I(\alpha) - I_0$$

in the interval $[a, b]$, where $a$ and $b$ are chosen such that $f(a) > 0$ and $f(b) < 0$. We use the bisection method: by evaluating the function in the middle of an interval and replacing whichever boundary has the same sign, the bisection method can halve the size of the interval in each iteration and eventually find the root up to the desired accuracy $\varepsilon$.

The prescribed intensity is chosen to be

$$I_0 \quad = \quad \xi \int_0^T dt \left( \frac{\pi}{T\mu_{01}} \sin(\omega_{01} \cdot t) \right)^2 = \xi I_1 \tag{5.51}$$

| $\xi$ | a | b | $\varepsilon$ |
|---|---|---|---|
| 0.5 | 0 | 500 | $10^{-7}$ |

Table 5.4: Parameters for the bisection method

As initial guess for $\alpha$ we choose 0.5.

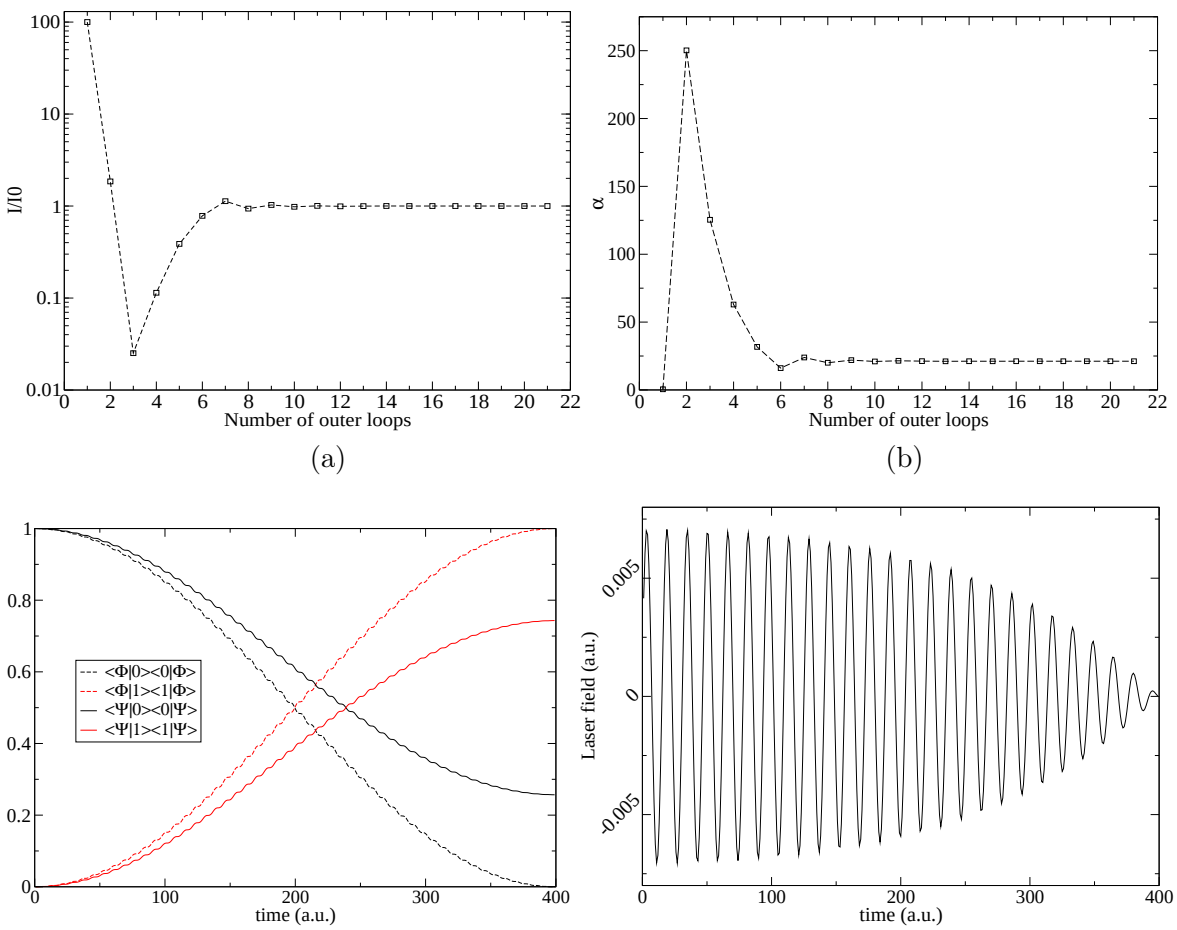


Figure 5.11: Ratio $I/I_0$ of the intensity of the calculated field and the intensity of the field which maximizes $J_1$ (a), $\alpha$ (b) $|\Psi_i(t)|^2$, $|\Phi_i(t)|^2$ (i = 0, 1)(d) and time-dependence of the optimal field (d) for $\alpha = 21.163$

In figure 5.11 (a) we see that the intensity converges to the desired value $I_0$. The penalty factor converges (see figure 5.11 (b)) after 20 loops with a precision of $10^{-7}$ to the value $\alpha = 21.163$. In figure 5.11 (c) and (d) are shown the optimal field with the prescribed intensity and the target and calculated population of the two levels.

We repeated the same calculation with another initial guess for the field (with constant envelope $A = 2\pi/T|\mu_{01}|$) and the Lagrange multiplier $\alpha$ converged to the same value as in the previous case.

For "traditional" optimal control theory the problem consists of finding the field that drives the system into the desired final state at $T$, but the trajectory followed by the system remains undetermined. This is the reason why there is usually more than one field that optimizes the target. If we give the trajectory that has to be followed by the system, the problem has much less degrees of freedom an therefore the flexibility that different field achieves the same task is much more restricted.

### 5.3.4 Targets with discontinuities

Until now we used as target wave-function either the solution of the Schrödinger equation for a known field or a *continuous* normalized function. In the previous section we have seen that also for the "artificial" function the algorithm finds a field that drives the system along the prescribed trajectory, very close to the time-dependent target. For this wave-function it was unclear if there is a field $E(t)$ so that $\Phi$ satisfies the time-dependent Schrödinger equation. This finding motivated following computer experiment. We want to test the ability of the algorithm in finding an optimal field for a discontinuous target and we analyze how close we can come to discontinuous targets.

We choose discontinuous functions for the coefficients of the two states $\Phi_0$ and $\Phi_1$, or functions with a discontinuous first time derivative. wave-functions discontinuous in the time do not satisfy the Schrödinger equation. Thus we can illustrate an important feature of the method presented in chapters 2, 3 and 4. Even if it does not find the exact solution of the problem ($J_1$ cannot reach the value 1.0), this method has the ability to find the solution that lies close to the desired target and satisfies the Schrödinger equation with a non-singular field. This is important, because in most cases one does not know if the goal ($J_1 = 1$) of the optimal control problem can be achieved to 100%.

In cases where the target is ill-posed an alternative approach such as tracking control would fail (see appendix H and also ref.[27]). Such a method is able to find the exact solution of a well posed problem, but has to deal with singularities in the case of ill-posed problems.

We present an example where the exact field calculated with the tracking method (see appendix H) would contain singularities, but where our optimal control finds continuous and finite fields that drive the system as close as possible, in the space of available solutions of the Schrödinger equation, to the target.

We know (see [27]) that for an operator $\widehat{O}_t$ we can impose a time-dependent trajectory $S(t)$ and calculate the exact field that drives the system along the given trajectory so that

$$\langle\Psi(t)|\widehat{O}(t)|\Psi(t)\rangle \quad = \quad S(t). \tag{5.52}$$

is satisfied. The exact field will depend on the time derivatives of the given trajectory as one can see in appendix H, so for trajectories discontinuous in time it will contain singularities.

**Target with the first time derivative discontinuous**

We choose as target wave-function

$$\widetilde{\Phi}_1(t) = \begin{cases} \sqrt{\frac{2t}{T}} & t \in [0, T/2] \\ \sqrt{\frac{t-T/2}{T/2}} & t \in (T/2, T] \end{cases} \tag{5.53}$$

$$\widetilde{\Phi}_0(t) = \sqrt{1 - \widetilde{\Phi}_1^2(t)} \tag{5.54}$$

The time derivatives of $|\widetilde{\Phi}_i^2(t)|$ $(i = 0, 1)$ have a discontinuity at $t = T/2$ (see figure 5.12 (a)).

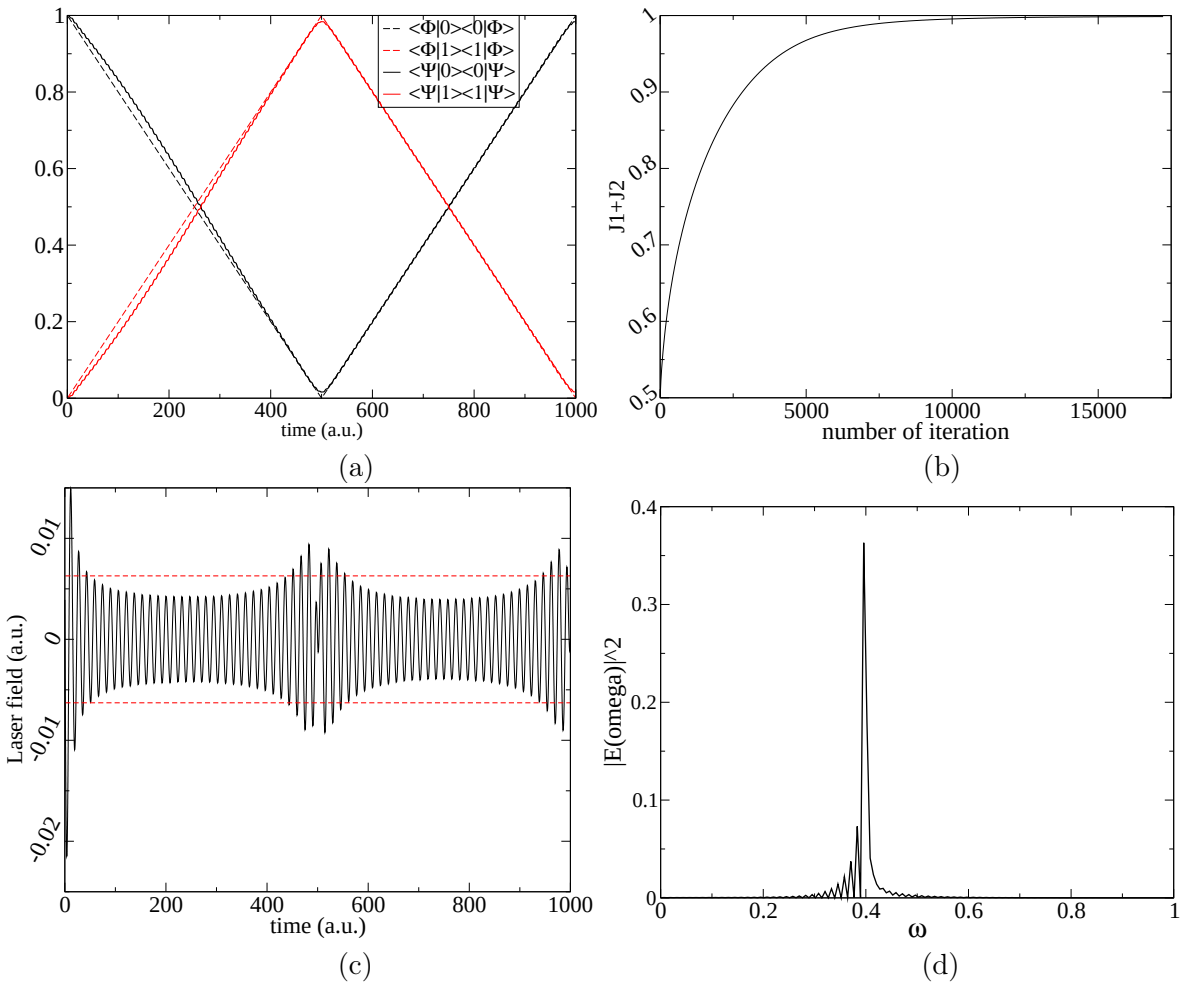


Figure 5.12: $|\Phi_i(t)|^2$ and $|\Psi_i(t)|^2$, $i = 0, 1$ (a), functional $J_1 + J_2$ (b), optimal field $E(t)$ (c) and its Fourier transform (d)

The initial guess field is $E_{guess}(t) = 0$.

In figure 5.12 (b) one can see that the functional $J_1 + J_2$ converges to a value larger than 99%. Since $J_1 \geq J_1 + J_2$, we conclude that also the time averaged overlap of the wave-function with the target reaches a value larger than 99%. The algorithm is therefore able to find a field

| $\mu_{01}$ | $\Delta t$ | $\omega_{01}$ | T | $\alpha$ |
|---|---|---|---|---|
| 1 | 0.01 | 0.4 | 1000 | 0.05 |

Table 5.5: Parameters for the calculation of the triangular target

that optimizes the overlap to this high accuracy even in the case of a target wave-function with discontinuous time derivative.

The evolution of the functional $J_1 + J_2$ over the number of iterations is typical for this kind of optimal control, and we found it in almost all calculations. We see at the beginning a strong enhancement from 0.5 to 0.9 over less than 3000 iterations. For the last 10% it takes approximatively 14000 iterations. In this very simple system it was possible to compute such a large number of iterations and to let the algorithm converge until the functional deviation in $J_1 + J_2$ between two consecutive loops was smaller than $10^{-7}$.

The optimal field (figure 5.12 (c)) oscillates mainly with the resonance frequency $\omega_{01}$ as one can see from its Fourier transform (figure 5.12 (d)). The dotted lines represent the constant envelope of a field with resonance frequency and amplitude $2\pi/T|\mu_{01}|$, which is strong enough to induce the two transitions $|0\rangle \to |1\rangle$ and $|1\rangle \to |0\rangle$ in the time $T$. Now if we evaluate

$$I = \int_0^T dt E^2(t) \tag{5.55}$$

for the optimal field and for the field with the RWA amplitude $2\pi/T|\mu_{01}|$ we obtain the ratio

$$\frac{I_{optimal}}{I_{RWA}} \approx 90\% \tag{5.56}$$

The results from [30] suggest that the optimal laser pulse that drives the system from state $|0\rangle$ to state $|1\rangle$ and back in time $T$ has a constant envelope and the amplitude $2\pi/T|\mu_{01}|$. Therefore it is surprising that another field, with smaller intensity achieves the same task. We can clarify this if we zoom in figure 5.12 (a) at time $t = T/2$ and $t = T$, see figure 5.13. We see that the wave-function does not reach 100% overlap with state $|1\rangle$ respectively $|0\rangle$. We suppose that the field that achieves this task must have an energy larger than $I_{RWA}$. In this example we can recognize the influence of the term $J_2$, which does not allow large values for the total intensity of the field.

**Step-like target**

As target function we choose

$$\widetilde{\Phi}_1(t) = \frac{1}{N}\sum_{n=1}^{N}\Theta(t-\tau_n), \tag{5.57}$$

$$\widetilde{\Phi}_0(t) = \sqrt{1-\widetilde{\Phi}_1^2(t)}, \tag{5.58}$$

$$\tau_n = \frac{nT}{N}. \tag{5.59}$$

$\widetilde{\Phi}_0(t)$, $\widetilde{\Phi}_1(t)$ and consequently $|\widetilde{\Phi}_0(t)|^2$ and $|\widetilde{\Phi}_1(t)|^2$ have discontinuities at $\tau_n$ as one can see in figure 5.14 (a). The initial guess field is $E_{guess}(t) = 0$. In this example we choose the length

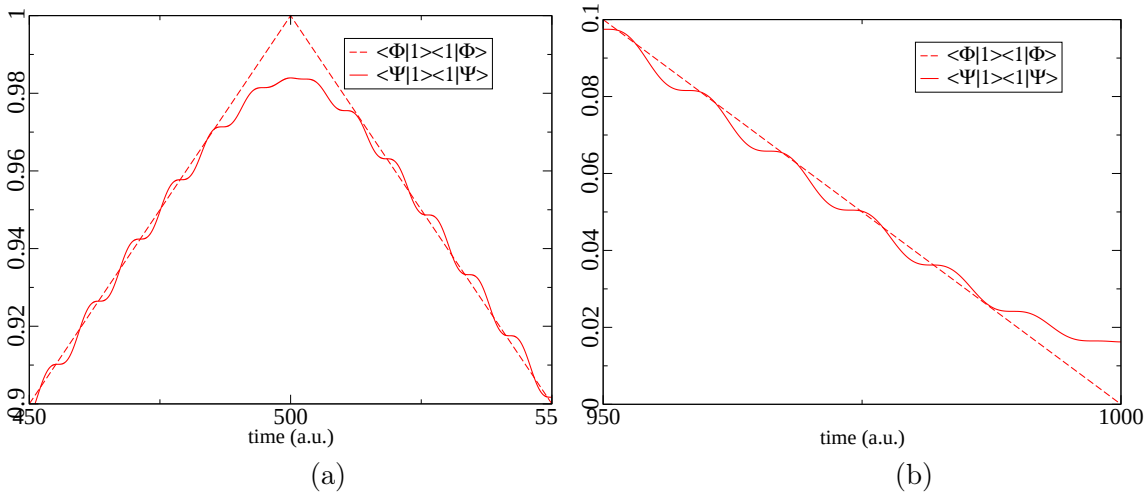


Figure 5.13: $|\Phi_1(t)|^2$ and $|\Psi_1(t)|^2$ at in the middle (a) and at the end of the time interval (a)

| $\mu_{01}$ | $\Delta t$ | $\omega_{01}$ | T | $\alpha$ |
|---|---|---|---|---|
| 1 | 0.01 | 0.4 | 500 | 0.05 |

Table 5.6: Parameters for calculation with the step-like target

of the time interval $T$ to be half of the one used in the previous example, because now we are only interested in the transition $|0\rangle \longrightarrow |1\rangle$.

We observe in figure 5.14 (b) a similar convergence behavior of $J_1 + J_2$ as in the previous example, figure 5.12 (b). Nevertheless, in this case a larger number of iterations is needed to achieve convergence. This is due to the more demanding task, and we can see in figure 5.14 (a) that the imposed trajectory is not followed as close by as in the previous example.

At the points where $|\widetilde{\Phi}_0(t)|^2$ becomes discontinuous, the field has intense pulses (see figure 5.14 (c)) consisting of only few oscillations with the resonance frequency (see figure 5.14 (d)). The dotted line represents the RWA amplitude $\pi/T|\mu_{01}|$ of the pulse that maximizes the overlap with state $|1\rangle$ at time $T$. At the discontinuity points the exact field (calculated using the Ehrenfest theorem, see Appendix H and [27]) would have $\delta$-peaks. The field that maximizes $J_1 + J_2$ cannot have singularities, because the total intensity is penalized by $J_2$ and cannot become infinite.

The population curves in figure 5.14 (a) do not match 100%, the calculated population is washed out at the discontinuity points of the target. For larger values of the penalty factor we notice that the broadening of the steps of the calculated population is more pronounced (see figure 5.15 (a)), the width of the envelope of the pulses is larger and the maximum peak lower (b).

Optimal control does not find the exact solution of the problem (5.52). But the approximate solution we are able to find with this method does not have singularities and consequently is more realistic from a physical point of view. This is a consequence of including the term $J_2$ in the functional, which penalizes the total intensity and thus excludes singularities in the electric field.

### 5.3.5 Control of the time-dependent dipole moment

In the previous examples we have shown how one can optimize the overlap of the wave-function with a time-dependent target. For this purpose we constructed "artificial" normalized wave-functions, without knowing for sure that they satisfy a Schrödinger equation. According to scheme 5.37 this corresponds to step (b). As we explained at the beginning of section 5.3, in most cases one is not interested in the time-dependent wave-function, but in the time evolution of an observable. If this observable has only positive values, we can insert it into the functional $J_1$. However, for the observable $\hat{\mu}$ this is not the case. In this section we want to control the time-dependent dipole moment. The dipole operator is not positive definite so we cannot use it in the formulation of chapter 2. We translate our goal into the form of the optimization of a time-dependent wave-function, which corresponds to step (a) of scheme 5.37. We have to choose this wave-function such that the expectation value of the dipole operator calculated with this function has the desired properties. The expectation value of the dipole moment

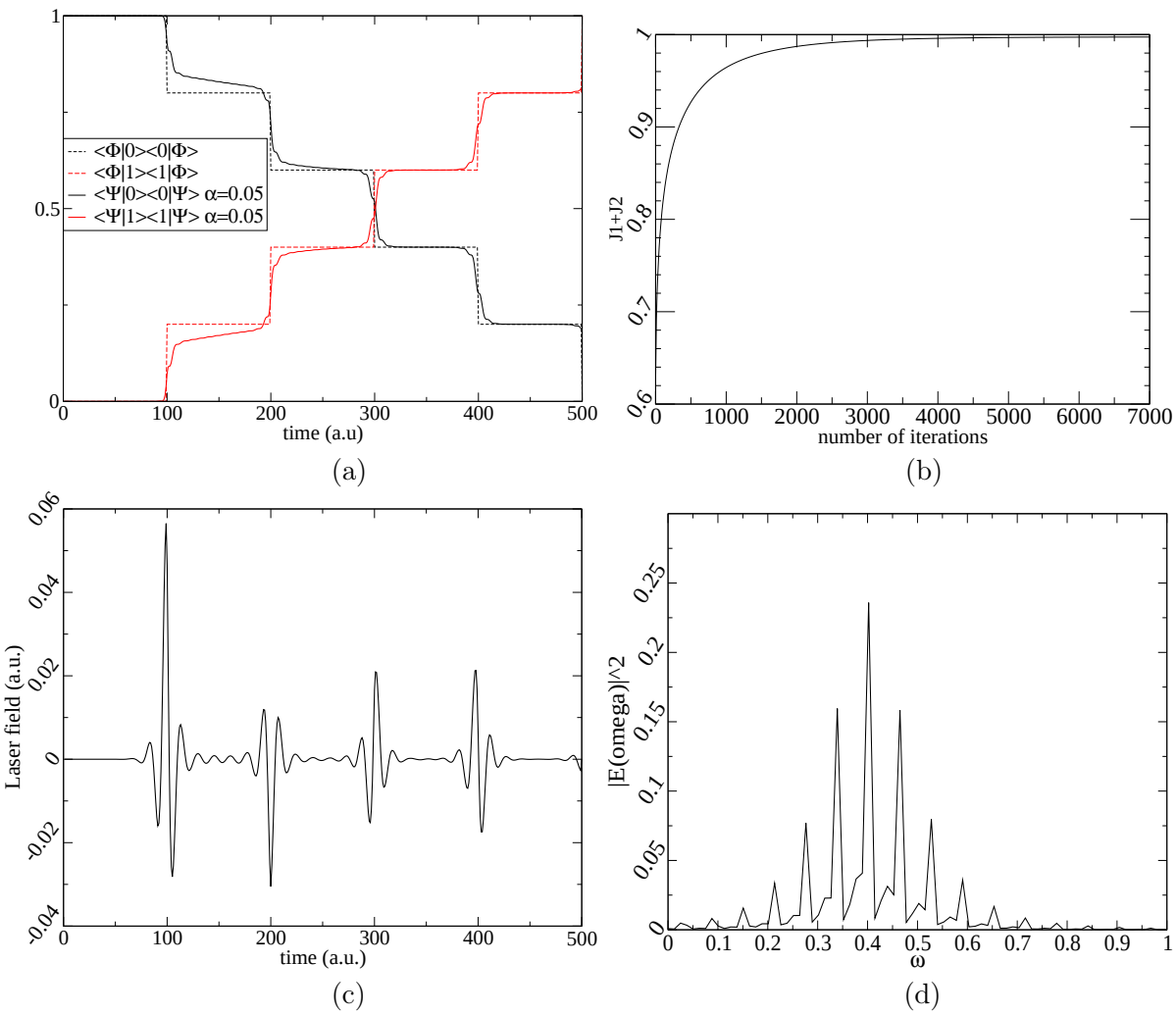


Figure 5.14: $|\Phi_0(t)|^2$, $|\Phi_1(t)|^2$,$|\Psi_0(t)|^2$ and $|\Psi_1(t)|^2$ (a), value of functional $J_1 + J_2$ (b), optimal field $E(t)$ (c) and its Fourier transform (d)

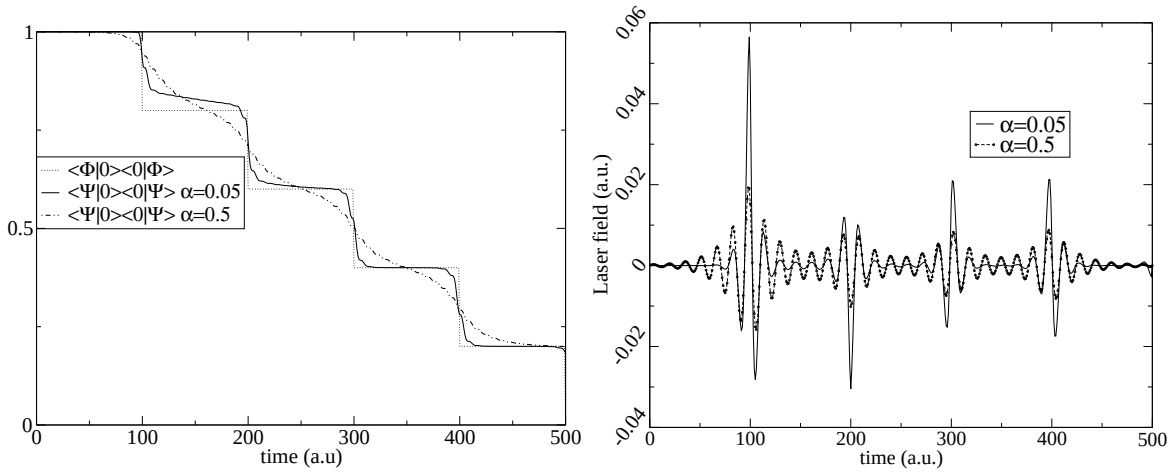


(a) (b)

Figure 5.15: $|\Phi_0(t)|^2$ and $|\Psi_0(t)|^2$ (a), optimal field (b) for different values of the penalty factor $\alpha$

operator in the two-level system is

$$\langle\Phi|\hat{\mu}|\Phi\rangle = 2\Re(\Phi_0^*\Phi_1\mu_{01}) \tag{5.60}$$
$$= 2\Re(\widetilde{\Phi}_0^*\widetilde{\Phi}_1\mu_{01}e^{i\omega_{01}t}), \tag{5.61}$$

where $\mu_{00} = \mu_{11} = 0$.

We define a target function with the goal to obtain a dipole moment that oscillates with the first, n$th$ and (n-2)$th$ harmonic of the frequency $\Omega$

$$\Phi_1(t) = \rho(t), \tag{5.62}$$
$$\Phi_0(t) = \sqrt{1-\rho^2(t)}, \tag{5.63}$$
$$\rho(t) = A\sin(\Omega\cdot t)\left(1+\frac{A}{2}\sin((n-1)\Omega\cdot t)\right). \tag{5.64}$$

In contrast to the previous sections we have chosen the wave-function $\Phi$, and not $\widetilde{\Phi}$ to be real. The reason for this is that in equation (5.61) the phase $e^{i\omega_{01}t}$ causes the dipole moment to oscillate also with the resonance frequency. We want to prevent this and use in equation 5.60 real functions for $\Phi_j$, $j = 0, 1$.

| $\mu_{01}$ | $\Delta t$ | $\omega_{01}$ | T | $\alpha$ | A | $\Omega$ | $n$ | $E_{guess}(t)$ |
|---|---|---|---|---|---|---|---|---|
| 1 | 0.0025 | 0.6 | 1000 | 0.0025 | 0.5 | 0.04 | 11 | $10^{-6}$ |

Table 5.7: Parameters for optimization of dipole moment

The algorithm reproduces the shape of the target (figure 5.16 (a) and (b)), at a smaller scale. The optimal field (f) is very strong. To obtain the target dipole moment, one would need an even stronger field, which could be obtained using a smaller value of the penalty factor $\alpha$. At the same time one would need to use a smaller time step $\Delta t$. The first, 9$th$ and 11$th$ harmonic of the frequency $\Omega$ are contained in the Fourier transform of the dipole

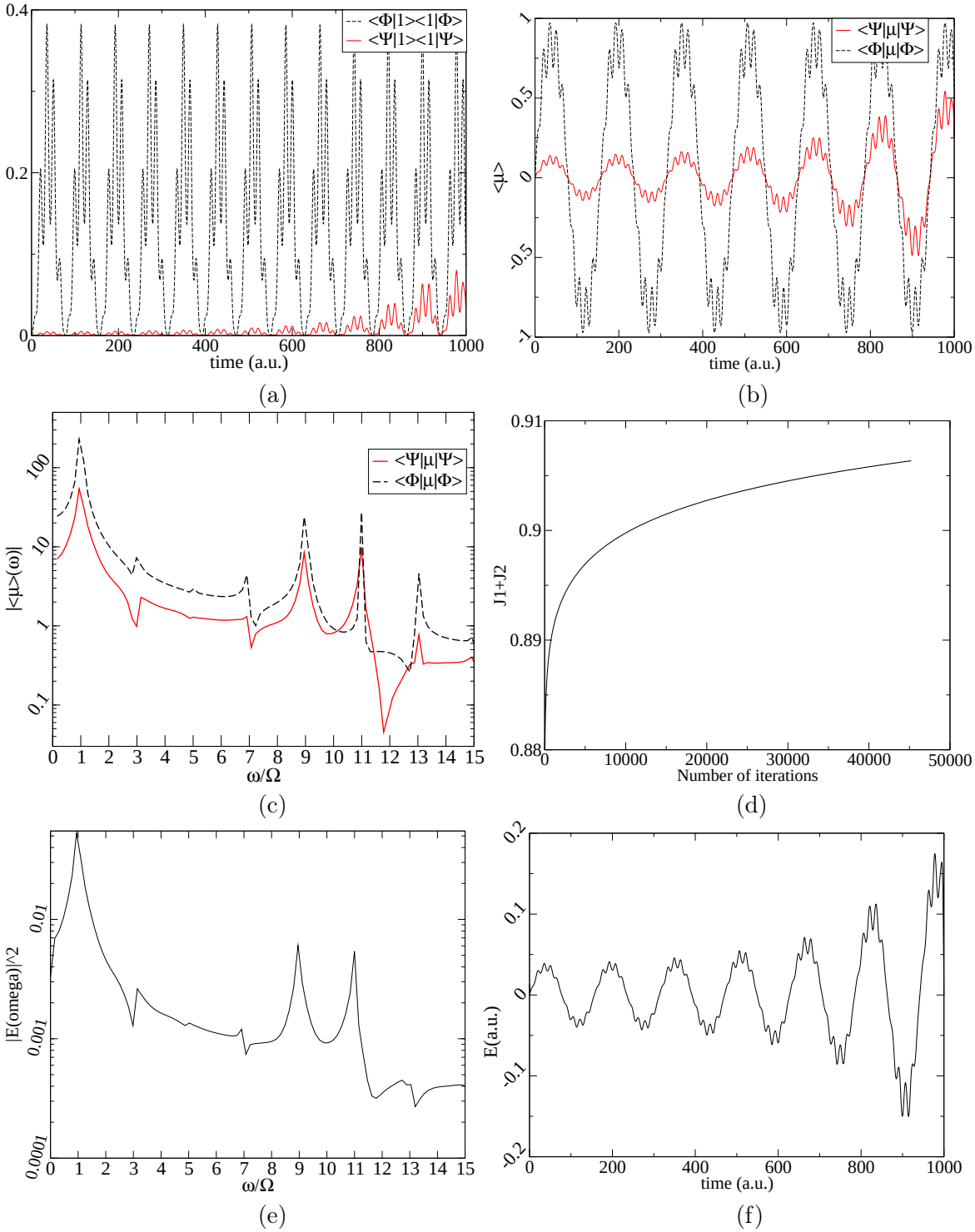


Figure 5.16: $|\Psi_1(t)|^2$ and$|\Phi_1(t)|^2$ (a), time-dependent dipole moment (b) and its Fourier transform (c), functional $J_1 + J_2$ (d), optimal field $E(t)$ (f) and its Fourier transform (e)

moment (figure 5.16(c)). The same frequencies are present in the Fourier transform of the field (see figure 5.16(e)). If one would wish to exclude the $9th$ and $11th$ harmonic of $\Omega$ form the spectrum of the external field $E$ one should impose a constraint on the frequencies of the field. A constraint in the Fourier space on the field would imply the knowledge of the field at *all* times. Since the iteration form chapter 4 relies on immediate feedback, it is incompatible with an constraint in the spectral domain.

We have constructed an "artificial" target wave-function, with no guarantee that it satisfies the Schrödinger equation. In this case the functional $J_1 + J_2$ does not reach its maximum value (figure 5.16(d)), and the convergence is very slow.

In this chapter we have applied on a very simple model the theory developed in chapters 2, 3 and 4. The two-level atom is a good test system, because the infinitesimal time evolution operator $\widehat{U}_{t_0}^{t}$ can be approximated very good. We have considered principle questions, as how does the parameter $\alpha$ affects the results and how we can find an optimal field with a given intensity.

We also presented two practical applications: the control of time-dependent occupation numbers and dipole moment. Here we have translated our goals into the optimization of wave-functions.

# Chapter 6

# Optimal control of a one dimensional hydrogen atom

Until now we have applied the theory developed in chapters 2, 3 and 4 to a very simple model, the two-level atom. This has numerical advantages, but remains a limited model. Since the method is very general, we can apply it to more complicated systems, which are more closely related to real systems.

We now apply the theory to a simplified, one-dimensional model of the hydrogen atom. We use the real space representation of the wave function on a numerical grid. The first part of this chapter is dedicated to the numerical methods used for the computations. In the second part we present the results obtained for this simplified hydrogen model. We use again the projection operator to control the time population of two or more eigenstates. Then we apply the method to an alternative type of operator.

## 6.1 Solution of the Schrödinger equation on the grid

In this section we present the method used to solve the homogeneous and inhomogeneous Schrödinger equation and we test it for two simple systems. Then we present the simplified model for the hydrogen atom, the method we use to obtain it's eigenstates, and make some considerations about the parameters to be used.

### 6.1.1 Split-operator method

To propagate the solution of the Schrödinger equation (2.28) we need an approximation for the infinitesimal time evolution operator

$$\widehat{U}_t^{t+\Delta t} = \mathcal{T} \exp\left(-i \int_t^{t+\Delta t} dt' \; \widehat{H}(t')\right). \tag{6.1}$$

We use the $2^{nd}$ order Split Operator method [39]: for small time intervals we can write

$$\widehat{U}_t^{t+\Delta t} \approx \exp\left(-i\Delta t \hat{H}(t)\right) = \exp(-i\left(\hat{T} + \hat{V}(t)\right)\Delta t) \tag{6.2}$$

Using the expression

$$e^{(A+B)\Delta t} = e^{A\Delta t/2} e^{B\Delta t} e^{A\Delta t/2} + \mathcal{O}(\Delta t^3), \tag{6.3}$$

for $A = \hat{T}$ and $B = V$, equation (6.2) becomes

$$\widehat{U}_t^{t+\Delta t} \approx \exp\left(-\frac{i}{2}\,\hat{T}\,\Delta t\right)\exp\left(-i\,\hat{V}(x,t)\,\Delta t\right)\exp\left((-\frac{i}{2}\,\hat{T}\,\Delta t\right) + \mathcal{O}(\Delta t^3). \tag{6.4}$$

Using (6.4) and $\hat{T} = -\nabla^2/2$, equation (3.9) becomes

$$\Psi(x,t+\Delta t) = \exp\left(-\frac{\Delta t}{4i}\nabla^2\right)\exp\left(-i\Delta t V(x,t)\right)\exp\left(-\frac{\Delta t}{4i}\nabla^2\right)\Psi(x,t). \tag{6.5}$$

Writing

$$\hat{T}\Psi(x,t) = -\frac{1}{2}\nabla^2\Psi(x,t), \tag{6.6}$$

we can use for $\Psi(x,t)$ the representation in the Fourier space

$$\begin{aligned}\hat{T}\Psi(x,t) &= -\frac{\nabla^2}{2}\int dk\, e^{-ikx}\Psi(k,t) = \int dk\, e^{-ikx}\frac{k^2}{2}\Psi(k,t)\\ &= [\mathfrak{F}\mathfrak{T}]^{-1}\left(\frac{k^2}{2}\cdot[\mathfrak{F}\mathfrak{T}]\left(\Psi(x,t)\right)\right),\end{aligned} \tag{6.7}$$

where $[\mathfrak{F}\mathfrak{T}]$ denotes the Fourier transform. Using the fact that the kinetic energy operator $\hat{T} = -\nabla^2/2$ and also $e^{-i\hat{T}/2}$ is diagonal in momentum space and the potential $V(x,t)$ and its exponential function are diagonal in the real space, equation (6.5) becomes

$$\begin{aligned}\Psi(x,t+\Delta t) &= [\mathfrak{F}\mathfrak{T}]^{-1}\Bigg[\exp\left(\frac{\Delta t k^2}{4i}\right)\cdot[\mathfrak{F}\mathfrak{T}]\Bigg[\exp\left(-i\Delta t V(x,t)\right)\cdot[\mathfrak{F}\mathfrak{T}]^{-1}\Big(\exp\left(\frac{\Delta t k^2}{4i}\right)\\ &\cdot\ [\mathfrak{F}\mathfrak{T}]\Psi(x,t)\Big)\Bigg]\Bigg] + \mathcal{O}((\Delta t)^3).\end{aligned} \tag{6.8}$$

In chapter 3 we have shown that

$$\chi(x,t+\Delta t) = \widehat{U}_t^{t+\Delta t}\left(\chi(x,t) + \int_t^{t+\Delta t} d\tau\,\widehat{U}_\tau^t f(x,\tau)\right). \tag{6.9}$$

For the time integral we use the simplest approximation

$$\int_t^{t+\Delta t} d\tau f(\tau) = \Delta t f(t) + \mathcal{O}(\Delta t^2), \tag{6.10}$$

so that the approximate solution of the inhomogeneous equation becomes

$$\chi(x,t+\Delta t) \approx \widehat{U}_t^{t+\Delta t}\left(\chi(x,t) - \frac{\Delta t}{T}\widehat{O}_t^{(1)}\Psi(x,t)\right). \tag{6.11}$$

We can propagate the Lagrange multiplier using the split-operator method for the infinitesimal time evolution operator

$$\begin{aligned}\chi(x,t+\Delta t) &\approx \exp(-\frac{i}{2}\,\hat{T}\,\Delta t)\exp(-i\,\hat{V}(x,t)\,\Delta t)\exp(-\frac{i}{2}\,\hat{T}\,\Delta t)\cdot\\ &\cdot\ \left(\chi(x,t) - \frac{\Delta t}{T}\widehat{O}_\tau^{(1)}\Psi(x,\tau)\right) +\\ &+\ \mathcal{O}((\Delta t)^2).\end{aligned} \tag{6.12}$$

The errors of the propagation of $\Psi$ due to split-operator method are of order $(\Delta t)^3$. For the propagation of $\chi$ the errors are of order $(\Delta t)^2$ due to the approximation for the time integral. In the calculations performed in this thesis we found this approximation to be sufficient.

### 6.1.2 Test of the numerical solution of the inhomogeneous Schrödinger equation

In section 3.2 we derived the analytical solution of the inhomogeneous Schrödinger equation for a particular type of inhomogeneity. Using this result we can test the numerical solution of the inhomogeneous Schrödinger equation. In appendix D one can find the analytical solution of the homogeneous Schrödinger equation for the free particle and the harmonic oscillator in an external field.

#### Free particle

For the free particle wave-function we choose a Gaussian distribution in momentum space, with the center at $k_0 = 0.05$ and a width of $\Delta_k = 0.05$. We consider an inhomogeneity of the form $\Psi(x,t)$ i.e. $\widetilde{f}(t) = 1$ in equation 3.28 and an initial state $\chi(x,t_0) = 0$, so that the norm of $\chi(x,t)$ must grow quadratically with time as one can read in equation (3.33), see figure 6.1 (a). To evaluate the errors we define

$$\Delta_a(t) = \frac{\int dx(|\chi(x,t)| - |\chi_a(x,t)|)^2}{\int dx|\chi_a(x,t)|^2}, \tag{6.13}$$

$$\Delta_r(t) = \frac{\int dx(\Re\chi(x,t) - \Re\chi_a(x,t))^2}{\int dx|\chi_a(x,t)|^2}. \tag{6.14}$$

where $\chi_a$ and $\chi$ are the analytical and numerical solution (compare appendix D). We find

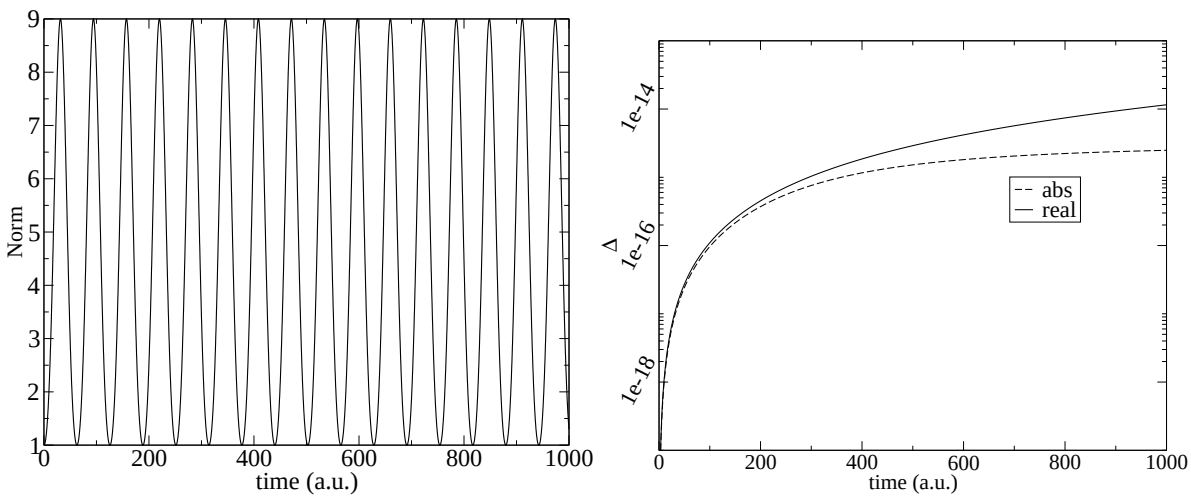


(a) (b)

Figure 6.1: $\Delta_a(t)$ and $\Delta_r(t)$ The norm of the analytical solution $\chi_a$ (a), $\Delta_a(t)$ and $\Delta_r(t)$ (b) ($x \in [-500, 500]$, $N = 2048$ points, $\Delta t = 0.01$ a.u.)

very good agreement between the analytical and numerical solution. We see in figure 6.1 (b) that the errors of the real part of the wave function are larger than the errors of the norm, but both are very small. The phase of the wave-function is more sensitive to numerical errors.

**Harmonic oscillator in an external field**

For the harmonic oscillator we choose $\omega = \sqrt{k} = \sqrt{2}$ and $\alpha = \sqrt{2}$. To analyze the errors we define

$$\Delta_n(t) = \frac{|\langle\chi_a(t)|\chi_a(t)\rangle - \langle\chi_{num}(t)|\chi_{num}(t)\rangle|}{\langle\chi_a(t)|\chi_a(t)\rangle}. \tag{6.15}$$

For the inhomogeneity of the Schrödinger equation for $\chi$ (3.28) we choose

$$f(t) = \omega_{inh}\sin(\omega_{inh}t), \tag{6.16}$$

$$\omega_{inh} = 0.1, \tag{6.17}$$

and as initial state for $\chi$ we start with $\chi(x,0) = \Psi(x,0)$, where the initial state of the wave function is the ground state of the harmonic oscillator. The external field has the amplitude $A = 0.05$ and frequency $\omega_0 = 0.03$. Using (3.33) we obtain

$$\chi_a(x,t) = (2 - \cos(\omega_{inh}t))\Psi_a(x,t). \tag{6.18}$$

We propagate both the homogeneous and the inhomogeneous equations from $t = 0$ to $t = T$ using equation (6.12)on a grid $x \in [-50, 50]$ with $N = 1024$ points. Looking at figure 6.2 we

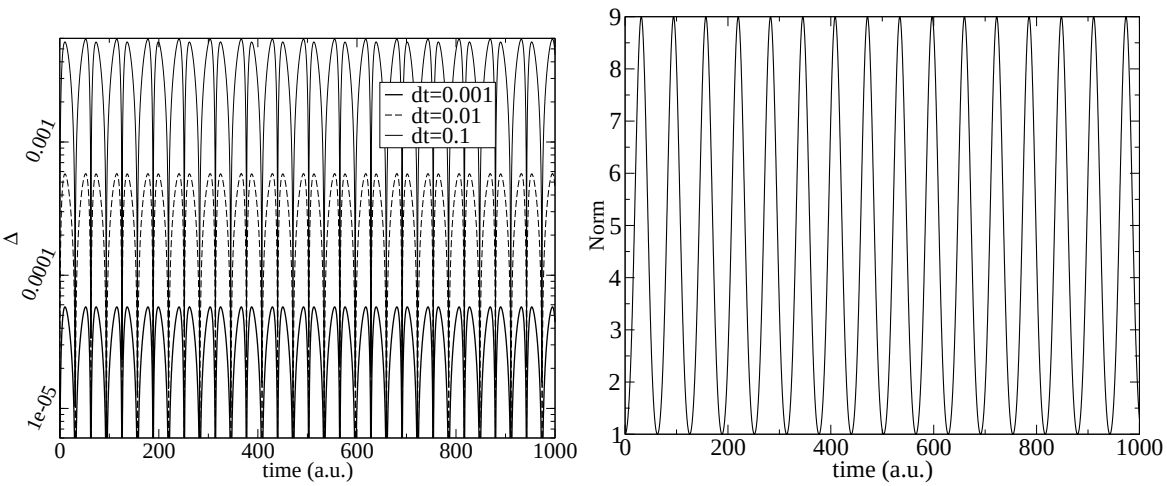


(a) (b)

Figure 6.2: $\Delta_n$(t) for different time steps $dt$ and the norm of the exact $\chi$

can see that the errors are linear in $\Delta t$. This is the consequence of the approximation of the integral, where we have an error $\mathcal{O}((\Delta t)^2)$ in every time step. For the whole time interval we have $n = T/\Delta t$ time steps so that the total error of the integral is proportional $\Delta t$.

### 6.1.3 "Soft" Coulomb potential

The field free Hamiltonian for the hydrogen atom is

$$\widehat{H}_0 = \widehat{T} + V(\vec{r}) \tag{6.19}$$

where $\widehat{T}$ is the kinetic energy operator and

$$V(\vec{r}) = -\frac{1}{\sqrt{x^2+y^2+z^2}}. \tag{6.20}$$

We consider only a one dimensional model

$$V(x) = -\frac{1}{x}, \tag{6.21}$$

which is less expensive to calculate. To avoid the singularity at $x = 0$, we approximate the potential $V$ following [40], with the function

$$V(x) = -\frac{Q}{\sqrt{x^2+a^2}}. \tag{6.22}$$

This is a so-called "soft" Coulomb potential (see figure 6.3). The parameters $a$ and $Q$ are introduced to remove the singularity at $x = 0$ and to adjust the depth of the potential well. For the calculations used here $Q = a = 1$.

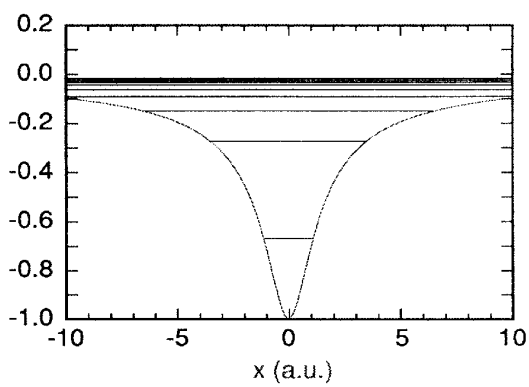


Figure 6.3: Potential V(x) of the 1D model for the hydrogen atom. The first few eigenlevels are drawn to scale with the potential (from [40]).

### 6.1.4 Ground state of the "soft" Coulomb potential

An arbitrary normalized time dependent wave function can be expressed as a linear combination of eigenstates of the field free Hamilton operator with time dependent coefficients

$$\Psi(x,t) = \sum_{n=0}^{\infty} c_n(t) e^{-iE_n t} \psi_n(x), \tag{6.23}$$

$$E_n < 0 \tag{6.24}$$

where we may replace $t$ with $-it$

$$\Psi(x,-it) = \sum_{n=0}^{\infty} c_n(t) e^{-E_n t} \psi_n(x). \tag{6.25}$$

The eigenenergies of $\widehat{H}_0$ satisfy the relation $E_0 < E_1 < \ldots E_n$, and $e^{-E_n t} > e^{-E_m t}$ for $n < m$. Thus, in imaginary time, the state with the lowest energy suffers less damping than the excited states. We begin with an arbitrary function and similar to the real time propagation, we use the split operator method to propagate in imaginary time. Due to the exponential damping it is necessary to re-normalize the wave function in each step. After a number of steps we obtain the ground state wave function. To find the first excited state, one subtracts the ground state component from the initial arbitrary wave function and repeats the whole procedure. Similarly one can obtain the other excited states.

The advantage of this procedure is that we obtain the eigenstates of the numerical (rather than the exact) Hamiltonian used for the propagation.

### 6.1.5 Absorbing boundaries

If one uses strong external fields (for example strong laser pulses) the atom can be ionized. In this case it is possible that the wave function reaches the boundary of the grid and reenters the grid form the opposite side due to the Fourier transform that imposes periodic boundary conditions. One way to avoid this effect is the use of absorbing boundaries [41]. In order to achieve this we multiply the real space wave function in every time step with a mask $\boldsymbol{M}(x)$, which falls off from 1 in the last 10% of the grid to zero at the grid boundary.

$$\begin{aligned}\Psi(x,t+\Delta t) &= [\mathfrak{F}\mathfrak{T}]^{-1}\left[\exp\left(\frac{\Delta t k^2}{4i}\right)\cdot[\mathfrak{F}\mathfrak{T}]\left[\boldsymbol{M}(x)\exp\left(-i\Delta t V(x,t)\right)\cdot[\mathfrak{F}\mathfrak{T}]^{-1}\left(\exp\left(\frac{\Delta t k^2}{4i}\right)\right.\right.\right.\\ &\cdot\ \left.\left.\left.[\mathfrak{F}\mathfrak{T}]\boldsymbol{M}(x)\Psi(x,t)\right)\right]\right], \qquad (6.26)\end{aligned}$$

where

$$f(x) = \begin{cases}\left[\cos\left(\frac{\pi}{2}\frac{x_{min}+\xi-x}{\xi}\right)\right]^{\gamma} & x\in[x_{min},x_{min}+\xi]\\ \left[\cos\left(\frac{\pi}{2}\frac{x-(x_{max}-\xi)}{\xi}\right)\right]^{\gamma} & x\in[x_{max}-\xi,x_{max}]\\ 1 & x\in(x_{min}+\xi,x_{max}-\xi)\end{cases}. \qquad (6.27)$$

The parameter $\xi$ determines the width of the absorption region and $\gamma$ the slope of the function in this region. Typical values for these parameters used in the calculations are $\xi = (x_{max} - x_{min})/10$ and $\gamma = 0.125$. With this choice of $\gamma$ and $\xi$ the reflection is negligible in the models we used. The use of the mask function may lead to decrease of the norm, if a part of the electronic density leaves the grid.

With a grid spacing $\Delta x$, the momentum-space grid is $[-p_{max}, p_{max}]$ with $p_{max} = \pi/\Delta x$. This value must be larger than the maximum momentum of the electron. The size of the grid must be large enough to contain the motion of the wave function in the electric field.

With a time step $\Delta t$ the maximum representable frequency is $\omega_{max} = \pi/\Delta t$. This value must be larger than the frequency difference corresponding to the difference between the maximum energy and the ground state energy. The maximum energy depends again on the strength and frequency of the field.

### 6.1.6 Modified iterative scheme

For the propagation of the Lagrange multiplier $\chi_k$ we need to know the wave function $\Psi_k$, not only to compute the field but also for the inhomogeneity. To avoid the storage of $\Psi_k(x,t)$, we

propagate it simultaneously with $\chi_k$. Similarly, to propagate $\Psi_{k+1}$ one needs to know $\chi_k$ in order to calculate the field, therefore we propagate $\chi_k$ together with $\Psi_{k+1}$. But to propagate $\chi_k$ one needs again $\Psi_k$, thus we need to propagate also $\Psi_k$. Thus we must include three more propagations in the iterative scheme of equations (4.6)-(4.7).

$$
\begin{array}{lll}
\textit{Step} & 0. & \boldsymbol{\Psi_1(0)} \xrightarrow{E_1} \Psi_1(T) \\
\textit{Step} & k. & \left[\Psi_k(T) \xrightarrow{E_k} \Psi_k(0)\right] \\
 & & \boldsymbol{\chi_k(T)} \xrightarrow{\widetilde{E}_k,\, \Psi_k} \chi_k(0) \\
 & & \left[\chi_k(0) \xrightarrow{\widetilde{E}_k,\, \Psi_k} \chi_k(T)\right] \\
 & & \left[\boldsymbol{\Psi_k(0)} \xrightarrow{E_k} \Psi_k(T)\right] \\
 & & \boldsymbol{\Psi_{k+1}(0)} \xrightarrow{E_{k+1}} \Psi_{k+1}(T)
\end{array}
\tag{6.28}
$$

Bold symbols indicate variables that are known analytically from equations (2.27) and (2.29). The fields used for the propagation are as before given in equations (4.12) and (4.17).

## 6.2 Results

In this section we use some of the operators used in chapter 5 and, extend the applications of the projection operator and apply the optimization to the hydrogen atom. Then we study a local operator, which permits us to control the movement of the electronic density. With this operator we calculate also the generalized functional of section 4.3.

### 6.2.1 Projection operator

The operator we use now is

$$\widehat{O}_t^{(1)} = |\Phi(t)\rangle\langle\Phi(t)|. \tag{6.29}$$

Similar to the two-level atom, it may be used to impose the behavior of the time-dependent occupation numbers of the eigenstates of the field-free Hamiltonian.

The operator $\widehat{O}^{(2)}$ is zero, so that the initial state of the Lagrange multiplier is also zero, $\chi(x,T) = 0$.

#### Population control of ground and first excited state

In the following section we use one of the projection operators which we already studied for the two-level system and transfer it to the present case of the 1D hydrogen atom. We define the target wave-function as

$$\Phi(x,t) = \Phi_0(t)|0\rangle + \Phi_1(t)|1\rangle, \tag{6.30}$$

$$\Phi_0(t) = e^{i\omega_0 t}\rho, \tag{6.31}$$

$$\Phi_1(t) = e^{i\omega_1 t}\sqrt{1-\rho^2}. \tag{6.32}$$

$|0\rangle$ and $|1\rangle$ here are ground and first excited state of the hydrogen atom in "soft" Coulomb approximation, respectively. For the absolute value of the time-dependent coefficients $\Phi_0(t)$ and $\Phi_1(t)$ we have chosen the same functions as in section 5.3.4:

$$\rho(t) \quad = \quad \begin{cases} \sqrt{\frac{2t}{T}} & t \in [0, T/2] \\ \sqrt{\frac{t-T/2}{T/2}} & t \in (T/2, T] \end{cases} . \tag{6.33}$$

The algorithm iterated until the difference in $\delta\mathcal{L}$ was smaller than $\varepsilon$.

| Grid | N | $\alpha$ | $\Delta t$ | T | $E_{guess}(t)$ | $\varepsilon$ |
|---|---|---|---|---|---|---|
| [-500, 500] | 2048 | 1.5 | 0.01 | 1500 | $10^{-3}$ | $10^{-5}$ |

Table 6.1: Parameters for the population control of the first two states of the 1D hydrogen atom

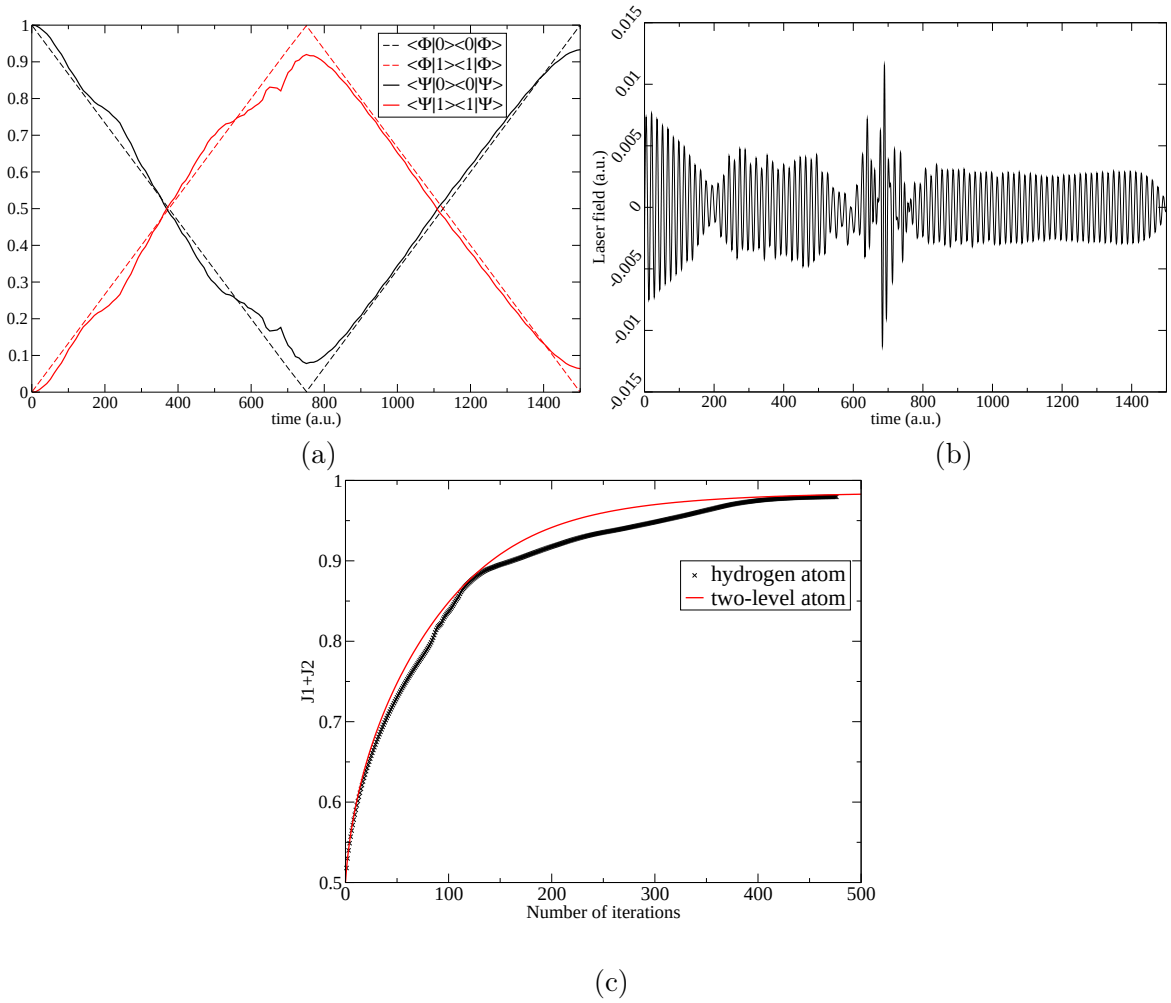


Figure 6.4: Target and optimal population of the ground and first excited state (a), optimal field (b), functional $J_1 + J_2$ (c)

We observe in figure 6.4 that the results are not as good as in the case of the two-level system. We expect the same structure because no other levels are involved. The optimal field (b) has, at least in the second half of the time interval a structure similar to corresponding one of of the two-level system (see figure 6.5 (b)) . In the first half of the time interval there appears to be little correspondence between the shape of the optimal field calculated in the two-level system and the one form the hydrogen atom.

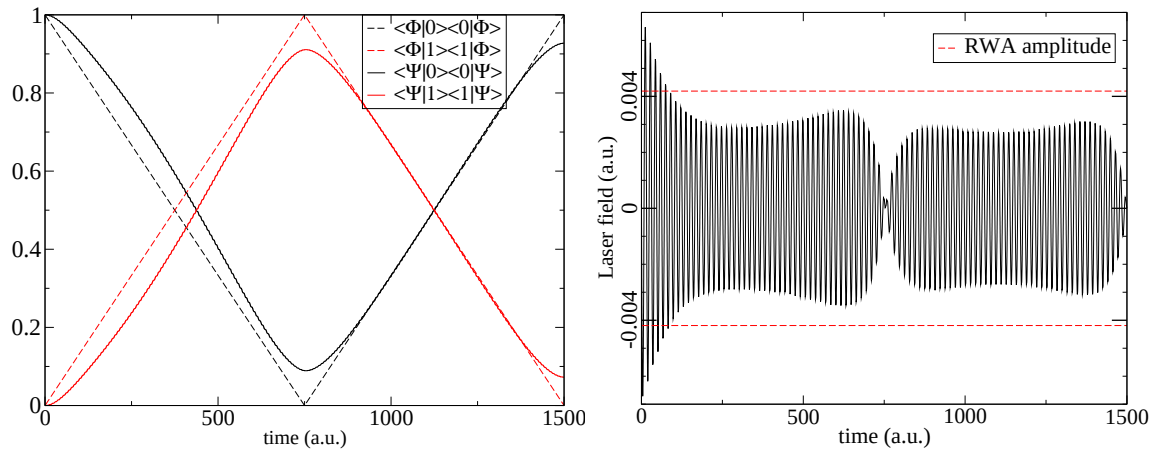


(a) (b)

Figure 6.5: Target and optimal population of the ground and first excited state (a), optimal field (b) calculated in the two-level atom, with $\alpha$ and $T$ given in table 6.1, after 500 iterations.

By comparing the results in the two-level atom and "soft" Coulomb potential one can see that the numerical errors are larger in the case of the real space calculation. The evolution of the functional $J_1 + J_2$ over iterations in (c) does not have the same smooth shape as in the two-level system, which probably is also a sign of numerical errors. From experience with the two-level system we know that the last few percents of the overlap are reached over a very large number of iterations, which in the present case of a grid calculation, are numerically much more expensive that in the two-level system. Although after almost 500 iterations the overlap reaches the value 0.98, the functional still grows monotonic.

### Control of population of the first three levels

In the "soft" Coulomb system we have an infinite number of levels, for which we can in principle do the same type of population control as used in section 5.3. We consider the first three eigenstates of the field free Hamiltonian and define as target

$$\Phi_1(t) = \sqrt{\exp\left(-\frac{(t-T)^2}{2(T/\sigma)^2}\right)}, \tag{6.34}$$

$$\Phi_0(t) = \begin{cases} \sqrt{1-\Phi_1^2(t)} & t < T/2 \\ 0 & t \geq T/2 \end{cases}, \tag{6.35}$$

$$\Phi_2(t) = \begin{cases} \sqrt{1-\Phi_1^2(t)} & t \geq T/2 \\ 0 & t < T/2 \end{cases}. \tag{6.36}$$

As we know form atom physics the direct transition $|0\rangle \rightarrow |2\rangle$ is forbidden. Therefore, we force the system to use an intermediary state, namely $|0\rangle$, since both transitions $|0\rangle \rightarrow |1\rangle$ and $|1\rangle \rightarrow |2\rangle$ are permitted.

| Grid | N | $\alpha$ | $\Delta t$ | T | $E_{guess}(t)$ | $\varepsilon$ | $\sigma$ |
|---|---|---|---|---|---|---|---|
| [-200, 200] | 1024 | 4 | 0.005 | 1200 | 0 | $10^{-7}$ | 7 |

Table 6.2: Parameters for the three level population control of the 1D hydrogen atom

In figure 6.6 one can see the imposed and calculated population of the three considered eigenstates (a). The absolute value of the calculated time-dependent wave-function$|\Psi(x,t)|$ is plotted in figure 6.6 (b). Vertical slices of this plot give graphs of $\Psi(x)$ at fixed time, where $\Psi(x)$ can be decomposed in the three eigenfunctions. In (c), (d) and (e) is plotted $|\Psi(x,t)|$ for $t = 0, T/t, T$. At $t = 0$, $\Psi(x)$ is the ground state, in agreement with (a) where the population of $|0\rangle$ has the value 1. At $t = T/2$ $\Psi$ becomes the first excited state and at $t = T$ it is the second excited state.

The optimal field (figure 6.7 (a)) oscillates in the first half of the time interval with the resonance frequency $\omega_{01} = \omega_1 - \omega_0$, where $\omega_i$ is the eigenenergy of state $i$. In the second part of the time interval the field oscillates with $\omega_{12}$, the resonance frequency between the first and second excited states. This was to be expected quantitatively from quantum theory describing the transitions between quantum states.

The functional converges monotonically as one can see in figure 6.8.

### 6.2.2 Local operator

A type of operator that can be used only in the real space representation is e.g. an $x$ dependent function. If we want to control the time-dependent density, we can define as operator

$$\widehat{O}_t^{(1)} = f(x,t) = T\delta(x - r(t)), \tag{6.37}$$

By inserting this operator in the functional $J_1$ we obtain

$$\begin{aligned} J_1 &= \int_0^T dt \;\; n(r(t),t) \\ n(x,t) &= \Psi^*(x,t)\Psi(x,t) \end{aligned} \tag{6.38}$$

in other words we want to maximize the density along the curve $r(t)$.

The dipole moment operator is not a positive definite operator. We can use the operator in equation (6.37) to control the movement of density. $\hat{x} = \hat{\mu}/q$, where $\hat{\mu}$ is the dipole moment operator, mimics this movement of the density, so we can use the operator (6.37) to control the time-dependent dipole moment. The control of time dependent dipole operator has application for example in the process of high harmonic generation.

One could apply the the control of operator $\widehat{O}_t^{(1)}$ (equation (6.37)) to transfer the electronic density of an atom or molecule from a point $A$ on the potential surface to a point $B$ and avoid a given region on the way from $A$ to $B$.

In this section we examine if we can use the local operator to control the time dependent expectation value of $\hat{x}$. To generate the function $r(t)$ we choose a field

$$E_{target}(t) = A\sin(\omega \cdot t)\exp\left(-\frac{(t - T/2)^2}{2(T/\sigma)^2}\right). \tag{6.39}$$

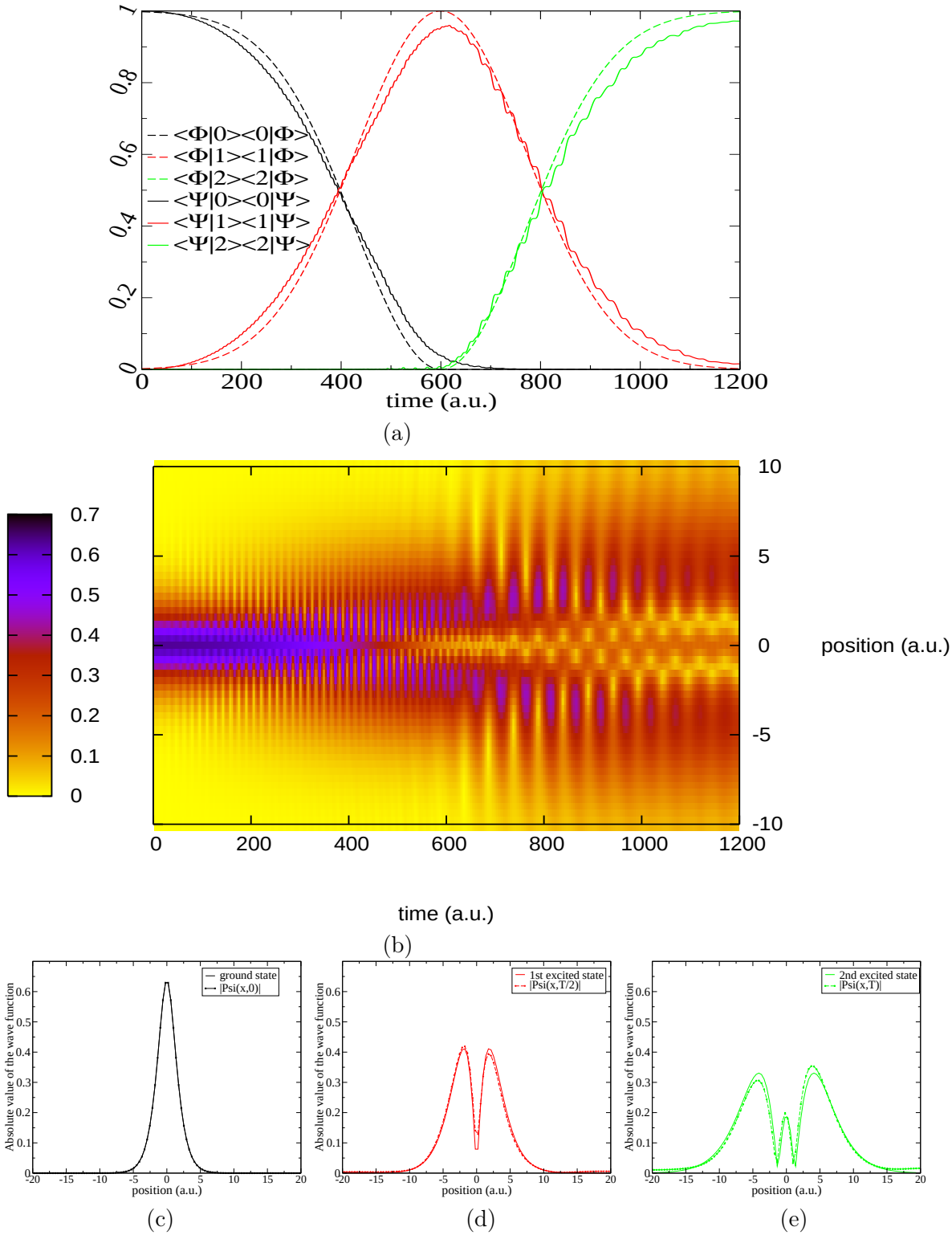


Figure 6.6: Projection of $\Psi$ and $\Phi$ on the ground and first two exited states (a), $|Psi(x,t)|$ as a function of both $x$ and $t$ (b), vertical cuts throught (b) at different times $t = 0$ (c), $t = T/2$ (d) and $t = T$ (e)

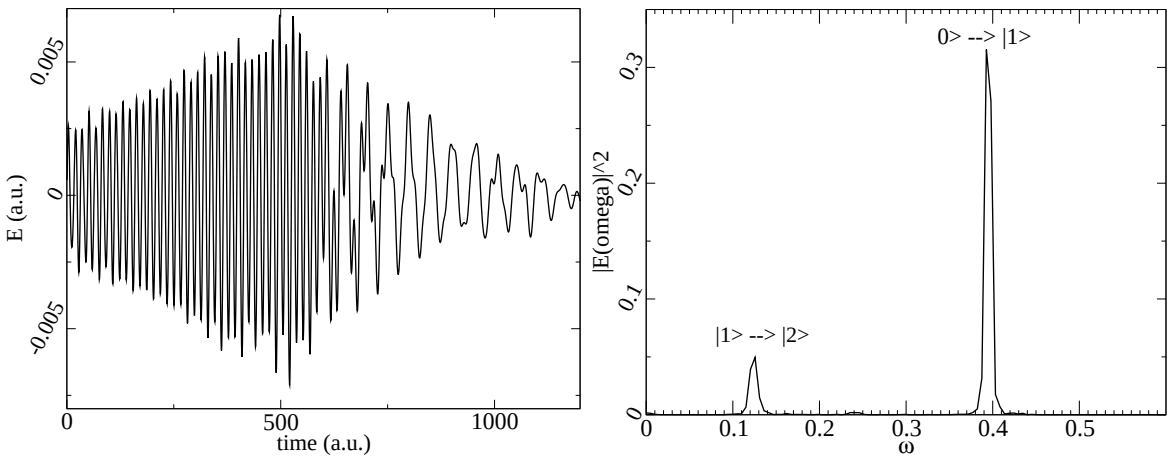


(a) (b)

Figure 6.7: Optimal field (a) and its Fourier transform (b)

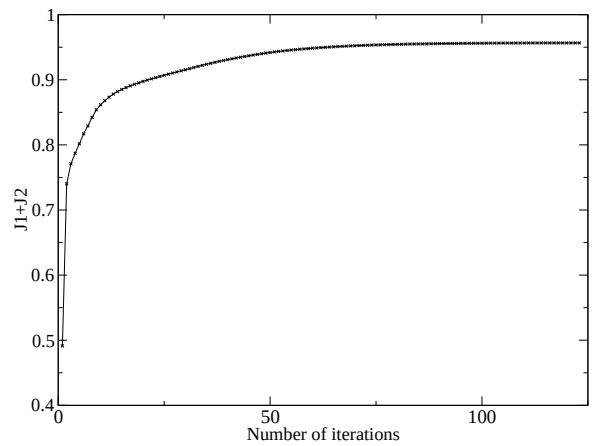


Figure 6.8: Functional $J_1 + J_2$

With this field we solve the Schrödinger equation, calculate the expectation value $\langle x \rangle$, and set

$$r(t) \quad = \quad \langle \Psi(t)|x|\Psi(t)\rangle. \tag{6.40}$$

The delta-function is approximated by

$$\delta(x - r(t)) \quad \approx \quad \sqrt[4]{\frac{\gamma}{\pi}} e^{-(x-r(t))^2\gamma}. \tag{6.41}$$

| Grid | N | $\alpha$ | $\Delta t$ | T | $E_{guess}(t)$ | $\varepsilon$ | $\gamma$ | A | $\omega$ | $\sigma$ |
|---|---|---|---|---|---|---|---|---|---|---|
| [-500,500] | 2048 | 0.5 | 0.005 | 300 | $10^{-3}$ | $10^{-6}$ | 25 | 0.03 | 0.12 | 6 |

Table 6.3: Parameters for the optimization of the time-dependent density

In figure 6.9 (a) we see that the expectation value $\langle x \rangle$ calculated with the optimal field follows the target $r(t)$. This is a consequence of the fact that the maximum of the density

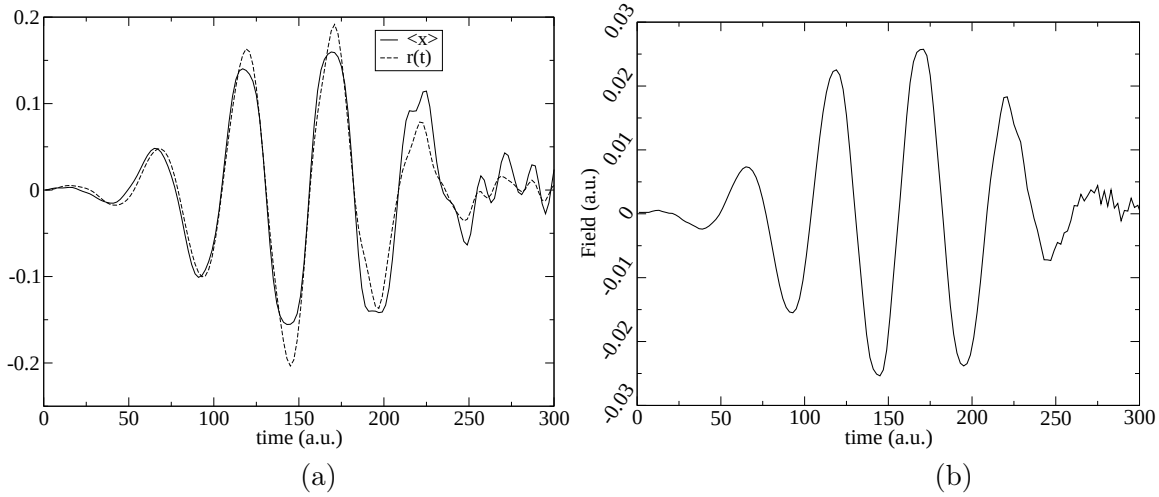


Figure 6.9: Expectation value $\langle x \rangle$ with the calculated wave-function and target $r(t)$ (a) and optimal field (b)

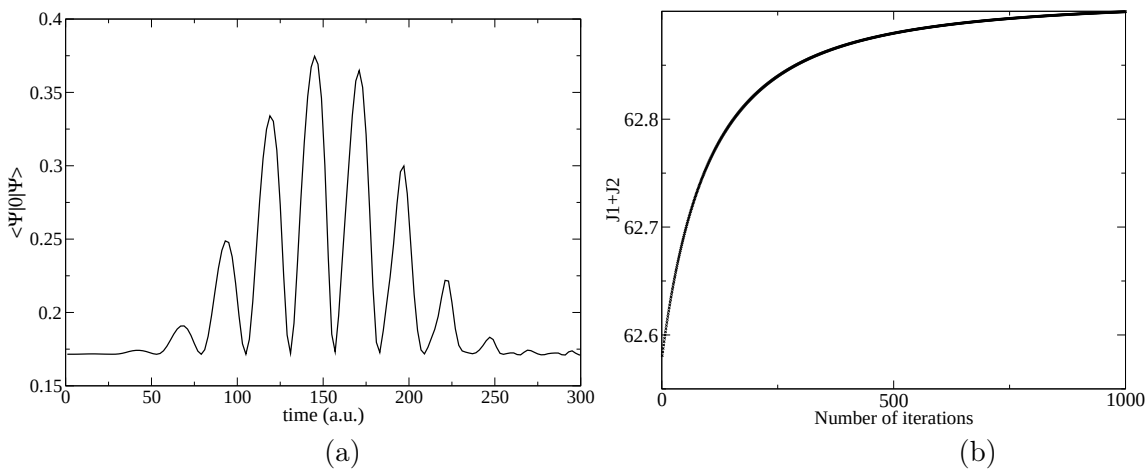


Figure 6.10: Expectation value of the time-dependent operator $\langle \Psi | \widehat{O} | \Psi \rangle$ (a) and value functional $J_1 + J_2$ (b)

approximatively corresponds to the expectation value of position operator $x$. We do not obtain a perfect correspondence between $\langle x \rangle(t)$ and $r(t)$, but the results confirm our expectation that $\langle x \rangle(t)$ should mimic $r(t)$. Thus, our method to control the expectation value of $\hat{x}$ is appropriate if we want to prescribe the approximative trajectory. The advantage of this approach with respect to tracking control is that the optimal field remains in the space of admissible control fields, i.e. has no singularities. Our algorithm is able to produce a physically reasonable field, given only a time-dependent target function. The optimal field (figure 6.10 (b)) is similar to the target generating field.

In figure 6.10 (a) one can see the density along the curve $r(t)$, $\langle \Psi(t) | \widehat{O}_t^{(1)} | \Psi(t) \rangle$, which is the quantity that we actually optimize. It has maxima at the points where $|r(t)|$ has maxima.

The convergence of the functional (figure 6.9 (a)) shows the same behavior as in the previous calculations. But in this system we are far from reaching 100%, since this would

mean that the whole electronic density is concentrated at $r(t)$ at time $t$. This is also the reason why we included the factor $T$ in the operator, so that $J_1$ weighs more in comparison to $J_3$. It follows that the maximal value of the functional $J_1 + J_2$ is $T$. The increase of the functional is very small, less then 1% of the maximal value which is $T$. For this calculation we used a smaller time step than usual, because one needs higher accuracy to obtain a monotonic convergent functional. The quite small differences in the functional $\mathcal{L}$ between two iterative steps make this more difficult.

### Generalized functional

For this particular type of operator we want to compare the results we obtain if we use the general functional of the form (4.33) instead of functional (2.6). For the power $n$ of the integrand we choose values between 1 and 5.

| Grid | N | $\alpha$ | $\Delta t$ | T | $E_{guess}(t)$ | $\varepsilon$ | $\gamma$ | A | $\omega$ | $\sigma$ |
|---|---|---|---|---|---|---|---|---|---|---|
| [-500,500] | 2048 | 0.5 | 0.005 | 300 | $10^{-3}$ | $10^{-6}$ | 25 | 0.03 | 0.12 | 6 |

Table 6.4: Parameters for the optimization of the generalized functional

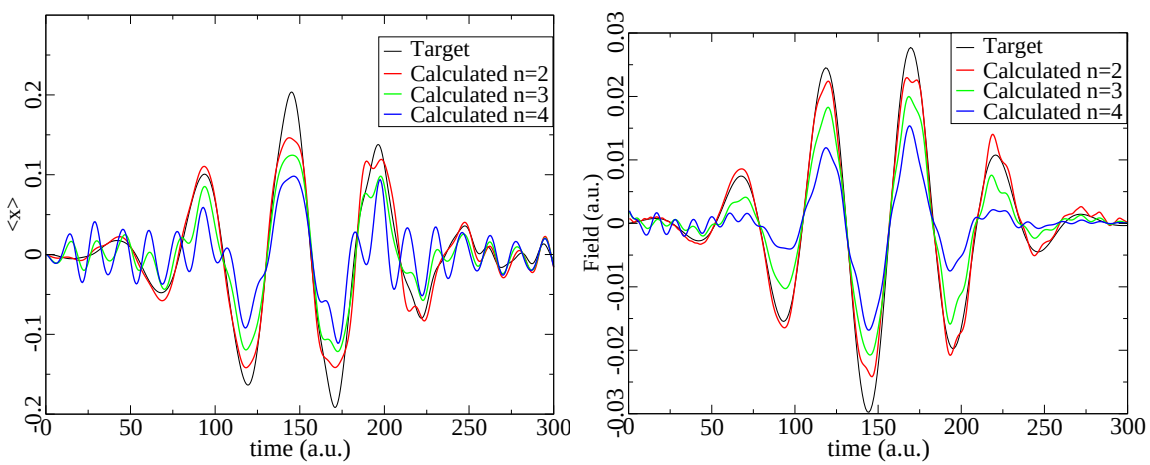


(a) (b)

Figure 6.11: Dipole moment (a) and optimal field (b) for different exponents $n$

In figure 6.11 we observe that for increasing value of the exponent $n$ the quality of the results decreases. We can understand this if we consider the values of the integrand in equation (4.33), which are smaller than one. Therefore, for larger values of the exponent $n$ this will result in a less favorable weight of $J_1$ against the other parts of the functional.

### Double-well

As a final example we want to apply the control of a local operator in a different system. All the considerations above remain valid if we replace the "soft-Coulomb" potential by a double-well potential, see fig.6.12 (a). In this system, the ground state density is equally distributed

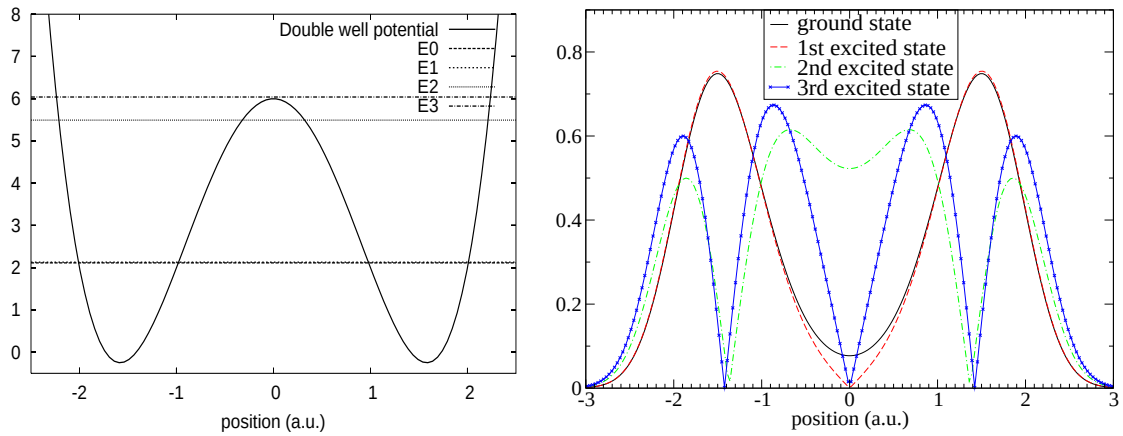


(a) (b)

Figure 6.12: Double-well potential $V(x) = ax^4 - bx^2 + b^2/(4a)$, $a = 1$ and $b = 5$, and the first four eigenenergies (a) and the density of the first four eigenstates (b).

| State | Energy (a.u.) |
|---|---|
| ground state | 2.114236 |
| $1st$ excited state | 2.130888 |
| $2nd$ excited state | 5.493239 |
| $3rd$ excited state | 6.039324 |

Table 6.5: Eigenenergies of the first four eigenstates

| Grid | N | $\alpha$ | $\Delta t$ | T | $E_{guess}(t)$ | $\varepsilon$ | $\gamma$ |
|---|---|---|---|---|---|---|---|
| [-32,32] | 512 | 10 | 0.01 | 250 | 0 | $10^{-3}$ | 15 |

Table 6.6: Parameters for the optimization in the double-well system

in the two wells. The energy difference between the ground and first excited state is small (compare table 6.5) and the density distributions of the two states are similar (fig.6.12 (b)).

The target $r(t)$ (see fig. 6.13 (a))

$$r(t) \quad = \quad 3 \cdot \exp\left(-\frac{(t - T/2)^2}{2(T/8)^2}\right) - 1.5$$

demands to concentrate the density at $t = 0$ in the left well, to push it into the right well at $t = T/2$ and back into the left well at $t = T$. We choose the ground-state of the double-well potential as initial state $\Psi(x, 0)$. As one can see in figure 6.13 (c) this goal is achieved very well for $t = T/2$ and $t = T$. For the times when $r(t) = 0$, i.e. when the goal is to maximize the density at $x = 0$, we observe the tunneling from one well to the other, without maximization of the density at the potential barrier.

The envelope of the optimal field becomes zero at $t = T/2$, when the density is localized in the left well, and at $t = T$, when the density is localized in the right well. Energy is needed to bring the density from one well to the other, therefore the field has a large amplitude between

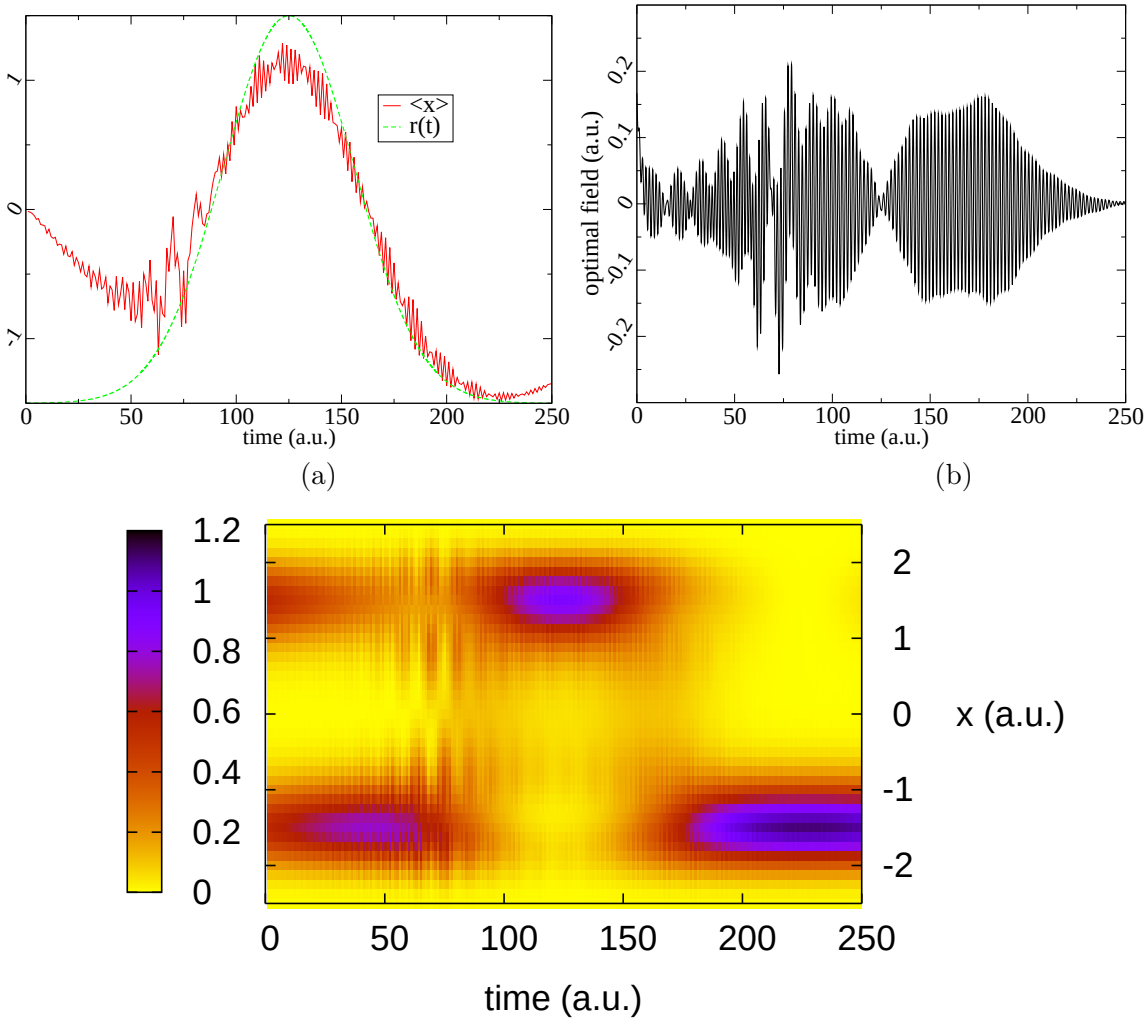


(a) (b)

(c)

Figure 6.13: Target trajectory $r(t)$ and $\langle x \rangle$ (a) optimal field (b) and time-dependent density (c).

$t = 0$ and $t = T/2$ and also in the second half of the time interval, for $t \in (T/2, T)$.

The transfer of density from the left to the right well and back is achieved via the $2nd$ excited state, for which the density has large values also near $x = 0$ (see fig. 6.12 (b)). This results from fig. 6.14 (a), where one can see an increase of the population of state $|2\rangle$ at the times when $r(t) = 0$. In the spectrum of the optimal field (fig. 6.14 (b)) one can see a large peak at the resonance frequency $\omega_{02} = \mathcal{E}_2 - \mathcal{E}_0$.

At the start of the optimisation the goal is to bring the density into the left well as quiqly as possible. In figure 6.14 (a) we can see an increase in the population of the $1st$ and $3rd$ excited state at the beginning of the time interval. The transition frequency $\omega_{03}$ between ground state and the $3rd$ excited state is also visible in the spectral representation of the optimal field. At the end of the time interval the maximization of the density in the left well is achieved through a linear combination of the first two eigenstates.

In conclusion, we are able control the time-dependent density of the system without knowl-

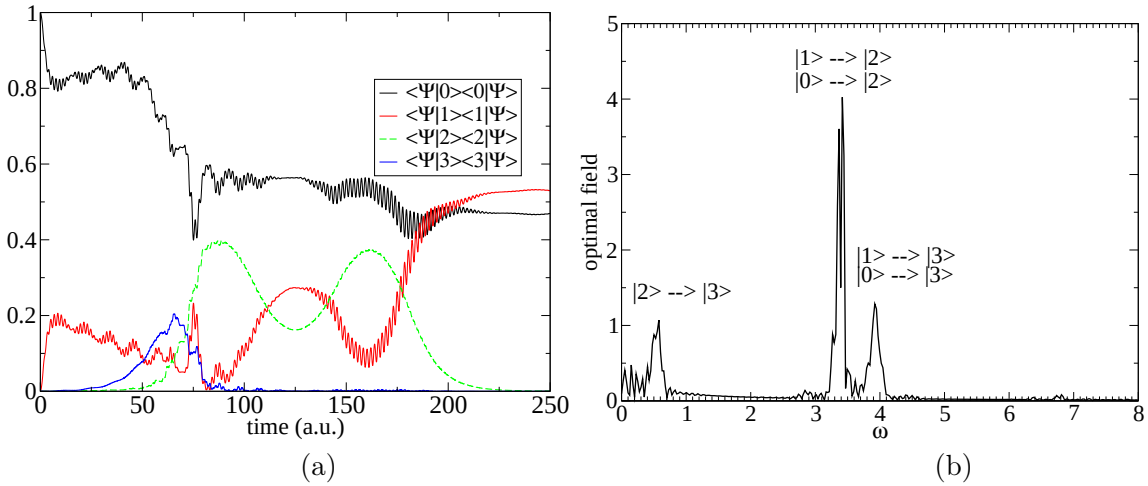


Figure 6.14: Occupation of the first 4 eigenstates (a) and Fourier transform of the optimal field (b)

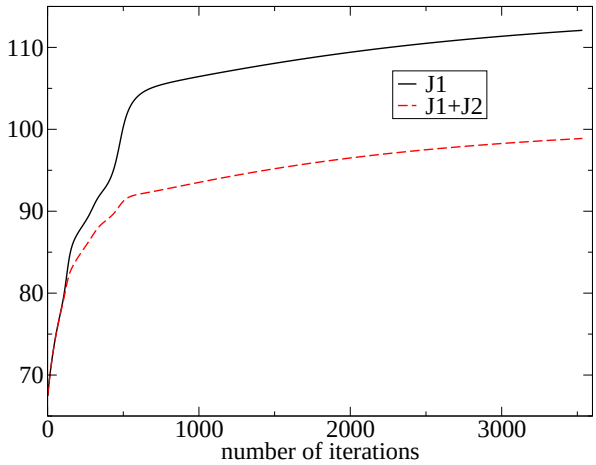


Figure 6.15: Functionals $J_1$ and $J_1 + J_2$

edge of the complete time-dependent wave-function, or even the time dependence of the occupation numbers of the eigenstates involved in the evolution of the system. It is sufficient to prescribe a simple time-dependent function $r(t)$ to control the approximate movement of the time-dependent density.

To summarize, we applied the formalism from chapters 2, 3 and 4 for a local operator, i.e. a delta-function in real space with time-dependent center $r(t)$. The expectation value of this operator is the value of the density at position $r(t)$. By maximizing the time-averaged expectation value of this operator we maximize the density at point $r(t)$ at time $t$. To control the trajectory followed by the dipole moment we used the fact that the movement of the density mimics the time-dependent dipole moment. We have observed that the dipole moment calculated with the optimal field follows the imposed trajectory $r(t)$, i.e. the method developed in this section can be used to control the time-dependent density and also the time-dependent dipole moment.

# Chapter 7

# Conclusion

The goal of this diploma thesis was to find a formulation of optimal control theory that makes it possible to control a quantum system at every point in time i.e., to control not only the final state but also the trajectory followed by the system. So far, physicists and chemists have mainly studied problems where one is only interested in the final state of a system, for example one wants to push the system into a final excited state, or to obtain only one of different possible sets of reaction products. This is a serious disadvantage in problems where one wants to favor only one particular of different possible paths that lead the initial to the final state. The novel formulation of this work makes it possible to selectively avoid or reach a specific intermediate state at a given time.

In this diploma thesis we have extended the optimal control theory to the control of time dependent targets, so that we can control the path followed by the system continuously. In chapter 2 we expressed this goal mathematically in the form of the maximization of a functional and derived the corresponding control equations. Chapters 3 and 4 were concerned with the solution of these equations. In chapter 4 we presented an iterative scheme, and for this scheme we proved the monotonic convergence of the functional to be maximized.

For a very simple (two-level) system we have tested the monotonic convergence of the iteration presented in chapter 4. We studied the importance of the penalty factor which sets the weight of the field intensity, for the functional $J_1 + J_2$, the optimal field and the number of iterations. As practical application, we have shown how one can transform the optimization of a wave-function into the control of time-dependent observables, using an "artificial" wave-function, that does not necessarily fulfill the Schrödinger equation. As two examples of such observables we used the occupation number of a level and the time-dependent dipole moment. We also developed a method which finds the optimal field in the subset of fields with a given intensity. The method developed in chapters 2, 3 and 4 is general and not restricted to a two-level system. In chapter 6 we applied this method to a more complicated system, the hydrogen atom. In this system we are furthermore able to optimize the expectation value of a local operator. By using a position and time-dependent $\delta$-function as operator, one can control the movement of the electronic density. Since the expectation value of the operator $\hat{x}$ (in this system) mimics the movement of the point of maximal density, we were able to control the trajectory of the time-dependent dipole moment. By extending the optimization of a time-dependent density to a two-dimensional system one could apply our method to problems where one wants to drive the density form an initial point on a potential surface to a final point, and at the same time, avoid a specific area on the potential surface, e.g. a conical

intersection of potential surfaces.

In chapters 5 and 6 we made an ansatz for the control of the time-dependent dipole moment. A possible application is the control of the process of high harmonic generation (HHG) i.e., the selective enhancement of a harmonic of the laser frequency in the spectrum of the dipole moment of an irradiated atom. This is crucial for the creation of attosecond laser pulses where one uses parts of the HHG spectrum to obtain a new coherent soft X-ray source [42, 43]. We have shown that it is possible to control the time-dependent dipole moment. But since the search for the optimal field was unrestricted with respect to the spectral domain in our formulation, the optimal field we found contained some undesired frequencies. Therefore, it is necessary to be able to restrict the laser field in the spectral domain. A formulation of optimal control with spectral restriction has already been suggested in [44], but no proof of convergence has been given for the iterative algorithm. Moreover, as one can see in [27] and appendix H, we have a one-to-one correspondence between the time-dependent dipole moment as operator whose expectation value is to be controlled and the external field as control variable. Therefore by choosing the time-dependent target trajectory for the dipole moment, one can uniquely determine the field. Therefore, only a "brute-force" restriction on the spectral representation of the control field is not sufficient to achieve the goal.

In this thesis we derived a novel and very general form of optimal control, namely the control of the trajectory of a quantum system. A challenge for future work remains the control of a trajectory with restrictions on the control field in the spectral domain and further research on the equation H.8.

# Appendix A

# Atomic units

Atomic units are convenient units to describe the properties of electrons. The atomic units have been chosen such that the fundamental electron properties such as mass and charge are all equal to one atomic unit. Other quantities can be obtained by combining these four basic

| Physical significance | Symbol | Conversion Factor |
|---|---|---|
| Electron mass | $m_e$ | 1 au = $9.10939 \times 10^{-31}$ kg |
| Electron charge | $e$ | 1 au = $1.60218 \times 10^{-19}$ C |
| $4\pi$ times the permittivity of free space | $4\pi\epsilon_0$ | 1 au = $1.11265 \times 10^{-10}$ F/m |
| Plank's constant divided by $2\pi$ | $\hbar$ | 1 au = $1.05457 \times 10{-}34$ J s/rad |

Figure A.1: Basic quantities for the atomic unit system and their SI equivalent

quantities. From the expression for the velocity we can see that the velocity of light has the

| Quantity | Physical significance | Symbol | Conversion Factor |
|---|---|---|---|
| Lenght | Bohr radius | $a_0 = 4\pi\epsilon_0\hbar^2/m_e e^2$ | 1 au = $5.29177 \times 10^{-11}$ m |
| Energy | Ionisation potential of the hydrogen atom | $E_h = e^2/4\pi\epsilon_0 a_0$ | 1 au = $4.35975 \times 10^{-18}$ J |
| Velocity | Electron velocity in first Bohr orbit | $v_0 = \alpha c$ | 1 au = $2.18769 \times 10^{6}$ m/s |
| Time | Time required for the electron in $1^{st}$ Bohr orbit to travel one Bohr radius | $a_0/v_0$ | 1 au = $2.41889 \times 10^{-17}$ s |
| Frequency | Angular frequency of electron in first Bohr orbit divided by $2\pi$ | $v_0/2\pi a_0$ | 1 au = $6.57968 \times 10^{15}$ $s^{-1}$ |
| Electric dipole moment | Dipole moment of electron in the first Bohr orbit | $d_0 = e\, a_0$ | 1 au = $8.47835 \times 10^{-30}$ Cm |
| Electric field | | $E_h/ea_0$ | 1 au = $5.14220 \times 1011$ V/m |

Figure A.2: Atomic units

value $\alpha^{-1} = 137.035$ in atomic units.

The use of atomic units simplifies Schrödinger's equation. The Hamiltonian for an electron in the hydrogen atom is

$$\widehat{H} = -\frac{\hbar^2\nabla^2}{2m_e} + \frac{-e}{4\pi\epsilon_0 r} \quad \text{(SI)} \tag{A.1}$$

$$\widehat{H} = -\frac{\nabla^2}{2} - \frac{1}{r} \quad \text{(Atomic units)} \tag{A.2}$$

# Appendix B

# Electrons in an external electromagnetic field

The dynamics of an electron in an electromagnetic field can be described [45] by the Hamiltonian

$$\widehat{H} = \frac{1}{2m}\left(\vec{p} - \frac{q}{c}\vec{A}\right)^2 - q\phi, \tag{B.1}$$

where $q$ is the charge, $m$ the mass and $\vec{p}$ the momentum of the electron. $\vec{A}$ and $\phi$ are the vector and scalar potential of the electromagnetic field. This minimum coupling Hamiltonian reproduces the equation of motion of the electron in an electromagnetic field when substituted into the classical canonical equations.

$$\begin{aligned} \frac{\partial q_i}{\partial t} &= \frac{\partial H}{\partial p_i} \;;\; \frac{\partial p_i}{\partial t} = -\frac{\partial H}{\partial q_i}, \\ (q_1, q_2, q_3) &= \vec{r} \;;\; (p_1, p_2, p_3) = \vec{p} \end{aligned} \tag{B.2}$$

Plugging (B.1) into (B.2) one finds the Lorenz equation of motion

$$m\frac{d\vec{v}}{dt} = q\left(\vec{E} + \frac{1}{c}\vec{v} \times \vec{B}\right). \tag{B.3}$$

The potentials are determined up to a gauge transformation

$$\vec{A} \rightarrow \vec{A}' = \vec{A} + \vec{\nabla}\chi, \tag{B.4}$$

$$\phi \rightarrow \phi' = \phi + \frac{1}{c}\dot{\chi}. \tag{B.5}$$

where $\chi(x,t)$ is an arbitrary scalar function. This transformation does not change the corresponding fields

$$\vec{E} = -\frac{1}{c}\dot{\vec{A}} + \vec{\nabla}\phi, \tag{B.6}$$

$$\vec{B} = \vec{\nabla} \times \vec{A}. \tag{B.7}$$

One can choose $\chi$ such that $\vec{\nabla} \cdot \vec{A} = 0$ (Coulomb gauge). The gauge transformed Schrödinger equation is then given by

$$i\hbar\frac{\partial\psi}{\partial t} = \left[\frac{1}{2m}\left(-i\hbar\vec{\nabla} - \frac{q}{c}\vec{A}' + \frac{q}{c}\vec{\nabla}\chi\right)^2 - e\phi' + \frac{q}{c}\frac{\partial\chi}{\partial t}\right]\psi, \tag{B.8}$$

which can be rewritten as:

$$i\hbar\frac{\partial}{\partial t}\psi e^{i(q/\hbar c)\chi} = \left[\frac{1}{2m}\left(-i\hbar\vec{\nabla}-\frac{q}{c}\vec{A'}\right)^2 - q\phi' + \right]\psi e^{i(q/\hbar c)\chi}. \tag{B.9}$$

In the Coulomb gauge the Maxwell wave equation of the vector potential is

$$\left(\nabla^2 - \frac{1}{c^2}\frac{\partial^2}{\partial t^2}\right)\vec{A} = 0, \tag{B.10}$$

with the solution

$$\vec{A}(\vec{r},t) = \sum_k \vec{\epsilon}_k A_{0,k}\cos(\vec{k}\cdot\vec{r}-\omega_k t+\delta), \tag{B.11}$$

$$\omega_k = ck, \tag{B.12}$$

$$e^{i\vec{k}\cdot\vec{r}} \simeq 1+\vec{k}\cdot\vec{r}+\cdots \tag{B.13}$$

If we take only the leading order term in the Taylor series above, we obtain for a monochromatic laser field

$$\vec{A}(t) = \epsilon_z A_0\cos(\omega_k t+\delta) \text{ (linear polarized)}, \tag{B.14}$$

$$\vec{A}(t) = \epsilon_x A_0\cos(\omega_k t) - \epsilon_y A_0\sin(\omega_k t) \text{ (circular polarized)}. \tag{B.15}$$

In the Coulomb gauge the Hamiltonian takes the form

$$H = -\frac{\hbar^2}{2m}\nabla^2 + V + \frac{iq\hbar}{mc}\vec{A}(t)\cdot\vec{\nabla} + \frac{q^2}{2mc^2}\vec{A}^2(t). \tag{B.16}$$

One can define a new transformation of the wave function $\Psi = e^{i(e/\hbar c)\vec{r}\cdot\vec{A}(t)}\psi$. The new variable $\Psi$ fulfills the equation

$$i\hbar\frac{\partial\Psi(x,t)}{\partial t} = \left[-\frac{\hbar^2}{2m}\nabla^2 + V(x) - q\vec{r}\cdot\vec{E}(t)\right]\Psi(x,t), \tag{B.17}$$

where the term in square brackets is called the *length form* of the Hamiltonian.

The dipole approximation is valid in the case $kr \ll 1$. Since $k = 2\pi/\lambda$, where $\lambda = cT$ is the wave length of the electromagnetic radiation, and $r = vT$ is describes the space hat can be occupied by the wave-function, the validity condition of the dipole approximation becomes

$$v \ll c \tag{B.18}$$

where $v$ is the speed of the electron.

# Appendix C

# Optimal control equations without dipole approximation

We write the Schrödinger equation with the minimum coupling Hamiltonian

$$i\hbar\partial_t\Psi(x,t) = \left(\hat{T} + \underbrace{V(x)}_{-q\phi(x)} + \frac{iq\hbar}{m_e c}A(x,t)\cdot\partial_x + \frac{q^2}{2m_e c^2}A^2(x,t)\right)\Psi(x,t), \tag{C.1}$$

$$\widehat{H} = \hat{T} + V(x) + \frac{iq\hbar}{m_e c}A(x,t)\cdot\partial_x + \frac{q^2}{2m_e c^2}A^2(x,t) \tag{C.2}$$

and the electric field

$$E(x,t) = -\frac{1}{c}\dot{A} + \partial_x\phi. \tag{C.3}$$

We construct again the functional $\mathcal{L}$ and take the variation with respect to $\Psi$, $\chi$ and $E$. The only equation that changes with respect to the ones derived in chapter 2 is the field equation. Instead of the field $E$ we now have to take the variation of the functional with respect to the vector potential.

$$J_2 = -\alpha\int dx\int_0^T dt E^2(t) = -\alpha\int dx\int_0^T dt\left(-\frac{1}{c}\dot{A}(x,t) + \partial_x\phi(x)\right)^2 \tag{C.4}$$

$$J_3 = 2\Re\int_0^T dt\,\left\langle\chi(t)\left|\left(\partial_t + i\widehat{H}\right)\right|\Psi(t)\right\rangle \tag{C.5}$$

The variation of $J_2$ with respect to $A$ is

$$\begin{aligned}\frac{\delta J_2}{\delta A(y,\tau)} &= 2\alpha\int dx\int_0^T dt\left(-\frac{1}{c}\dot{A}(x,t) + \partial_x\phi(x)\right)\frac{1}{c}\frac{\delta}{\delta A(y,\tau)}\dot{A}(x,t)\\ &= 2\alpha\int dx\int_0^T dt\left(-\frac{1}{c}\dot{A}(x,t) + \partial_x\phi(x)\right)\frac{1}{c}\delta(x-y)\dot{\delta}(t-\tau).\end{aligned} \tag{C.6}$$

After a partial integration we obtain

$$\begin{aligned}
\frac{\delta J_2}{\delta A(y,\tau)} &= 2\alpha \int dx \left[ \left( -\frac{1}{c}\dot{A}(x,t) + \partial_x \phi(x) \right) \frac{1}{c}\delta(x-y)\delta(t-\tau) \right]_0^T \\
&- 2\alpha \int dx \frac{d}{d\tau} \left( -\frac{1}{c}\dot{A}(x,\tau) + \partial_x \phi(x) \right) \frac{1}{c}\delta(x-y) \\
&= 2\alpha \left[ \left( -\frac{1}{c}\dot{A}(y,t) + \partial_x \phi(y) \right) \frac{1}{c}\delta(t-\tau) \right]_0^T + \frac{2\alpha}{c^2}\ddot{A}(y,\tau). \qquad \text{(C.7)}
\end{aligned}$$

The variation of $J_3$ with respect to $A$ gives

$$\begin{aligned}
\frac{\delta J_3}{\delta A(y,\tau)} &= 2\Re \int_0^T dt \left\langle \chi(t) \left| i \frac{\delta}{\delta A(y,\tau)} \left( \frac{iq\hbar}{m_e c} A(t) \cdot \partial_x + \frac{q^2}{2m_e c^2} A^2(t) \right) \right| \Psi(t) \right\rangle \\
&= 2\Re \int_0^T dt \left\langle \chi(t) \left| i \left( \frac{iq\hbar}{m_e c} \delta(x-y)\delta(t-\tau)\partial_x + \frac{q^2}{2m_e c^2} 2A(x,t)\delta(x-y)\delta(t-\tau) \right) \right| \Psi(t) \right\rangle \\
&= -2\Re \left( \chi^*(y,\tau)\partial_x \Psi(y,\tau) \frac{q\hbar}{m_e c} + \frac{iq^2}{2m_e c^2} 2A(y,\tau)\ \chi^*(y,\tau)\Psi(y,\tau) \right). \qquad \text{(C.8)}
\end{aligned}$$

If we request the vector potential to be a continuous function of time at every point $t$ (0 and $T$ included), we obtain a $2nd$ order differential equation with boundary conditions at 0 and $T$ for $\dot{A}$. To show this we make the same considerations as in the case of the boundary condition for the Lagrange multiplier $\chi$ (see chapter 2). We obtain

$$\frac{2\alpha}{c^2}\ddot{A}(y,\tau) = -2\Re \left( \chi^*(y,\tau)\partial_y \Psi(y,\tau) \frac{q\hbar}{m_e c} + A(y,\tau) \frac{iq^2}{m_e c^2}\ \chi^*(y,\tau)\Psi(y,\tau) \right), \qquad \text{(C.9)}$$

with boundary conditions

$$2\alpha \left[ \left( -\frac{1}{c}\dot{A}(y,0) + \partial_y \phi(y) \right) \frac{1}{c} \right] = 0, \qquad \text{(C.10)}$$

$$2\alpha \left[ \left( -\frac{1}{c}\dot{A}(y,T) + \partial_y \phi(y) \right) \frac{1}{c} \right] = 0. \qquad \text{(C.11)}$$

The boundary conditions are equivalent to $E(x,0) = E(x,T) = 0$. In the cases where the dipole approximation is not valid i.e. when the condition $kr \ll 1$ is not fulfilled, one has to solve equation (C.9) instead of equation (2.30). The solution of (C.9) is more complex than the solution of (2.30), and due to the fact that (C.9) is a second order differential equation, it makes immediate feedback, see section 4.1, impossible. In this thesis we will consider the dipole approximation valid.

# Appendix D

# Analytical solution of the Schrödinger equation

## D.1 Free particle

The Schrödinger equation of a free particle has the form

$$-\frac{1}{2}\frac{\partial^2}{\partial x^2}\Psi(x,t) = i\frac{\partial}{\partial t}\Psi(x,t). \tag{D.1}$$

The well known solution is

$$\Psi(x,t) = \frac{1}{\sqrt[4]{\pi}}\sqrt{\frac{\Delta_k}{1+it\Delta_k^2}}\exp\left(\frac{-ik_0^2t+2ik_0x-\Delta_k^2x^2}{2(1+i\Delta_k^2t)}\right) \tag{D.2}$$

where $\Delta_k$ is the width of the Gauss wave packet in momentum space. For $\chi$ we therefore have

$$\chi(x,t) = \left(\int_T^t d\tau f(\tau)+c_T\right)\sqrt[4]{\pi}\sqrt{\frac{\Delta_k}{1+it\Delta_k^2}}\exp\left(\frac{-ik_0^2t+2ik_0x-\Delta_k^2x^2}{2(1+i\Delta_k^2t)}\right). \tag{D.3}$$

## D.2 Harmonic oscillator in laser field

Another system we can solve exactly is the harmonic oscillator with frequency $\omega$ in a laser field $E(t)$. The Schrödinger equation has the form

$$-\frac{\hbar^2}{2m}\frac{\partial^2}{\partial x^2}\Psi(x,t)+\left(\frac{m\omega^2}{2}x^2-E(t)qx\right)\Psi(x,t) = i\hbar\frac{\partial\Psi(x,t)}{\partial t}. \tag{D.4}$$

The propagator from point $y$ at time $t=0$ to point $x$ at time $t$ is given by [46, 47]

$$K(x,t,y)=\frac{\alpha}{\sqrt{2\pi i\sin(\omega t)}}\exp\left[\frac{i}{\sin(\omega t)}\left(\alpha^2\left(\frac{x^2+y^2}{2}\cos(\omega t)-xy\right)+\frac{xx_0+yy_0}{\hbar}+\frac{\chi}{2\alpha^2\hbar^2}\right)\right], \tag{D.5}$$

where we introduced the following abbreviations

$$
\begin{aligned}
x_0 &= -G, && \text{(D.6)}\\
y_0 &= G\cos(\omega t) - F\sin(\omega t), && \text{(D.7)}\\
\chi &= G^2\cos(\omega t) - (FG + 2H)\sin(\omega t), && \text{(D.8)}\\
G(t) &= \int_0^t d\tau E(\tau)\sin(\omega\tau), && \text{(D.9)}\\
F(t) &= \int_0^t d\tau E(\tau)\cos(\omega\tau), && \text{(D.10)}\\
H(t) &= \frac{1}{2}\int_0^t d\tau E(\tau)\left(\cos(\omega\tau)G(\tau) - \sin(\omega\tau)F(\tau)\right). && \text{(D.11)}
\end{aligned}
$$

If $\Psi(x,0) = \phi(x)$, where $\phi$ is the ground state of the harmonic oscillator, then the time-dependent wave-function is

$$
\begin{aligned}
\Psi(x,t) &= \left(\frac{\alpha^2}{\pi}\right)^{\frac{1}{4}} \int dy K(x,t,y)\exp\left[-\frac{\alpha^2}{2}y^2\right], && \text{(D.12)}\\
&= \sqrt[4]{\frac{\alpha^2}{\pi}} e^{-i\omega t/2}\exp\left[-\frac{\alpha^2}{2}(x-\widetilde{x}_0(t))^2 - \widetilde{\chi}(t)\right]. && \text{(D.13)}
\end{aligned}
$$

with

$$
\begin{aligned}
\widetilde{\chi}(t) &= \frac{i}{2\hbar^2\alpha^2}\left[2H + e^{-i\omega t}(G - iF)(F(\cos\omega)t + G\sin(\omega t))\right], && \text{(D.14)}\\
\widetilde{x}_0(t) &= -i\frac{F + iG}{\hbar\alpha^2}e^{-i\omega t}, && \text{(D.15)}\\
\omega &= \sqrt{k}, && \text{(D.16)}\\
\alpha &= \sqrt{\frac{m\omega}{\hbar}}. && \text{(D.17)}
\end{aligned}
$$

For a laser field

$$
E(t) = A\cdot\sin(\omega_0\cdot t),
$$

we can integrate F, G and H analytically

$$
\begin{aligned}
G(t) &= A\left(\frac{\sin(t\ (\omega_0-\omega))}{2\ (\omega_0-\omega_{ho})} - \frac{\sin(t\ (\omega_0+\omega))}{2\ (\omega_0+\omega)}\right), && \text{(D.18)}\\
F(t) &= A\left(\frac{1}{2\ (\omega_0-\omega)} - \frac{\cos(t\ (\omega_0-\omega))}{2\ (\omega_0-\omega)} + \frac{1}{2\ (\omega_0+\omega)} - \frac{\cos(t\ (\omega_0+\omega))}{2\ (\omega_0+\omega)}\right), && \text{(D.19)}\\
H(t) &= \frac{A^2\left(4\cos(t\omega_0)\sin(t\omega)\omega_0^3 - 4\cos(t\omega)\sin(t\omega_0)\omega_0^2\omega\right)}{8\omega_0(\omega_0^2-\omega^2)^2}\\
&- \frac{A^2(\sin(2t\omega_0) - 2t\omega_0)\omega(\omega_0^2-\omega^2)}{8\omega_0(\omega_0^2-\omega^2)^2} && \text{(D.20)}
\end{aligned}
$$

# Appendix E

# Rotating wave approximation

We consider a two level atom in an external time-dependent field

$$E(t) = A\cos(\omega t), \tag{E.1}$$

where $A$ is the amplitude and $\omega$ the frequency of the field. We write the wave-function as a linear combination of the two eigenstates of the field free Hamiltonian $\widehat{H}_0$, $\Psi(t) = \Psi_0(t)|0\rangle + \Psi_1(t)|1\rangle$. The Schrödinger equation reads

$$\partial_t \Psi(t) = -i\widehat{H}\Psi(t), \tag{E.2}$$

where

$$\widehat{H} = \widehat{H}_0 - \hat{\mu}E(t), \tag{E.3}$$

$$\widehat{H}_0 = \begin{pmatrix} \omega_0 & 0 \\ 0 & \omega_1 \end{pmatrix} \tag{E.4}$$

We consider $\mu_{00}\mu_{11} = 0$, and $\mu_{10} = \mu_{01}^*$, where $\mu_{ab} = \langle a|\hat{\mu}|b\rangle$. The equations of motion for the amplitudes $\Psi_0(t)$ and $\Psi_1(t)$ can be written as

$$\dot{\Psi}_0(t) = -\omega_0 + i\Omega_R e^{-i\phi}\cos(\omega t)\Psi_0(t), \tag{E.5}$$

$$\dot{\Psi}_1(t) = -\omega_1 + i\Omega_R e^{i\phi}\cos(\omega t)\Psi_1(t), \tag{E.6}$$

where $\Omega_R = |\mu_{01}|A$ is the Rabi frequency and $\mu_{01} = |\mu_{01}|e^{i\phi}$. We transform the coefficients $\Psi_j(t) = \widetilde{\Psi}_j e^{i\omega j t}$, $j = 0, 1$, The transformed variables satisfy

$$\dot{\widetilde{\Psi}}_0(t) = i\Omega_R e^{-i\phi} e^{i\omega_{01}t}\cos(\omega t)\Psi_0(t), \tag{E.7}$$

$$\dot{\widetilde{\Psi}}_1(t) = i\Omega_R e^{i\phi} e^{-i\omega_{01}t}\cos(\omega t)\Psi_1(t), \tag{E.8}$$

with $\omega_{01} = \omega_0 - \omega_1$. The rotating wave approximation consists in ignoring the terms $e^{\pm(\omega+\omega_{01})}$, i.e. the fast oscillating terms. The motion equations are

$$\dot{\widetilde{\Psi}}_0(t) = \frac{i\Omega_R}{2} e^{-i\phi} e^{i(\omega_{01}-\omega)t}, \tag{E.9}$$

$$\dot{\widetilde{\Psi}}_1(t) = \frac{i\Omega_R}{2} e^{i\phi} e^{-i(\omega_{01}-\omega)t}. \tag{E.10}$$

They can be solved and the solution is

$$\widetilde{\Psi}_0(t) = \left(a_1 e^{i\Omega_R t/2} + a_2 e^{-i\Omega_R t/2}\right) e^{i(\omega_{01}-\omega)t/2}, \tag{E.11}$$

$$\widetilde{\Psi}_1(t) = \left(b_1 e^{i\Omega_R t/2} + b_2 e^{-i\Omega_R t/2}\right) e^{-i(\omega_{01}-\omega)t/2}, \tag{E.12}$$

where $a_j$ and $b_j$, $j = 1, 2$ are integration constants which have to be determined from the initial conditions.

$$a_1 = \frac{1}{2\Omega}[(\Omega - \Delta)\widetilde{\Psi}_0(0) + \Omega_R e^{-i\phi}\widetilde{\Psi}_1(0)], \tag{E.13}$$

$$a_2 = \frac{1}{2\Omega}[(\Omega + \Delta)\widetilde{\Psi}_0(0) - \Omega_R e^{-i\phi}\widetilde{\Psi}_1(0)], \tag{E.14}$$

$$b_1 = \frac{1}{2\Omega}[(\Omega + \Delta)\widetilde{\Psi}_1(0) + \Omega_R e^{i\phi}\widetilde{\Psi}_1(0)], \tag{E.15}$$

$$b_2 = \frac{1}{2\Omega}[(\Omega - \Delta)\widetilde{\Psi}_1(0) - \Omega_R e^{i\phi}\widetilde{\Psi}_1(0)], \tag{E.16}$$

where

$$\Omega = \sqrt{\Omega_R^2 + \Delta^2}, \tag{E.17}$$

$$\Delta = \omega_{01} - \omega. \tag{E.18}$$

For $\widetilde{\Psi}_0(0) = 1$ and $\omega = \omega_{01}$ it follows that

$$|\widetilde{\Psi}_0(t)|^2 = \sin^2\left(\frac{\Omega_R t}{2}\right) \tag{E.19}$$

For further details see ref. [37].

Since one can solve equations (E.9) and (E.10) only for fields of the form (E.1), i.e., with only spectral component, we will use for the calculations in chapter 5 a numerical solution of the Schrödinger equation.

# Appendix F

# Relevance of numerical errors

In some runs we found that the monotonic convergence was violated: this is due to numerical errors. Suppose that (2.28) and (2.26) are subject to numerical errors which we can write in the following form:

$$\left(\frac{\partial}{\partial t} + i\widetilde{H}_k\right)\chi_k(x,t) = -\frac{1}{T}\widehat{O}_t^{(1)}\Psi_k(x,t) + \delta_c\chi_k(x,t), \tag{F.1}$$

$$\left(\frac{\partial}{\partial t} + i\widehat{H}_k\right)\Psi_k(x,t) = \delta_c\Psi_k(x,t), \tag{F.2}$$

$$\chi_k(T) = \widehat{O}_T^{(2)}\Psi_k(x,T) + \delta_c f_k(x), \tag{F.3}$$

$$\Psi_k(0) = \phi(x) + \delta_c\phi_k(x). \tag{F.4}$$

Then the variation of the Lagrange functional between two iterations is

$$\begin{aligned}\delta\mathcal{L}_{k+1,k} &= \int_0^T dt\Big(\frac{1}{T}\langle\delta\Psi_{k+1,k}(t)|\widehat{O}_t|\delta\Psi_{k+1,k}(t)\rangle \\ &+ \frac{2}{T}\Re\langle\delta\Psi_{k+1,k}(t)|\widehat{O}_t^{(1)}|\Psi_k(t)\rangle - \alpha\left(E_{k+1}^2(t) - E_k^2(t)\right)\Big) \\ &+ 2\Re\underbrace{\langle\Psi_k(T)|\widehat{O}_T^{(2)}|\delta\Psi_{k+1,k}(T)\rangle}_{\langle\chi_k(T)-\delta_c f_k|\delta\Psi_{k+1,k}(T)\rangle} - \underbrace{2\Re\int_0^T dt\langle\chi(t)|\delta_c\Psi_{k+1}(t) - \delta_c\Psi_k(t)\rangle}_{J_3}.\end{aligned} \tag{F.5}$$

Since the Schrödinger equation is not fulfilled we have in addition to the previous case also the contribution from $J_3$. We use the fact that $\widehat{O}_t^{(1)}$ is hermitian and the equation (F.1) and obtain

$$\begin{aligned}&\frac{1}{T}\int_0^T dt\langle\Psi_k(t)|\widehat{O}_t^{(1)}|\delta\Psi_{k+1,k}(t)\rangle = \\ &- \int_0^T dt\Big\langle\left(\frac{\partial}{\partial t} + i\widetilde{H}_k\right)\chi_k(t) - \delta_c\chi_k(t)\Big|\delta\Psi_{k+1,k}(t)\Big\rangle.\end{aligned} \tag{F.6}$$

We use a partial integration

$$\begin{aligned}
\frac{1}{T}\int_0^T dt\langle\Psi_k(t)|\widehat{O}_t^{(1)}|\delta\Psi_{k+1,k}(t)\rangle &= -\langle\chi_k(t)|\delta\Psi_{k+1,k}(t)\rangle|_0^T \\
&+ \int_0^T dt\Big(\Big\langle\chi_k(t)\Big|\left(\frac{\partial}{\partial t}+i\widetilde{H}_k\right)\delta\Psi_{k+1,k}(t)\Big\rangle \\
&- \langle\delta_c\chi_k(t)|\delta\Psi_{k+1,k}(t)\rangle\Big) = \\
&= \langle\chi_k(0)|\delta_c\phi_{k+1}-\delta_c\phi_k\rangle - \langle\chi_k(T)|\delta\Psi_{k+1,k}(T)\rangle \\
&+ \int_0^T dt\Big(\Big\langle\chi_k(t)\Big|\left(\frac{\partial}{\partial t}+i\widetilde{H}_k\right)\delta\Psi_{k+1,k}(t)\Big\rangle \\
&- \langle\delta_c\chi_k(t)|\delta\Psi_{k+1,k}(t)\rangle. \qquad \text{(F.7)}
\end{aligned}$$

Using the Schrödinger equation (F.2) we get

$$\begin{aligned}
\frac{1}{T}\int_0^T dt\langle\Psi_k(t)|\widehat{O}_t^{(1)}|\delta\Psi_{k+1,k}(t)\rangle &= \langle\chi_k(0)|\delta_c\phi_{k+1}-\delta_c\phi_k\rangle - \langle\chi_k(T)|\delta\Psi_{k+1,k}(T)\rangle \\
&+ \int_0^T dt\Bigg(\Big\langle\chi_k(t)\Big|i\left(\widetilde{H}_k-\widehat{H}_{k+1}\right)\Big|\Psi_{k+1}(t)\Big\rangle \\
&- \langle\chi_k(t)|i\left(\widetilde{H}_k-\widehat{H}_k\right)|\Psi_k(t)\rangle \\
&+ \langle\chi_k(t)|\left(\delta_c\Psi_{k+1}(t)-\delta_c\Psi_k(t)\right)\rangle \\
&- \langle\delta_c\chi_k(t)|\delta\Psi_{k+1,k}(t)\rangle\Bigg). \qquad \text{(F.8)}
\end{aligned}$$

We use the fact that two Hamilton operators differ only in the laser fields

$$\begin{aligned}
\frac{1}{T}\int_0^T dt\langle\Psi_k(t)|\widehat{O}_t^{(1)}|\delta\Psi_{k+1,k}(t)\rangle &= \langle\chi_k(0)|\delta_c\phi_{k+1}-\delta_c\phi_k\rangle - \langle\chi_k(T)|\delta\Psi_{k+1,k}(T)\rangle + \\
&+ \int_0^T dt\Bigg(\Big\langle\chi_k(t)\Big|i\hat{\mu}\Big|\Psi_{k+1}(t)\Big\rangle\left(\widetilde{E}_k(t)-E_{k+1}(t)\right) - \\
&+ \langle\chi_k(t)|i\hat{\mu}|\Psi_k(t)\rangle\left(\widetilde{E}_k(t)-E(t)_k\right) + \\
&- \langle\chi_k(t)|\left(\delta_c\Psi_{k+1}(t)-\delta_c\Psi_k(t)\right)\rangle - \\
&- \langle\delta_c\chi_k(t)|\delta\Psi_{k+1,k}(t)\rangle\Bigg). \qquad \text{(F.9)}
\end{aligned}$$

We use the field equations and regroup the terms containing the fields to squared differences as before and obtain

$$\begin{aligned}
\delta\mathcal{L}_{k+1,k} &= \int_0^T dt\left(\langle\delta\Psi_{k+1,k}(t)|\frac{1}{T}\widehat{O}_t|\delta\Psi_{k+1,k}(t)\rangle + \alpha\left(E_{k+1}(t)-\widetilde{E}_k(t)\right)^2 + \alpha\left(E_k(t)-\widetilde{E}_k(t)\right)^2\right) \\
&+ 2\Re\int_0^T dt\Big(\langle\chi_k(t)|(\delta_c\Psi_{k+1}(t)-\delta_c\Psi_k(t))\rangle - \langle\chi_k(t)|(\delta_c\Psi_{k+1}(t)-\delta_c\Psi_k(t))\rangle \\
&- \langle\delta_c\chi_k(t)|\delta\Psi_{k+1,k}(t)\rangle\Big) - 2\Re\langle\chi_k(T)|\delta\Psi_{k+1,k}(T)\rangle + 2\Re\langle\chi_k(T)|\delta\Psi_{k+1,k}(T)\rangle \\
&- \langle\delta_c f_k|\delta\Psi_{k+1,k}(T)\rangle + \langle\chi_k(0)|\delta_c\phi_{k+1}-\delta_c\phi_k\rangle. \qquad \text{(F.10)}
\end{aligned}$$

We use the field equations (4.12) and (4.17) and group the fields

$$\begin{aligned}
\delta\mathcal{L}_{k+1,k} &= \int_0^T dt\Big(\langle\delta\Psi_{k+1,k}(t)|\frac{1}{T}\widehat{O}_t|\delta\Psi_{k+1,k}(t)\rangle \\
&+ \alpha\left(\frac{2}{\gamma}-1\right)\left(E_{k+1}(t)-\widetilde{E}_k(t)\right)^2+\alpha\left(\frac{2}{\eta}-1\right)\left(E_k(t)-\widetilde{E}_k(t)\right)^2\Big) \\
&- 2\Re\int_0^T dt\Big(\langle\delta_c\chi_k(t)|\delta\Psi_{k+1,k}(t)\rangle\Big) \\
&- \langle\delta_c f_k|\delta\Psi_{k+1,k}(T)\rangle+\langle\chi_k(0)|\delta_c\phi_{k+1}-\delta_c\phi_k\rangle. \qquad \text{(F.11)}
\end{aligned}$$

The sum of the last three terms in equation (F.11) is not necessarily greater than 0. Therefore, if the wave-function and the Lagrange multiplier do not satisfy the Schrödinger equation (homogeneous and inhomogeneous), the proof of convergence does not hold.

In (F.11) we have a time integral over the error term from the inhomogeneous Schrödinger equation. Since the errors for $\chi$ are of the order $\mathcal{O}(\Delta t)$, as we have shown in chapter 6, one can see that the first error term from $\delta\mathcal{L}_{k+1,k}$ does not explicitly depend on $(\Delta t)$, and can become sizable.

# Appendix G

# Generalized functional - relations

Consider two real positive numbers $a$ and $b$ and $n$ a positive integer, $n > 1$ . We have:

$$a^n - b^n = nb^{n-1}(a-b) + a^n + (n-1)b^n - nb^{n-1}a \tag{G.1}$$

We want to show that $a^n + (n-1)b^n - nb^{n-1}a$ is always positive. For this we define a new variable $\delta$: $a = b + \delta$, $\delta \in [-b, \infty)$
I. case: $\delta \in (0, \infty)$

$$\begin{aligned} a^n + (n-1)b^n - nb^{n-1}a &= (b+\delta)^n + (n-1)b^n - nb^{n-1}(b+\delta) = \\ &= b^n + nb^{n-1}\delta + \cdots + n\delta^{n-1}b + \delta^n + (n-1)b^n - nb^{n-1}\delta = \\ &= \frac{n!}{(n-2)!2!}b^{n-2}\delta^2 + \cdots + n\delta^{n-1}b + \delta^n \geq 0 \end{aligned} \tag{G.2}$$

II. case: $\delta \in [-b, 0]$

$$(b+\delta)^n + (n-1)b^n - nb^{n-1}(b+\delta) = \underbrace{b^n}_{\geq 0}\left[\left(1+\frac{\delta}{b}\right)^n + n - 1 - n - n\frac{\delta}{b}\right] \tag{G.3}$$

Now we define $x = 1 + \frac{\delta}{b}$, $x \in [0, 1)$. We need to show that the function $f(x)$ is positive:

$$f(x) = x^n - nx + n - 1$$

The function $f$ has the properties:

$$\begin{aligned} f(0) &= n - 1 > 0 \\ f(1) &= 0 \\ f'(x) &= n\underbrace{(x^{n-1} - 1)}_{<0} \Longrightarrow f(x) \in [0, n-1] \Longrightarrow f(y) \geq 0 \end{aligned}$$

Since $f'(x) \leq 0$, the function $f$ must fall monotonically from $n-1$ to 0, so it cannot become negative. In conclusion:

$$a^n - b^n = nb^{n-1}(a-b) + \underbrace{a^n + (n-1)b^n - nb^{n-1}a}_{A \geq 0} \tag{G.4}$$

# Appendix H

# Tracking control

We consider the dipole approximation of the Hamiltonian

$$\widehat{H} = \widehat{H}_0 - \hat{\mu}E(t) = -\frac{\nabla^2}{2} + V(x) - \hat{\mu}E(t) \tag{H.1}$$

Given the equation

$$S(t) = \langle\Psi(t)|\hat{O}|\Psi(t)\rangle \tag{H.2}$$

one can determine [27] the Schrödinger equation (i.e. the laser field) whose solution $\Psi$ satisfies it. We use the Ehrenfest theorem and obtain

$$\frac{dS(t)}{dt} = \langle\Psi(t)|\frac{\partial\hat{O}}{\partial t}|\Psi(t)\rangle - \langle\Psi(t)|i[\hat{O},\widehat{H}]|\Psi(t)\rangle. \tag{H.3}$$

It follows

$$E(t) = \frac{\frac{dS(t)}{dt} + \langle\Psi(t)|i[\hat{O},\widehat{H}_0]|\Psi(t)\rangle - \langle\Psi(t)|\frac{\partial\hat{O}}{\partial t}|\Psi(t)\rangle}{\langle\Psi(t)|i[\hat{O},\hat{\mu}]|\Psi(t)\rangle}. \tag{H.4}$$

For $[\hat{O},\hat{\mu}] = 0$ the denominator is zero for every $t$. In this case we apply again [27] the Ehrenfest theorem

$$\begin{aligned}
\frac{d^2S(t)}{dt^2} &= \left\langle\Psi(t)\left|\frac{\partial^2\hat{O}}{\partial t^2}\right|\Psi(t)\right\rangle - 2\left\langle\Psi(t)\left|i\left[\frac{\partial\hat{O}}{\partial t},\widehat{H}_0\right]\right|\Psi(t)\right\rangle \\
&+ 2\left\langle\Psi(t)\left|i\left[\frac{\partial\hat{O}}{\partial t},\hat{\mu}\right]\right|\Psi(t)\right\rangle E(t) + \left\langle\Psi(t)\left|i\left[\hat{O},\hat{\mu}\right]\right|\Psi(t)\right\rangle\frac{\partial E(t)}{\partial t} \\
&- \left\langle\Psi(t)\left|\left[\left[\hat{O},\widehat{H}_0\right],\widehat{H}_0\right]\right|\Psi(t)\right\rangle + \left\langle\Psi(t)\left|\left[\left[\hat{O},\widehat{H}_0\right],\hat{\mu}\right]\right|\Psi(t)\right\rangle E(t) \\
&+ \left\langle\Psi(t)\left|\left[\left[\hat{O},\hat{\mu}\right],\widehat{H}_0\right]\right|\Psi(t)\right\rangle E(t) - \left\langle\Psi(t)\left|\left[\left[\hat{O},\hat{\mu}\right],\hat{\mu}\right]\right|\Psi(t)\right\rangle E^2(t)
\end{aligned} \tag{H.5}$$

The terms containing $[\hat{O},\hat{\mu}] = 0$ vanish so that

$$\begin{aligned}
\frac{d^2S(t)}{dt^2} &= \left\langle\Psi(t)\left|\frac{\partial^2\hat{O}}{\partial t^2}\right|\Psi(t)\right\rangle - 2\left\langle\Psi(t)\left|i\left[\frac{\partial\hat{O}}{\partial t},\widehat{H}_0\right]\right|\Psi(t)\right\rangle \\
&+ 2\left\langle\Psi(t)\left|i\left[\frac{\partial\hat{O}}{\partial t},\hat{\mu}\right]\right|\Psi(t)\right\rangle E(t) \\
&- \left\langle\Psi(t)\left|\left[\left[\hat{O},\widehat{H}_0\right],\widehat{H}_0\right]\right|\Psi(t)\right\rangle + \left\langle\Psi(t)\left|\left[\left[\hat{O},\widehat{H}_0\right],\hat{\mu}\right]\right|\Psi(t)\right\rangle E(t)
\end{aligned} \tag{H.6}$$

We rewrite this equation

$$E(t) = \frac{\frac{d^2S(t)}{dt^2} - \left\langle \Psi(t) \left| \frac{\partial^2 \hat{O}}{\partial t^2} + 2i \left[ \frac{\partial \hat{O}}{\partial t}, \widehat{H}_0 \right] + \left[ \left[ \hat{O}, \widehat{H}_0 \right], \widehat{H}_0 \right] \right| \Psi(t) \right\rangle}{2 \left\langle \Psi(t) \left| i \left[ \frac{\partial \hat{O}}{\partial t}, \hat{\mu} \right] \right| \Psi(t) \right\rangle + \left\langle \Psi(t) \left| \left[ \left[ \hat{O}, \widehat{H}_0 \right], \hat{\mu} \right] \right| \Psi(t) \right\rangle} \tag{H.7}$$

For $\widehat{O} = \hat{\mu} = x$ this equation becomes

$$E(t) = -\left( \ddot{S}(t) + \langle \Psi(t) | \partial_x V | \Psi(t) \rangle \right) \tag{H.8}$$

which means that the second time derivative of the imposed trajectory determines the field.

In the process of high harmonic generation (HHG) the atom irradiated with a strong laser field of frequency $\omega_0$ responds in a nonlinear way and radiates odd harmonics of $\omega_0$. As one can see in equation (H.8) this is possible only if the term $\langle \Psi(t) | \partial_x V | \Psi(t) \rangle$ compensates the harmonics in the spectrum of the imposed trajectory $\ddot{S}(t)$, otherwise the spectrum of $E$ would contain more than only $\omega_0$. As one can see the type of potential plays a crucial role. It is well known that in the harmonic oscillator potential, there is no HHG [48]. Therefore, for such a potential the term $\langle \Psi(t) | \partial_x V | \Psi(t) \rangle$ cannot compensate any harmonic higher than the first from the spectrum of $\ddot{S}(t)$.

# Bibliography


[1] L.S. Pontryagin V.G Boltyanskii P.V. Gamkrelidtze and E.F Mischenko. *L.S. Pontryagin - Selected works*, volume 4. The mathematical theory of optimal processes. L.W. Neustadt, 1986.

[2] A.M. Weiner et al. Programmable shaping of femtosecond pulses by use of a 128-element liquid-crystal phase modulator. *IEEE J. Quant. Electron.*, 28:908–920, 1992.

[3] R. B. Walker and R. K. Preston. Quantum versus classical dynamics in the treatment of multiple photon excitation of the anharmonic oscillator. *J. Chem. Phys.*, 67:2017, 1977.

[4] P.S Dardi and S. K. Gray. Classical and quantum mechanical studies of hf in an intense laser field. *J. Chem. Phys.*, 77:1345, 1982.

[5] G.M. Huang, T.J. Tarn, and J.W. Clark. On the controllability of quantum-mechanical systems. *J. Math. Phys.*, 24:2608, 1983.

[6] A.P. Pierce M.A. Dahleh and H. Rabitz. Optimal control of quantum-mechanical systems: Existence, numerical approximation, and applications. *Phys. Rev. A*, 37:4950, 1988.

[7] M. Zhao and S.A.Rice. Comment concerning the optimum control of transformations in an unbounded quantum system. *J. Chem. Phys.*, 95:2465, 1991.

[8] D.Tannor and S. Rice. Control of selectivity of chemical reactions via control of wave packet evolution. *J. Chem. Phys.*, 83:5013, 1985.

[9] D.Tannor R.Kosloff and S. Rice. Coherent pulse sequence induced control of selectivity of reactions: Exact quantum mechanical calculation. *J. Chem. Phys.*, 83:5013, 1985.

[10] R.Kosloff et al. Wavepacket dancing: achieving chemical selectivity by shaping light pulses. *Chem. Phys.*, 139:201, 1989.

[11] R.S. Judson and H. Rabitz. Teaching lasers to control molecules. *Phys. Rev. Lett.*, 68:1500, 1992.

[12] C.J. Bardeen et al. Feedback quantum control of molecular electronic population transfer. *Chem. Phys. Lett.*, 280:151, 1997.

[13] A. Assion et al. Control of chemical reactions by feedback-optimized phase-shaped femtosecond laser pulses. *Science*, 282:919, 1998.

[14] C. Daniel et al. Deciphering the reaction dynamics underlying optimal control laser fields. *Science*, 299:536, 2003.

[15] R.J. Levis, G. M. Menkir, and H. Rabitz. Selective bond dissociation and rearrangement with optimally tailored, strong field laser pulses. *Science*, 292:709, 2001.

[16] *Time-Dependent Quantum Molecular Dynamics*, chapter Control of photochemical branching: Novel procedures for finding optimal pulses and global upper bounds, page 347. Plenum Press, New York, 1992.

[17] V.F. Krotov. *Global methods in optimal control theory.* Marcel Dekker, 1995.

[18] Wusheng Zhu, Jair Botina, and H. Rabitz. Rapidly convergent iteration methods for quantum optimal control of population. *J. Chem. Phys.*, 108:1953, 1997.

[19] Wusheng Zhu and H. Rabitz. A rapid monotonically convergent iteration algorithm for quantum optimal control over the expectation value of a positive definite operator. *J. Chem. Phys.*, 109:385, 1998.

[20] Y. Maday and G. Turinici. New formulations of monotonically convergent quantum control algorithms. *J. Chem. Phys.*, 118:8191, 2003.

[21] W. Zhu and H. Rabitz. Noniterative algorithms for finding quantum optimal controls. *J. Chem. Phys.*, 110:7142, 1999.

[22] I. Grigorenko, M. Garcia, and K.H. Bennemann. Theory for the optimal control of time-averaged quantities in quantum systems. *Phys. Rev. Lett.*, 89:233003–1, 2002.

[23] Y. Ohtsuki K.Nakagami Y. Fujimura W. Zhu H. Rabitz. Quantum optimal control of multiple targets. *J. Phys. Chem.*, 114:8867, 2001.

[24] M. Sugawara. General formulation of locally designed coherent control theory for quantum system. *J. Chem. Phys.*, 118:6784, 2003.

[25] M. Sugawara S.Yoshizawa and S. Yabushita. Coherent control of wavepachet dynamics by locally designed external field. *Chem. Phys. Lett.*, 350:253, 2001.

[26] M. Sugawara. Tracking of wave packet dynamics by locally designed control field. *Chem. Phys. Lett.*, 378:603, 2003.

[27] W. Zhu and H. Rabitz. Quantum control design via adaptive tracking. *J. Chem. Phys.*, 119:3619, 2003.

[28] Y. Chen P.Gross V. Ramakrishna H. Rabitz. Competitive tracking of molecular objectives described by quantum mechanics. *J. Phys. Chem.*, 102:8001, 1995.

[29] W. Zhu M. Smit H. Rabitz. Managing singular behavior in the tracking control of quantum dynamical observables. *J. Phys. Chem.*, 110:1905, 1998.

[30] J. Werschnik. *Optimal Control for One-Body and Many-Body systems.* PhD thesis, Freie Universität Berlin, to be published.

[31] A.L. Fetter and J.D. Walecka. *Quantum theory of many particle systems.* McGraw-Hill, 1971.

[32] F.R. Gantmacher. *Matrizenrechnung*, chapter Anwendungen der Matrizenrechnung zur Untersuchung linearer Differentialgleichungssysteme, page 114. Deutscher Verlag der Wissenschaften, 1959.

[33] J. Bosse. Theoretische vielteilchenphysik. Manuskript zur Vorlesung Theoretische Vieltelichenphysik, 2003.

[34] Th. Hornung M. Motzkus and R. de Vivie-Riedle. Teaching optimal control theory to distill robust pulses even under experimental constraints. *Phys. Rev. A*, 65:021403(R), 2002.

[35] C. Search W.Zhang and P. Meystre. Molecular micromaser. *Phys. Rev. Lett.*, 91:190401, 2003.

[36] M.A. Nielsen ans I.L Chuang. *Quantum computation and quantum information.* Cambridge University Press, 2004.

[37] M.O. Scully and M. S. Zubairy. *Quantum optics.* Cambridge University Press, 1997.

[38] L.Allen and J.H. Eberly. *Optical resonance and two-level atoms.* John Wiley, 1975.

[39] J.A. Fleck, Jr. J.R.Morris, and M.D.Feit. *Appl. Phys.*, 10:129, 1976.

[40] Q. Su and J.H. Eberly. Model atom for multiphoton physics. *Phys. Rev. A*, 44:5997, 1991.

[41] J.L. Krause K.J. Schafer and K.C Kulander. Calculation of photoemission from atoms subject to intense laser fields. *Phys. Rev. A.*, 45:4998, 1992.

[42] R. Bartels et al. Shaped pulse-optimisation of coherent emission of high-harmonic soft x-rays. *Nature*, 406:164, 2000.

[43] A. Baltuska et al. Attosecond control of electronic processes by by intense light fields. *Nature*, 421:611, 2003.

[44] R. de Vivie-Riedle T. Hornung, M. Motzkus. Adapting optimal control theory and using learning loops to provide experimentally feasible shaping mask patterns. *J. Chem. Phys*, 115:3105, 2001.

[45] Fahrad H. M. Faisal. *Theory of multiphoton processes.* Plenum Press, 1987.

[46] H. Kleinert. *Path Integrals in Quantum Mechanics, Statistics and Polymer Physics.* World Scientific, 1995.

[47] B. Hamprecht. Exact solutions of the time-dependent Schrödinger equation in one space dimension. *http://www.physik.fu-berlin.de/~hamprecht/*, 1997.

[48] S. Erhardt. Atome in ultrastarken Laserpulsen: Simulation der erzeugung hoher harmonischer. Physikalischen Institut der Bayerischen Julius-Maximilanus-Universitaet Wuerzburg, 1996.

# Acknowledgment

I wish to thank to professor E.K.U. Gross for giving me an interesting and challenging diploma thesis. He constantly motivated me and guided me through the difficulties I encountered. For the completion of this work, the pleasant environment in his group was of great importance.

My direct advisor and most frequent discussion partner was Jan Werschnik, who shared his experience in optimal control with me and whose help and ideas played an important role in this work. Furthermore, he kindly introduced me to his code, which was the basis for the calculations of chapter 6 and supported me in computer problems of all kind.

Many thanks also to Stefan Kurth for useful discussions. He, together with Nicole Helbig and Tobias Munk, carefully read early versions of this thesis and made useful suggestions.

Finally, none of this would have been possible without the constant support from my parents.